Developed at the request of:

Department of Energy & Climate Change

Research conducted by:

Met Office Hadley Centre

The University of Nottingham
UNITED KINGDOM · CHINA · MALAYSIA

Walker Institute

Centre for Ecology & Hydrology
Natural Environment Research Council

University of Leeds

Tyndall Centre for Climate Change Research

Climate: Observations, projections and impacts

Mexico

We have reached a critical year in our response to climate change. The decisions that we made in Cancún put the UNFCCC process back on track, saw us agree to limit temperature rise to 2 °C and set us in the right direction for reaching a climate change deal to achieve this. However, we still have considerable work to do and I believe that key economies and major emitters have a leadership role in ensuring a successful outcome in Durban and beyond.

To help us articulate a meaningful response to climate change, I believe that it is important to have a robust scientific assessment of the likely impacts on individual countries across the globe. This report demonstrates that the risks of a changing climate are wide-ranging and that no country will be left untouched by climate change.

I thank the UK's Met Office Hadley Centre for their hard work in putting together such a comprehensive piece of work. I also thank the scientists and officials from the countries included in this project for their interest and valuable advice in putting it together. I hope this report will inform this key debate on one of the greatest threats to humanity.

The Rt Hon. Chris Huhne MP, Secretary of State for Energy and Climate Change

There is already strong scientific evidence that the climate has changed and will continue to change in future in response to human activities. Across the world, this is already being felt as changes to the local weather that people experience every day.

Our ability to provide useful information to help everyone understand how their environment has changed, and plan for future, is improving all the time. But there is still a long way to go. These reports – led by the Met Office Hadley Centre in collaboration with many institutes and scientists around the world – aim to provide useful, up to date and impartial information, based on the best climate science now available. This new scientific material will also contribute to the next assessment from the Intergovernmental Panel on Climate Change.

However, we must also remember that while we can provide a lot of useful information, a great many uncertainties remain. That's why I have put in place a long-term strategy at the Met Office to work ever more closely with scientists across the world. Together, we'll look for ways to combine more and better observations of the real world with improved computer models of the weather and climate; which, over time, will lead to even more detailed and confident advice being issued.

Julia Slingo, Met Office Chief Scientist

Introduction

Understanding the potential impacts of climate change is essential for informing both adaptation strategies and actions to avoid dangerous levels of climate change. A range of valuable national studies have been carried out and published, and the Intergovernmental Panel on Climate Change (IPCC) has collated and reported impacts at the global and regional scales. But assessing the impacts is scientifically challenging and has, until now, been fragmented. To date, only a limited amount of information about past climate change and its future impacts has been available at national level, while approaches to the science itself have varied between countries.

In April 2011, the Met Office Hadley Centre was asked by the United Kingdom's Secretary of State for Energy and Climate Change to compile scientifically robust and impartial information on the physical impacts of climate change for more than 20 countries. This was done using a consistent set of scenarios and as a pilot to a more comprehensive study of climate impacts. A report on the observations, projections and impacts of climate change has been prepared for each country. These provide up to date science on how the climate has already changed and the potential consequences of future changes. These reports complement those published by the IPCC as well as the more detailed climate change and impact studies published nationally.

Each report contains:

- A description of key features of national weather and climate, including an analysis of new data on extreme events.
- An assessment of the extent to which increases in greenhouse gases and aerosols in the atmosphere have altered the probability of particular seasonal temperatures compared to pre-industrial times, using a technique called 'fraction of attributable risk.'
- A prediction of future climate conditions, based on the climate model projections used in the Fourth Assessment Report from the IPCC.
- The potential impacts of climate change, based on results from the UK's Avoiding Dangerous Climate Change programme (AVOID) and supporting literature. For details visit: http://www.avoid.uk.net

The assessment of impacts at the national level, both for the AVOID programme results and the cited supporting literature, were mostly based on global studies. This was to ensure consistency, whilst recognising that this might not always provide enough focus on impacts of most relevance to a particular country. Although time available for the project was short, generally all the material available to the researchers in the project was used, unless there were good scientific reasons for not doing so. For example, some impacts areas were omitted, such as many of those associated with human health. In this case, these impacts are strongly dependant on local factors and do not easily lend themselves to the globally consistent framework used. No attempt was made to include the effect of future adaptation actions in the assessment of potential impacts. Typically, some, but not all, of the impacts are avoided by limiting global average warming to no more than 2 °C.

The Met Office Hadley Centre gratefully acknowledges the input that organisations and individuals from these countries have contributed to this study. Many nations contributed references to the literature analysis component of the project and helped to review earlier versions of these reports.

We welcome feedback and expect these reports to evolve over time. For the latest version of this report, details of how to reference it, and to provide feedback to the project team, please see the website at www.metoffice.gov.uk/climate-change/policy-relevant/obs-projections-impacts

In the longer term, we would welcome the opportunity to explore with other countries and organisations options for taking forward assessments of national level climate change impacts through international cooperation.

Summary

Climate observations

- Mexico has seen widespread warming since 1960.
- The frequency of cool days has decreased since 1960 and the frequency of warm nights has increased.
- There has been a general increase in winter temperatures averaged over the country as a result of human influence on climate, making the occurrence of warm winter temperatures more frequent and cold winter temperatures less frequent.
- There has been a decrease in precipitation in the far south-east of the country since 1960.

Climate change projections

- For the A1B emissions scenario projected temperature increases from CMIP3 over Mexico are up to around 4°C close to the US border, with the rest of the country showing increases of around 2.5- 3.5°C. Agreement between models is generally high.
- Mexico is located in a region of projected decreased precipitation with typical decreases of around 5 to 10%. However, ensemble agreement is generally quite low.

Climate change impacts projections

Crop yields

- A definitive conclusion on the impact of climate change on crop yields in Mexico cannot be drawn from the studies included here. However, the majority of these studies project a decrease in the yield of maize, Mexico's major crop, by the 2050s.

- Results from the AVOID programme for Mexico show that under both emissions scenarios, no models project an increase in suitability for cultivation for current Mexican croplands. For both scenarios, between 40% and 70% of current Mexican croplands are projected to undergo declining suitability by 2030. By 2100 this rises to 50%-80% under the mitigation scenario and 60%-100% under A1B.

Food security

- Mexico is currently a country of extremely low undernourishment. Global- and regional-scale studies suggest a mixed outlook for food security issues under climate change, although the majority of these studies suggest that the country is not likely to face severe food security issues in the next 40 years.

- However, research by the AVOID programme indicates that adaptation measures, such as reducing food for exports, may be required to avoid major food security issues in Mexico with climate change.

Water stress and drought

- Global-scale studies included here concur that Mexico is currently highly vulnerable to water security threats.

- There is large uncertainty in how climate change could affect water stress in Mexico, which partly arises from climate modelling uncertainty. However, the majority of global-scale studies included here project that that the population exposed to water stress could increase substantially with climate change.

- Recent simulations by the AVOID programme support this.

Pluvial flooding and rainfall

- The IPCC AR4 reported a general decrease in mean precipitation with climate change for Mexico and recent studies confirm this.

- However, studies of extreme precipitation suggest the possibility of increases, but with a large uncertainty attached to future projections of tropical cyclone occurrence.

Fluvial flooding

- Few studies have investigated changes in flood hazard in Mexico under climate change scenarios. However, at least one global-scale assessments suggests that flood frequency and magnitude may decrease with climate change.

- Simulations by the AVOID programme showed a greater tendency among models towards decreasing flood risk early in the 21st century. Later in the century the balance shifted towards an increase in flood risk under the A1B scenario, while under a mitigation scenario the majority of the models still showed a decrease.

Tropical cyclones

- The majority of studies reviewed here suggest that tropical cyclone intensities could increase in both the Gulf of Mexico and East Pacific basins with climate change.

- The uncertainty in the magnitude of this change, coupled with the uncertainty in cyclone frequencies, makes estimates of future cyclone damages in Mexico due to climate change highly uncertain.

Coastal regions

- Two global-scale studies suggest that Mexico's population is not highly vulnerable to sea level rise (SLR), relative to other countries across the globe.

- One of these studies suggests that SLR could have little or no affect on Mexico's population.

- However, one study found that out of 84 developing countries considered, Mexico was ranked the 7th highest with respect to the amount of agricultural land that could be submerged with a simulated 1m SLR.

Table of contents

Chapter 1 – Climate Observations

Rationale

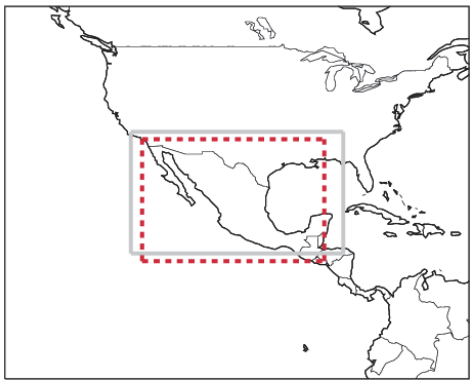

Figure 1. *Location of boxes for the regional average time series (red dashed box) in Figures 3 and 5 and attribution (grey box) in Figure 4.*

Present day weather and climate play a fundamental role in the day to day running of society. Seasonal phenomena may be advantageous and depended upon for sectors such as farming or tourism. Other events, especially extreme ones, can sometimes have serious negative impacts posing risks to life and infrastructure, and significant cost to the economy. Understanding the frequency and magnitude of these phenomena, when they pose risks or when they can be advantageous and for which sectors of society, can significantly improve societal resilience. In a changing climate it is highly valuable to understand possible future changes in both potentially hazardous events and those reoccurring seasonal events that are depended upon by sectors such as agriculture and tourism. However, in order to put potential future changes in context, the present day must first be well understood both in terms of common seasonal phenomena and extremes.

The purpose of this chapter is to summarise the weather and climate from 1960 to present day. This begins with a general climate overview including an up to date analysis of changes in surface mean temperature. These changes may be the result of a number of factors including climate change, natural variability and changes in land use. There is then a focus on extremes of temperature, precipitation and storms selected from 2000 onwards reported in the World Meteorological Organisation (WMO) Annual Statement on the Status of the Global Climate and/or the Bulletin of the American Meteorological Society (BAMS) State of the Climate reports. This is followed by a discussion of changes in moderate extremes from 1960 onwards using an updated version of the HadEX extremes database (Alexander et al., 2006) which categorises extremes of temperature and precipitation. These are core climate variables which have received significant effort from the climate research community in terms of data acquisition and processing and for which it is possible to produce long high quality records for monitoring. No new analysis is included for storms (see the methodology annex that follows for background). For seasonal temperature extremes, an attribution analysis then puts the seasons with highlighted extreme events into context of the recent climate versus a hypothetical climate in the absence of anthropogenic emissions (Christidis et al., 2011). It is important to note that we carry out our attribution analyses on seasonal

mean temperatures over the entire country. Therefore these analyses do not attempt to attribute the changed likelihood of individual extreme events. The relationship between extreme events and the large scale mean temperature is likely to be complex, potentially being influenced by *inter alia* circulation changes, a greater expression of natural internal variability at smaller scales, and local processes and feedbacks. Attribution of individual extreme events is an area of developing science. The work presented here is the foundation of future plans to systematically address the region's present and projected future weather and climate and the associated impacts.

The methodology annex that follows provides details of the data shown here and of the scientific analyses underlying the discussions of changes in the mean temperature and in temperature and precipitation extremes. It also explains the methods used to attribute the likelihood of occurrence of seasonal mean temperatures.

Climate overview

A primary factor moulding the climate of Mexico is its tropical to sub-tropical latitude range from 15-32°N which, as well as ensuring reasonably high temperatures, sandwiches the country between relatively high pressure towards the north and the Inter-tropical Convergence Zone which approaches the south of the country for a time in summer. Between these systems north-easterly 'trade' winds blow onto Mexico's eastern coastline from the warm Caribbean Sea. Along the north-western (Pacific) coastline of Baja California, the cold Californian ocean current, combined with the proximity of high atmospheric pressure, reduce both temperature and rainfall, giving desert conditions. The impact of Mexico's low latitude on temperature is tempered by much of the country being high plateaux or mountain with temperature reduced by altitude. Low lying areas are confined to narrow coastal strips on the west coast and a broader coastal strip on the eastern side of the country which, towards the south, expands into the low-lying Yukatan peninsula. Another influence on the climate is that Mexico forms an extension of the much larger land mass of the USA, the north of Mexico sharing in its more continental temperature extremes. In particular, 'cold waves' sweeping south from the USA occasionally bring very cold conditions to northern Mexico and the east coast as far south as Tampico (only 22°N) where snow has fallen. Meanwhile the west coast is protected from such cold waves by the high Sierra Madra mountain chain immediately inland.

Mean annual temperature at low-altitude varies from 26-28°C in Yukatan (far south-east) and Acapulco (southerly latitude on the Pacific coast) to 25°C at Tampico (east coast) but only 18°C at Tijuana at the northward extent of the Mexico's Pacific coast. At about 1500m altitude, mean annual temperature ranges from 21°C at Guadalajara in the south-central mountains to 18°C at Chilhuahua on the north-central plateau. The seasonal variation in monthly mean temperature is very small (±1-2°C) in the south at both Acapulco and Merida (Yukatan) but increases northwards and inland to around ±4-5°C in more northerly coastlands and ±8°C well inland in the north at Chilhuahua.

The north-west coastal zone is the driest area of Mexico, with, for instance, only 255mm annual average rainfall at Tijuana, falling almost entirely in winter and early spring, when southward migration of the North Pacific anticyclone allows eastward moving Pacific weather systems to reach the region. Elsewhere in Mexico precipitation is more plentiful and has a strong summer and early autumn maximum. Examples of annual average rainfall are Merida 1050mm, Tampico 1149mm and Acapulco 1284mm. However values inland are somewhat

lower despite higher altitude, for instance 972mm at Guadalajara towards the south and only 477mm at Chilhuahua towards the north.

Both the west and east coasts of Mexico are occasionally affected by tropical storms which develop in the Pacific or the Caribbean and bring two or three days of heavy rain. These are most likely to occur in the months August to October. Very few of these reach the strength of fully developed hurricanes, but if they do, the east-coast districts are more liable to severe damage. Other climate hazards are floods, droughts and occasional cold waves.

Analysis of long-term features in the mean temperature

CRUTEM3 data (Brohan et al., 2006) have been used to provide an analysis of mean temperatures from 1960 to 2010 over Mexico using the median of pairwise slopes method to fit the trend (Sen, 1968; Lanzante, 1996). The methods are fully described in the methodology annex. In agreement with increasing global average temperatures (Sánchez-Lugo et al., 2011), over the period 1960 to 2010 there is a spatially consistent warming signal for temperature over Mexico with widespread high confidence as shown in Figure 2. For both summer (June to August) and winter (December to February) the spatial pattern is similar. Regionally averaged trends (over grid boxes included in the red dashed box in Figure 1) calculated by the median of pairwise slopes show warming. Grid boxes in which the 5^{th} to 95^{th} percentiles of the slopes are of the same sign can be more confidently regarded as showing this signal: they are widespread for both summer (June to August) and winter (December to February). For the summer the trend is 0.17 ^{o}C per decade (5^{th} to 95^{th} percentile of slopes: 0.10 to 0.24 ^{o}C per decade) and for the winter the trend is 0.26 ^{o}C per decade (5^{th} to 95^{th} percentile of slopes: 0.16 to 0.36 ^{o}C per decade).

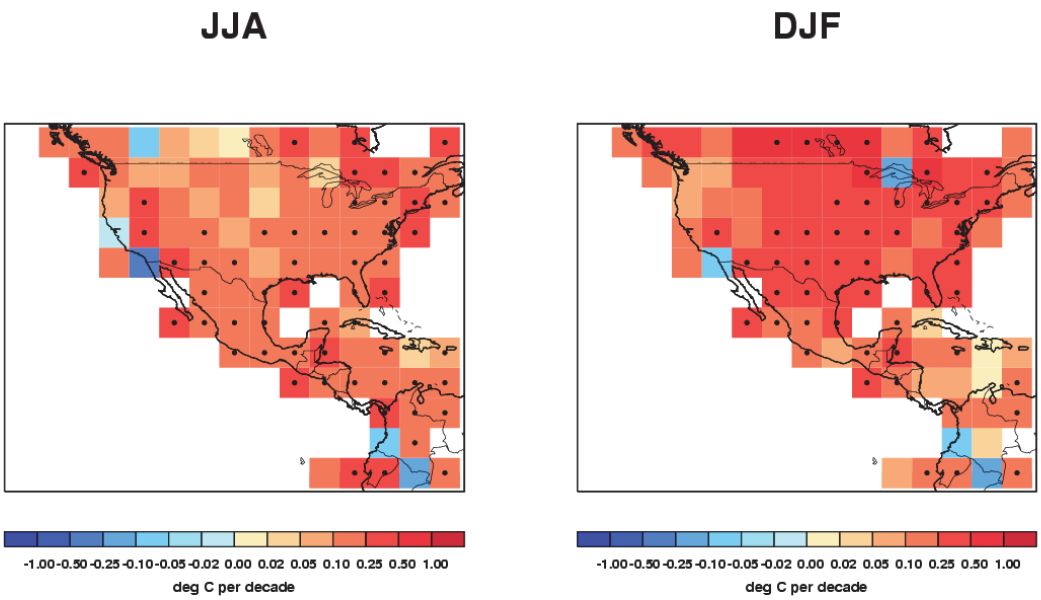

Figure 2. *Decadal trends in seasonally averaged temperatures for Mexico and the surrounding area over the period 1960 to 2010. Monthly mean anomalies from CRUTEM3 (Brohan et al., 2006) are averaged over each 3 month season (June-July-August – JJA and December-January-February – DJF). Trends are fitted using the median of pairwise slopes method (Sen, 1968; Lanzante, 1996). There is higher confidence in the trends shown if the 5th to 95th percentiles of the pairwise slopes do not encompass zero because here the trend is considered to be significantly different from a zero trend (no change). This is shown by a black dot in the centre of the respective grid-box.*

Temperature extremes

Both hot and cold temperature extremes can place many demands on society. While seasonal changes in temperature are normal and indeed important for a number of societal sectors (e.g. tourism, farming etc.), extreme heat or cold can have serious negative impacts. Importantly, what is 'normal' for one region may be extreme for another region that is less well adapted to such temperatures.

Table 1 shows selected extreme events since 2000 that are reported in WMO Statements on Status of the Global Climate and/or BAMS State of the Climate reports. The cold event of 2010 is highlighted below as an example of extreme temperatures which affected Mexico.

Year	Month	Event	Details	Source
2000	Jul-Sept	Hot	Very hot and dry conditions caused crop stress and wildfires	WMO (2001)
2009/10	Nov-Mar	Cold	Temperatures well below normal.	BAMS (Davydova-Belitskaya & Romero-Cruz, 2010 and 2011)

***Table 1**. Selected extreme temperature events reported in WMO Statements on Status of the Global Climate and/or BAMS State of the Climate reports since 2000.*

Recent extreme temperature events

Cold, winter 2009/10

The unusually cold temperatures of winter 2009/10 were due to intense humidity from the tropical Pacific and its interaction with cold fronts. These conditions brought heavy rain and cloudier-than normal skies, which led to low diurnal temperatures in most of the country (Davydova-Belitskaya & Romero-Cruz, 2010). From the end of November and throughout December 2009, unusually low temperatures were seen across the northwestern, northern, western, and central regions of Mexico; in the states of the northern Gulf coast; and in the Sierra Madre Oriental and the Eje Neovolcanico regions. Anomalies for Mexico were as much as 4.0°C below normal at the end of 2009 (Davydova-Belitskaya & Romero-Cruz, 2010). In February and March 2010, strong negative anomalies continued, ranging between 2.0°C–5.0°C below normal (Davydova-Belitskaya & Romero-Cruz, 2011).

Analysis of long-term features moderate temperature extremes

Temperature data provided by the Servicio Meteorológico Nacional have been used to update the HadEX extremes analysis for Mexico from 1960 to 2010 using daily maximum and minimum temperatures. Here we discuss changes in the frequency of cool days and nights and warm days and nights which are moderate extremes. Cool days/nights are defined as being below the 10^{th} percentile of daily maximum/minimum temperature and warm days/nights are defined as being above the 90^{th} percentile of the daily maximum/minimum temperature. The methods are fully described in the methodology annex.

The number of cool days is clearly decreasing, with high confidence that the trends are different from zero for each grid box, for all regions apart from the far east of the country surrounding the Yucatan peninsula (Figure 3 e to h). This cooling in the east of the country is also picked out in the number of cool nights, which also have increased in this area. However the rest of the signal from the number of cool nights is mixed, with further increases observed on the western coast, contrasting with the decreases seen in the rest of the country, albeit with lower confidence (Figure 3 a to d).

The signal for the number of warm nights is also fairly coherent, with higher confidence of an increase in all grid boxes, and lower confidence along the western coast and the Yucatan peninsula. There is a clear difference in the coverage from the number of warm days, which results from a much smaller decorrelation length scale being calculated for this index. This has led to a very mixed signal, but on a regional average, the number of warm days has increased. The behaviour of all four indices ties in with the general increase in average temperatures observed in the region (Figure 2).

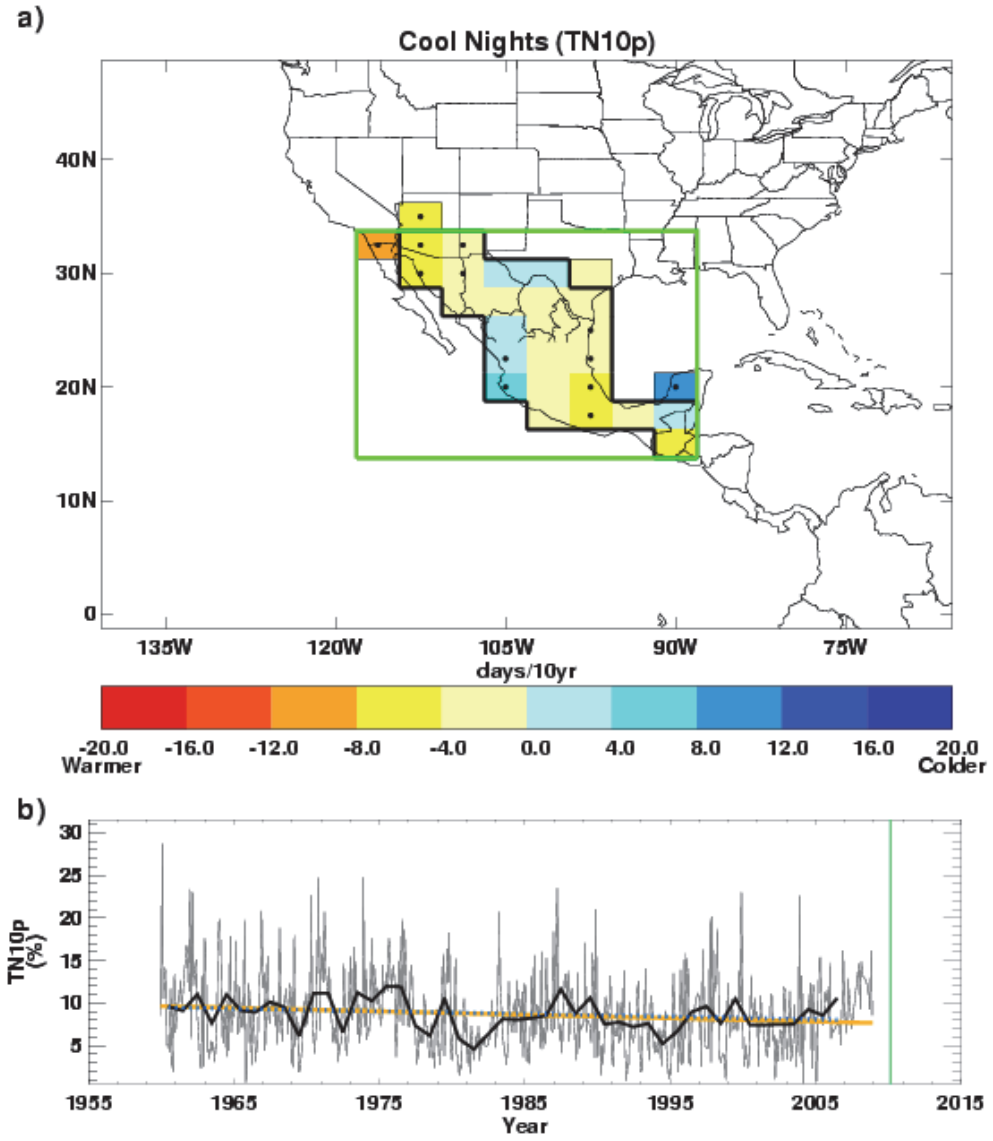
a)
Cool Nights (TN10p)
40N
30N
20N
10N
0
135W
120W
105W
90W
75W
days/10yr
-20.0
-16.0
-12.0
-8.0
-4.0
0.0
4.0
8.0
12.0
16.0
20.0
Warmer
Colder
b)
TN10P (%)
30
25
20
15
10
5
1955
1965
1975
1985
1995
2005
2015
Year
Monthly: -0.40% per decade (-0.67 to -0.14)
Total change of -1.62% from 1960 to 2008 (-2.68% to -0.55%)
Annual: -0.32% per decade (-0.67 to 0.19)
Total change of -1.28% from 1960 to 2006 (-2.69% to 0.77%)

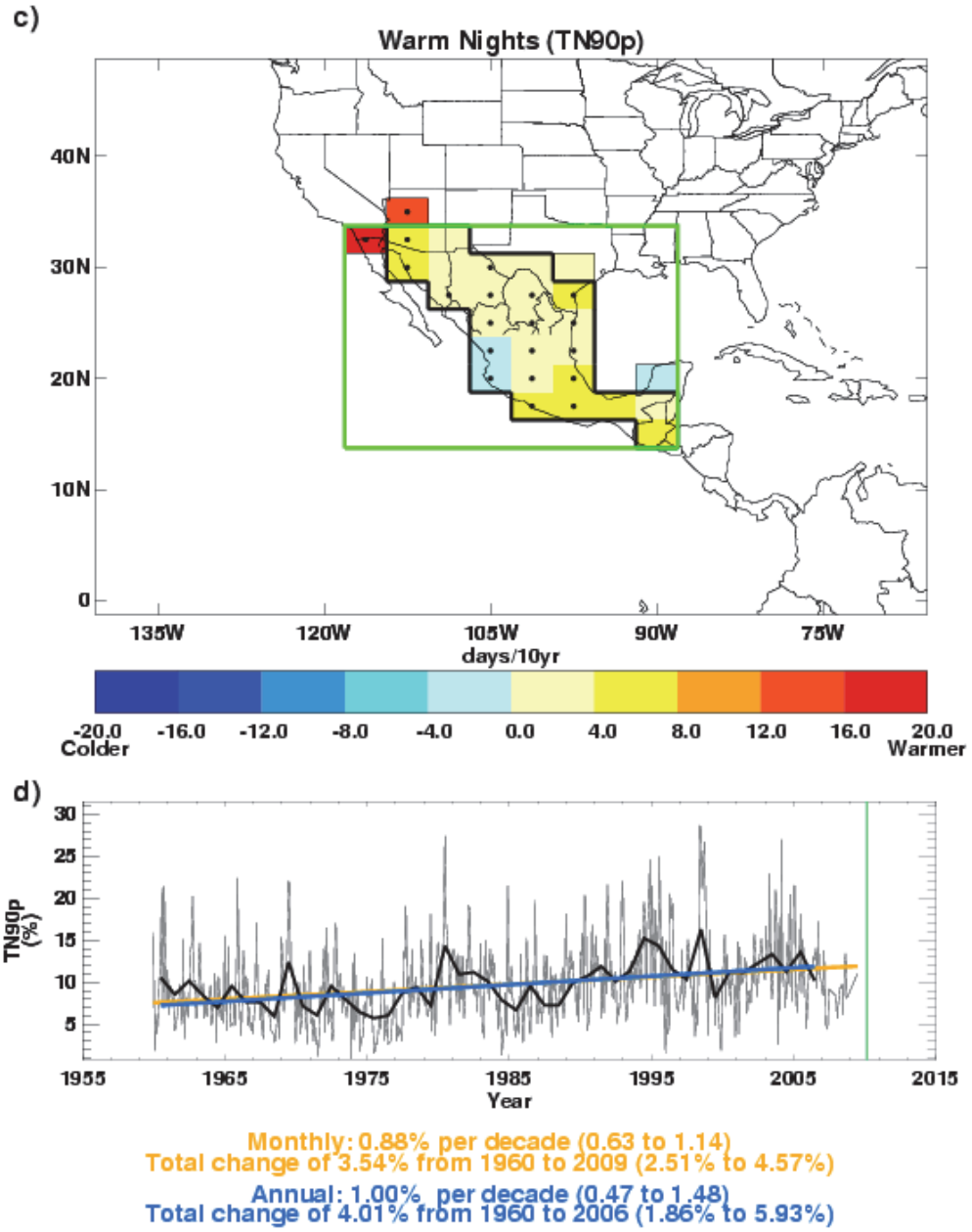
c)
Warm Nights (TN90p)
40N
30N
20N
10N
0
135W
120W
105W
90W
75W
days/10yr
-20.0
Colder
-16.0
-12.0
-8.0
-4.0
0.0
4.0
8.0
12.0
16.0
20.0
Warmer
d)
TN90p (%)
30
25
20
15
10
5
1955
1965
1975
1985
1995
2005
2015
Year
Monthly: 0.88% per decade (0.63 to 1.14)
Total change of 3.54% from 1960 to 2009 (2.51% to 4.57%)
Annual: 1.00% per decade (0.47 to 1.48)
Total change of 4.01% from 1960 to 2006 (1.86% to 5.93%)

e)

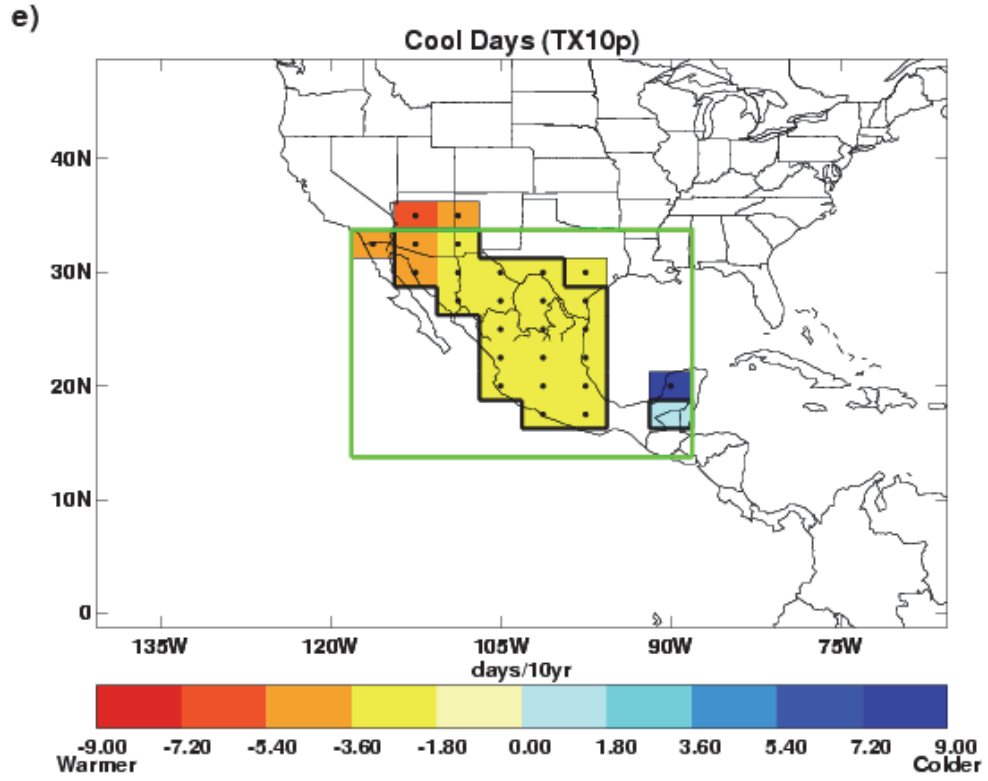

f)

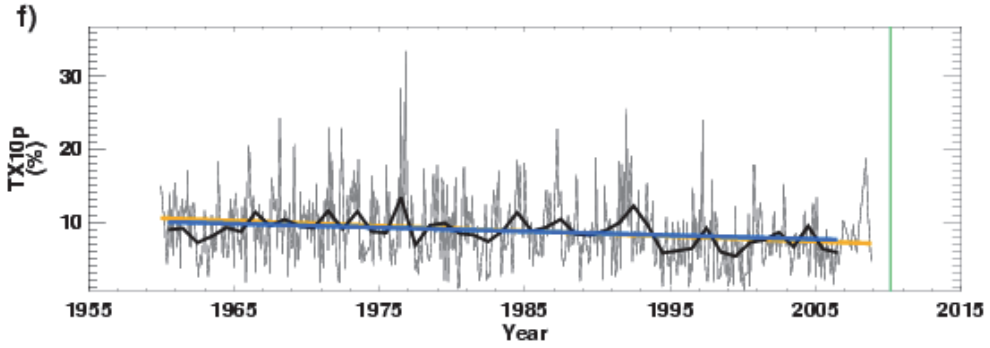

Monthly: -0.71% per decade (-0.96 to -0.46)
Total change of -2.85% from 1960 to 2008 (-3.84% to -1.85%)

Annual: -0.53% per decade (-0.91 to -0.14)
Total change of -2.12% from 1960 to 2006 (-3.62% to -0.58%)

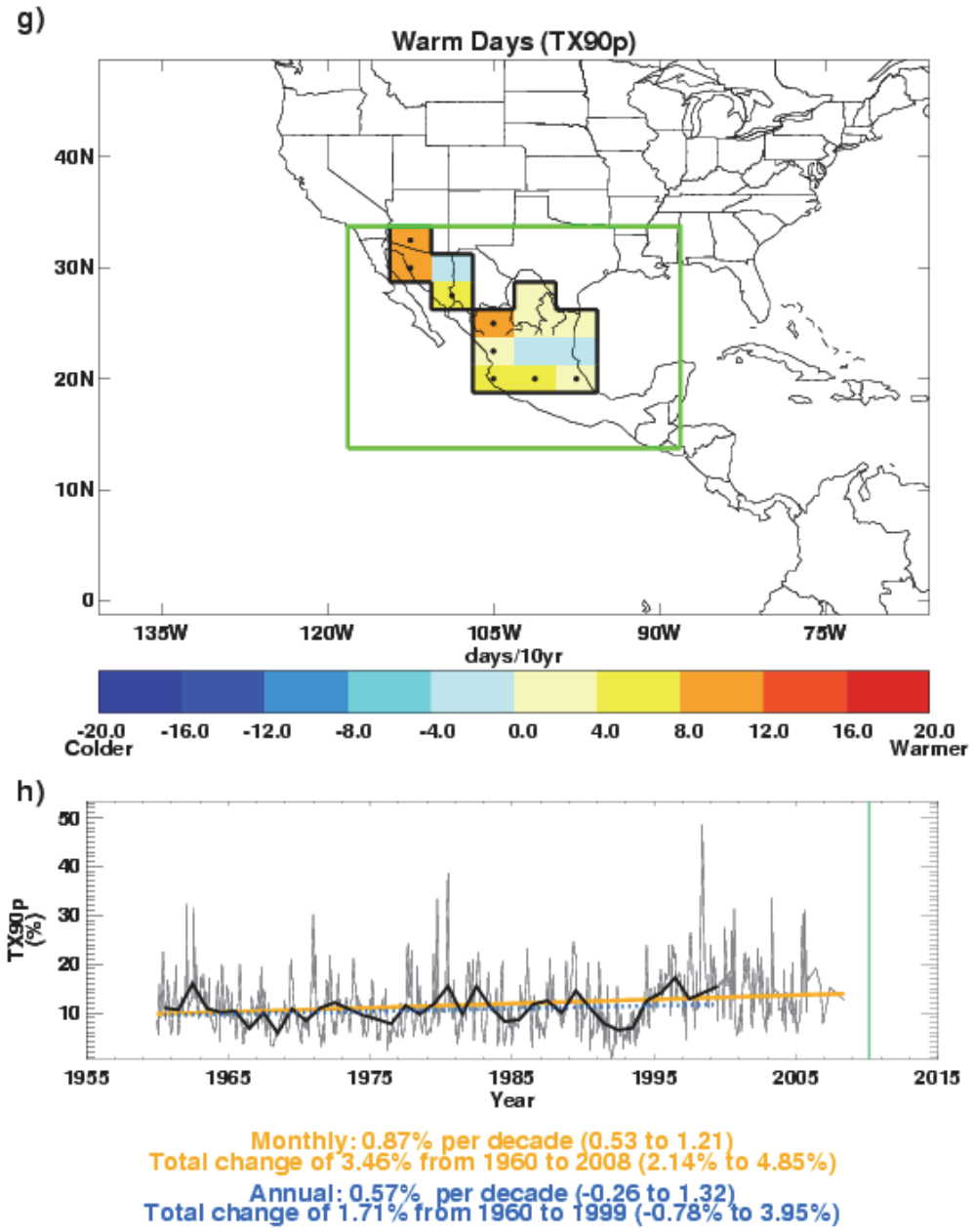

Figure 3. *Change in cool nights (a,b), warm nights (c,d), cool days (e,f) and warm days (g,h) for Mexico over the period 1960 to 2010 relative to 1961-1990 from data provided by the Servicio Meteorológico Nacional. a,c,e,g) Grid-box decadal trends. Grid-boxes outlined in solid black contain at least 3 stations and so are likely to be more representative of the wider grid-box. Trends are fitted using the median of pairwise slopes method (Sen, 1968; Lanzante, 1996). Higher confidence in a long-term trend is shown by a black dot if the 5th to 95th percentile slopes are of the same sign. Differences in spatial coverage occur because each index has its own decorrelation length scale (see methodology annex). b,d,f,h) Area averaged annual time series for 118.125° to 88.125° W and 13.75° to 33.75° N as shown by the green box on the map and red box in Figure 1. Thin and thick black lines show the monthly and annual variation respectively. Monthly (orange) and annual (blue) trends are fitted as described above. The decadal trend and its 5th to 95th percentile confidence intervals are stated along with the change over the period for which there are data available. Higher confidence in the trends, as denoted above, is shown by a solid line as opposed to a dotted one. The green vertical lines show the dates of the cold spell in 2010.*

Attribution of changes in likelihood of occurrence of seasonal temperatures

Today's climate covers a range of likely extremes. Recent research has shown that the temperature distribution of seasonal means would likely be different in the absence of anthropogenic emissions (Christidis et al., 2011). Here we discuss the seasonal means, within which the highlighted extreme temperature events occur, in the context of recent climate and the influence of anthropogenic emissions on that climate. The methods are fully described in the methodology annex.

Winter 2009/10

The distributions of the winter mean regional temperature in recent years in the presence and absence of anthropogenic forcings are shown in Figure 4. Analyses with both models suggest that human influences on the climate have shifted the distribution to higher temperatures. Considering the average over the entire region, the 2009/10 winter is cold, as it lies in the cold tail of the temperature distributions for the climate influenced by anthropogenic forcings (distributions plotted in red). In the absence of human influences on the climate (green distributions) the season would be less extreme, as it lies closer to the central sector of the temperature distribution. The winter of 2009/10 is considerably warmer than the winter of 1904/05, the coldest in the CRUTEM3 dataset. It should be noted that the attribution results shown here refer to temperature anomalies over the entire region and over an entire season, whereas the actual cold extreme event had a shorter duration and affected a smaller region.

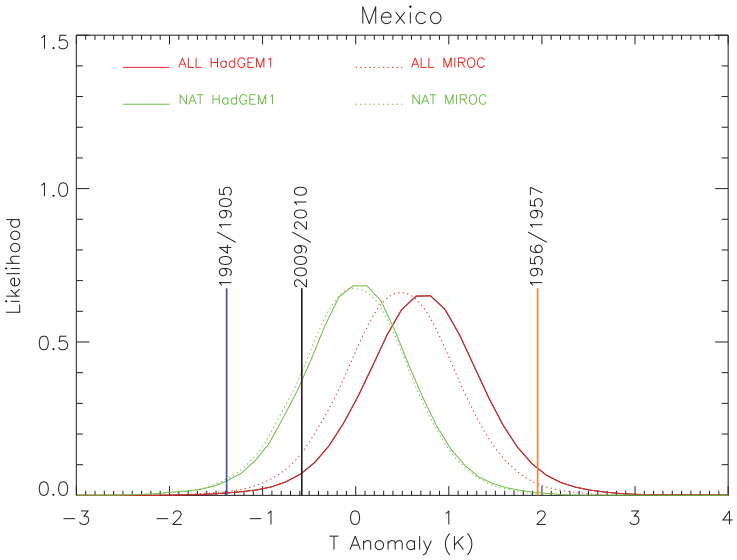

Figure 4. *Distributions of the December-January-February mean temperature anomalies (relative to 1961-1990) averaged over the Mexican region (120-85W, 15-35N – as shown in Figure 1) including (red lines) and excluding (green lines) the influence of anthropogenic forcings. The distributions describe the seasonal mean temperatures expected in recent years (2000-2009) and are based on analyses with the HadGEM1 (solid lines) and MIROC (dotted lines) models. The vertical black line marks the observed anomaly in 2009/10 and the vertical orange and blue lines correspond to the maximum and minimum anomaly in the CRUTEM3 dataset since 1900 respectively.*

Precipitation extremes

Precipitation extremes, either excess or deficit, can be hazardous to human health, societal infrastructure, and livestock and agriculture. While seasonal fluctuations in precipitation are normal and indeed important for a number of societal sectors (e.g. tourism, farming etc.), flooding or drought can have serious negative impacts. These are complex phenomena and often the result of accumulated excesses or deficits or other compounding factors such as spring snow-melt, high tides/storm surges or changes in land use. The analysis section below deals purely with precipitation amounts.

Table 2 shows selected extreme events since 2000 that are reported in WMO Statements on Status of the Global Climate and/or BAMS State of the Climate reports. The drought of 2009 and heavy rainfall of July 2010 are highlighted below as examples of extreme precipitation events experienced in Mexico.

Year	Month	Event	Details	Source
2003	Aug-Oct	Flooding	Mexico was hit by a series of hurricanes and tropical storms during August, September and October that brought heavy rains, flooding, and landslides to areas across the country.	WMO (2004)
2004	Apr	Flooding	Severe flooding in April along the Escondido River. In April, a storm brought heavy rain to the south-western United States and adjoining Mexico, causing the worst flash floods in the region.	WMO (2005)
2005	Oct	Flooding	Hurricane Stan caused flooding and mudslides over parts of Mexico leading to the deaths of hundreds of people.	WMO (2006)
2006	Sept	Flooding	Hurricane Lane had maximum winds at landfall of 204 km/h and caused widespread flooding and landslides.	WMO (2007)
2007	Nov	Flooding	Heavy rain caused the worst flooding in 5 decades, and the worst natural disaster in Mexico's history. Triggered by storms, massive flooding in Mexico in early November destroyed the homes of half a million people and seriously affected the country's oil industry.	WMO (2008)
2009		Drought	Experienced severe to exceptional drought conditions	WMO (2010)
2010	Jan-Feb	Flooding	January was the third wettest month on record, and February the wettest. Intense rainfall from 1-5 Feb led to landslides and flooding in many states, including Mexico City.	BAMS (Davydova-Belitskaya & Romero-Cruz, 2011)
2010	Jul	Wet	Wettest July since 1941 due to the transition to La Nina conditions. Total rainfall of 244 mm against average of 140 mm.	WMO (2011) BAMS (Davydova-Belitskaya & Romero-Cruz, 2011)
2010	Oct	Dry	Driest October since 1948, with only 6.7 mm of rainfall compared to the average of 27.5 mm.	WMO (2011) BAMS (Davydova-Belitskaya & Romero-Cruz, 2011)

Table 2. *Selected extreme precipitation events reported in WMO Statements on the Status of the Global Climate and/or BAMS State of the Climate reports since 2000.*

Recent extreme precipitation events

Drought, 2009

By September the drought conditions in Mexico were considered to be severe-to-exceptional (WMO, 2010). The northwest and central Mexico experienced its worst drought in 70 years, impacting agricultural, cattle, and water sectors across most of Mexico (NOAA, 2009; Davydova-Belitskaya & Romero-Cruz, 2010). About 3.5 million farmers were affected as over 50,000 cattle died, and up to 17 million acres of cropland were wiped out. Also due to the drought conditions around 80 of the country's largest reservoirs were less than half full (NOAA, 2009).

Heavy precipitation, July 2010

Under El Niño conditions Mexico saw record precipitation levels at the beginning of the year. In July, a transition to La Nina brought with it intense rainfall across most of the country, with a monthly total estimated at 244.2 mm, compared with a climatological average of around 140 mm (Davydova-Belitskaya & Romero-Cruz, 2011). This became the wettest July on record since 1941 (WMO, 2011).

Analysis of long-term features in precipitation

Precipitation data provided by the Servicio Meteorológico Nacional have been used to update the HadEX extremes analysis for Mexico from 1960 to 2010 for daily precipitation totals. Here we discuss changes in the annual total precipitation, and in the frequency of prolonged (greater than 6 days) wet and dry spells. The methods are fully described in the methodology annex.

For the majority of Mexico there is no strong signal in the change of the total precipitation amount and none of the grid boxes have high confidence that the trend is different from zero (Figure 5). However, in the far south-east there is a strong decrease which has higher confidence. The restricted nature of this signal is such that it should be treated with caution as it is at the edge of the data region. The data coverage of the number of continuous wet days is very poor (resulting from a short decorrelation length scale for this index). Therefore we are not able to draw any firm conclusions from the map. Similarly, the time series, which ends prematurely, although showing higher confidence in a decrease, should be interpreted with caution.

The number of continuous dry days shows a decrease for most of the country, but with lower confidence for all regions, apart from the far south east, where the same caveats apply as for the precipitation index. Both of the notable events outlined above occurred after the end of the time series, and so nothing can be said about their position in the time series.

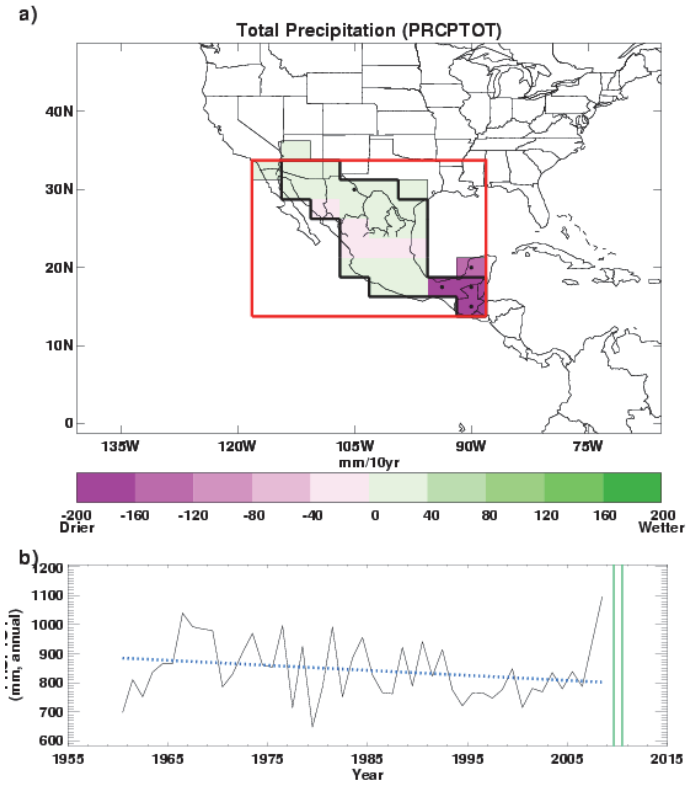

Annual: -17.33mm per decade (-37.11 to 4.61)
Total change of -69.31mm from 1960 to 2008 (-148.45mm to 18.42mm)

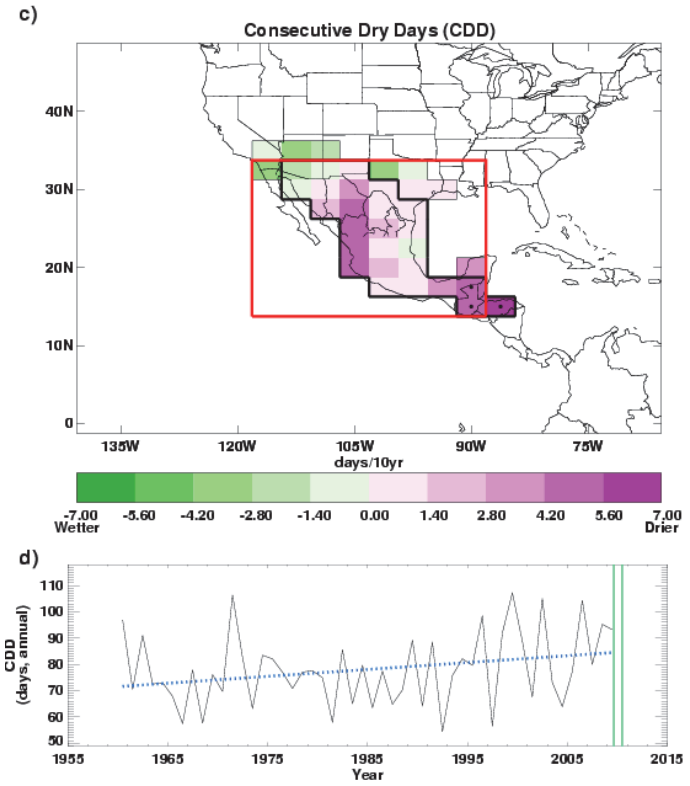

Annual: 2.62days per decade (-0.53 to 5.13)
Total change of 10.49days from 1960 to 2009 (-2.14days to 20.52days)

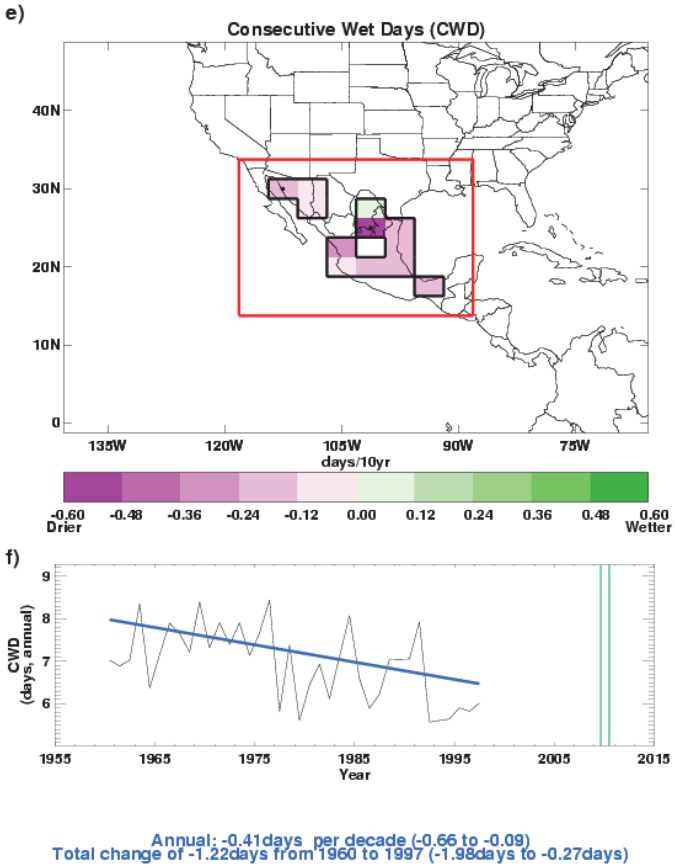

Figure 5. *Change in annual total rainfall (a,b), the annual number of continuous dry days (c,d) and the annual number of continuous wet days (e,f) over the period 1960-2010. The maps and time series have been created in exactly the same way as Figure 3. The green lines show the dates of the drought of 2009 and the floods of 2010. Only annual regional averages are shown in b,d,f).*

Storms

Storms can be very hazardous to all sectors of society. They can be small with localised impacts or spread across multiple states. There is no systematic observational analysis included for storms because, despite recent progress (Peterson et al., 2011; Cornes & Jones, 2011), wind data are not yet adequate for worldwide robust analysis (see methodology annex). Further progress awaits studies of the more reliable barometric pressure data through the new 20th Century Reanalysis (Compo et al., 2011) and its planned successors.

Table 3 shows selected extreme events since 2000 that are reported in WMO Statements on Status of the Global Climate and/or BAMS State of the Climate reports. Hurricane Alex, which made landfall in Mexico in June 2010, is highlighted below as an example of storms that affect Mexico.

Year	Month	Event	Details	Source
2000	Aug	Storm	Hurricane Beryl	WMO (2001)
2000	Oct	Storm	Hurricane Keith	WMO (2001)
2001	May	Storm	Hurricane Adolph - Strongest May hurricane (233 km/h)	WMO (2002)
2001	Sept	Storm	Hurricane Juliette - Second lowest centralpressure in the East Pacific (923 hPa)	WMO (2002)
2002	Oct	Storm	Hurricane Kenna- Third most violent hurricane in Mexico. Storm surge caused US$ 5 million damage in Puerto Vallarta	WMO (2003) BAMS (Lyon & Waple. 2003)
2005	Oct	Storm	Hurricane Wilma - category 4 at landfall in Mexico.	WMO (2006)
2008	Oct	Storm	Hurricane Norbert - Maximum winds 220 km/h. Most powerful 2008 East Pacific hurricane; the first October hurricane to make landfall on the Baja Peninsula since 1968	WMO (2009)
2009	Oct	Storm	Hurricane Rick had maximum winds 285 km/h. It was the second most intense Eastern North Pacific hurricane on record, behind Linda of 1997, and the strongest hurricane to form in October since reliable records began	WMO (2010)
2010	Jun	Storm	Hurricane Alex Maximum winds 175 km/h First June hurricane in the Atlantic basin since 1995; strongest June hurricane since 1966. Hurricane Alex led to flooding, affecting thousands of people and damage costing millions of pesos	WMO (2011) BAMS (Davydova-Belitskaya & Romero-Cruz, 2011)

***Table 3**. Selected extreme storm events reported in WMO Statements on Status of the Global Climate and/or BAMS State of the Climate reports since 2000.*

Recent storm events

Hurricane Alex, June 2010

Hurricane Alex was the first June hurricane in the Atlantic basin since 1995 and the strongest June hurricane since 1966 (WMO, 2011). The hurricane lasted from 25th June–2nd

July, and initially formed off of the Caribbean coast of Honduras. Alex acquired tropical storm status on 26th June (Amador, 2011).

In Mexico it was estimated that up to 700 mm of rain fell between the 30th June and 2nd July causing severe floods and some dam overflows (Davydova-Belitskaya & Romero-Cruz, 2011). Very strong winds also caused much damage as maximum wind speeds reached up to 175 km/h (WMO, 2011). Serious destruction was caused as the storm impacted Campeche, Tamaulipas and Nuevo Leon, where thousands of people were affected and millions of pesos were lost in damages (Davydova-Belitskaya & Romero-Cruz, 2011).

Summary

The main features seen in observed climate over Mexico from this analysis are:

- Mexico has seen widespread warming since 1960.
- The frequency of cool days has decreased since 1960 and the frequency of warm nights has increased.
- There has been a general increase in winter temperatures averaged over the country as a result of human influence on climate, making the occurrence of warm winter temperatures more frequent and cold winter temperatures less frequent.
- There has been a decrease in precipitation in the far south-east of the country since 1960.

Methodology annex

Recent, notable extremes

In order to identify what is meant by ‘recent’ events the authors have used the period since 1994, when WMO Status of the Global Climate statements were available to the authors. However, where possible, the most notable events during the last 10 years have been chosen as these are most widely reported in the media, remain closest to the forefront of the memory of the country affected, and provide an example likely to be most relevant to today’s society. By ‘notable’ the authors mean any event which has had significant impact either in terms of cost to the economy, loss of life, or displacement and long term impact on the population. In most cases the events of largest impact on the population have been chosen, however this is not always the case.

Tables of recent, notable extreme events have been provided for each country. These have been compiled using data from the World Meteorological Organisation (WMO) Annual Statements on the Status of the Global Climate. This is a yearly report which includes contributions from all the member countries, and therefore represents a global overview of events that have had importance on a national scale. The report does not claim to capture all events of significance, and consistency across the years of records available is variable. However, this database provides a concise yet broad account of extreme events per country. This data is then supplemented with accounts from the monthly National Oceanic and Atmospheric Administration (NOAA) State of the Climate reports which outline global extreme events of meteorological significance.

We give detailed examples of heat, precipitation and storm extremes for each country where these have had significant impact. Where a country is primarily affected by precipitation or heat extremes this is where our focus has remained. An account of the impact on human life, property and the economy has been given, based largely on media reporting of events, and official reports from aid agencies, governments and meteorological organisations. Some data has also been acquired from the Centre for Research on Epidemiological Disasters (CRED) database on global extreme events. Although media reports are unlikely to be

completely accurate, they do give an indication as to the perceived impact of an extreme event, and so are useful in highlighting the events which remain in the national psyche.

Our search for data has not been exhaustive given the number of countries and events included. Although there are a wide variety of sources available, for many events, an official account is not available. Therefore figures given are illustrative of the magnitude of impact only (references are included for further information on sources). It is also apparent that the reporting of extreme events varies widely by region, and we have, where possible, engaged with local scientists to better understand the impact of such events.

The aim of the narrative for each country is to provide a picture of the social and economic vulnerability to the current climate. Examples given may illustrate the impact that any given extreme event may have and the recovery of a country from such an event. This will be important when considering the current trends in climate extremes, and also when examining projected trends in climate over the next century.

Observational record

In this section we outline the data sources which were incorporated into the analysis, the quality control procedure used, and the choices made in the data presentation. As this report is global in scope, including 23 countries, it is important to maintain consistency of methodological approach across the board. For this reason, although detailed datasets of extreme temperatures, precipitation and storm events exist for various countries, it was not possible to obtain and incorporate such a varied mix of data within the timeframe of this project. Attempts were made to obtain regional daily temperature and precipitation data from known contacts within various countries with which to update existing global extremes databases. No analysis of changes in storminess is included as there is no robust historical analysis of global land surface winds or storminess currently available.

Analysis of seasonal mean temperature

Mean temperatures analysed are obtained from the CRUTEM3 global land-based surface-temperature data-product (Brohan et al. 2006), jointly created by the Met Office Hadley Centre and Climatic Research Unit at the University of East Anglia. CRUTEM3 comprises of more than 4000 weather station records from around the world. These have been averaged together to create 5° by 5° gridded fields with no interpolation over grid boxes that do not

contain stations. Seasonal averages were calculated for each grid box for the 1960 to 2010 period and linear trends fitted using the median of pairwise slopes (Sen 1968; Lanzante 1996). This method finds the slopes for all possible pairs of points in the data, and takes their median. This is a robust estimator of the slope which is not sensitive to outlying points. High confidence is assigned to any trend value for which the 5th to 95th percentiles of the pairwise slopes are of the same sign as the trend value and thus inconsistent with a zero trend.

Analysis of temperature and precipitation extremes using indices

In order to study extremes of climate a number of indices have been created to highlight different aspects of severe weather. The set of indices used are those from the World Climate Research Programme (WCRP) Climate Variability and Predictability (CLIVAR) Expert Team on Climate Change Detection and Indices (ETCCDI). These 27 indices use daily rainfall and maximum and minimum temperature data to find the annual (and for a subset of the indices, monthly) values for, e.g., the 'warm' days where daily maximum temperature exceeds the 90th percentile maximum temperature as defined over a 1961 to 1990 base period. For a full list of the indices we refer to the website of the ETCCDI (http://cccma.seos.uvic.ca/ETCCDI/index.shtml).

Index	Description	Shortname	Notes
Cool night frequency	Daily minimum temperatures lower than the 10th percentile daily minimum temperature using the base reference period 1961-1990	TN10p	---
Warm night frequency	Daily minimum temperatures higher than the 90th percentile daily minimum temperature using the base reference period 1961-1990	TN90p	---
Cool day frequency	Daily maximum temperatures lower than the 10th percentile daily maximum temperature using the base reference period 1961-1990	TX10p	---
Warm day frequency	Daily maximum temperatures higher than the 90th percentile daily maximum temperature using the base reference period 1961-1990	TX90p	---
Dry spell duration	Maximum duration of continuous days within a year with rainfall <1mm	CDD	Lower data coverage due to the requirement for a 'dry spell' to be at least 6 days long resulting in intermittent temporal coverage
Wet spell duration	Maximum duration of continuous days with rainfall >1mm for a given year	CWD	Lower data coverage due to the requirement for a 'wet spell' to be at least 6 days long resulting in intermittent temporal coverage
Total annual precipitation	Total rainfall per year	PRCPTOT	---

Table 4. *Description of ETCCDI indices used in this document.*

A previous global study of the change in these indices, containing data from 1951-2003 can be found in Alexander et al. 2006, (HadEX; see http://www.metoffice.gov.uk/hadobs/hadex/). In this work we aimed to update this analysis to the present day where possible, using the most recently available data. A subset of the indices is used here because they are most easily related to extreme climate events (Table 4).

Use of HadEX for analysis of extremes

The HadEX dataset comprises all 27 ETCCDI indices calculated from station data and then smoothed and gridded onto a 2.5° x 3.75° grid, chosen to match the output from the Hadley Centre suite of climate models. To update the dataset to the present day, indices are calculated from the individual station data using the RClimDex/FClimDex software; developed and maintained on behalf of the ETCCDI by the Climate Research Branch of the

Meteorological Service of Canada. Given the timeframe of this project it was not possible to obtain sufficient station data to create updated HadEX indices to present day for a number of countries: Brazil; Egypt; Indonesia; Japan (precipitation only); South Africa; Saudi Arabia; Peru; Turkey; and Kenya. Indices from the original HadEX data-product are used here to show changes in extremes of temperature and precipitation from 1960 to 2003. In some cases the data end prior to 2003. Table 5 summarises the data used for each country. Below, we give a short summary of the methods used to create the HadEX dataset (for a full description see Alexander et al. 2006).

To account for the uneven spatial coverage when creating the HadEX dataset, the indices for each station were gridded, and a land-sea mask from the HadCM3 model applied. The interpolation method used in the gridding process uses a decorrelation length scale (DLS) to determine which stations can influence the value of a given grid box. This DLS is calculated from the e-folding distance of the individual station correlations. The DLS is calculated separately for five latitude bands, and then linearly interpolated between the bands. There is a noticeable difference in spatial coverage between the indices due to these differences in decorrelation length scales. This means that there will be some grid-box data where in fact there are no stations underlying it. Here we apply black borders to grid-boxes where at least 3 stations are present to denote greater confidence in representation of the wider grid-box area there. The land-sea mask enables the dataset to be used directly for model comparison with output from HadCM3. It does mean, however, that some coastal regions and islands over which one may expect to find a grid-box are in fact empty because they have been treated as sea

Data sources used for updates to the HadEX analysis of extremes

We use a number of different data sources to provide sufficient coverage to update as many countries as possible to present day. These are summarised in Table 5. In building the new datasets we have tried to use exactly the same methodology as was used to create the original HadEX to retain consistency with a product that was created through substantial international effort and widely used, but there are some differences, which are described in the next section.

Wherever new data have been used, the geographical distributions of the trends were compared to those obtained from HadEX, using the same grid size, time span and fitting method. If the pattern of the trends in the temperature or precipitation indices did not match that from HadEX, we used the HadEX data despite its generally shorter time span. Differences in the patterns of the trends in the indices can arise because the individual

stations used to create the gridded results are different from those in HadEX, and the quality control procedures used are also very likely to be different. Countries where we decided to use HadEX data despite the existence of more recent data are Egypt and Turkey.

GHCND:
The Global Historical Climate Network Daily data has near-global coverage. However, to ensure consistency with the HadEX database, the GHCND stations were compared to those stations in HadEX. We selected those stations which are within 1500m of the stations used in the HadEX database and have a high correlation with the HadEX stations. We only took the precipitation data if its r>0.9 and the temperature data if one of its r-values >0.9. In addition, we required at least 5 years of data beyond 2000. These daily data were then converted to the indices using the *fclimdex* software.

ECA&D and SACA&D:
The European Climate Assessment and Dataset and the Southeast Asian Climate Assessment and Dataset data are pre-calculated indices comprising the core 27 indices from the ETCCDI as well as some extra ones. We kindly acknowledge the help of Albert Klein Tank, the KNMI[1] and the BMKG[2] for their assistance in obtaining these data.

Mexico:
The station data from Mexico has been kindly supplied by the SMN[3] and Jorge Vazquez. These daily data were then converted to the required indices using the *Fclimdex* software. There are a total of 5298 Mexican stations in the database. In order to select those which have sufficiently long data records and are likely to be the most reliable ones we performed a cross correlation between all stations. We selected those which had at least 20 years of data post 1960 and have a correlation with at least one other station with an *r*-value >0.95. This resulted in 237 stations being selected for further processing and analysis.

Indian Gridded:
The India Meteorological Department provided daily gridded data (precipitation 1951-2007, temperature 1969-2009) on a 1° x 1° grid. These are the only gridded daily data in our analysis. In order to process these in as similar a way as possible the values for each grid were assumed to be analogous to a station located at the centre of the grid. We keep these

[1] Koninklijk Nederlands Meteorologisch Instituut – The Royal Netherlands Meteorological Institute

[2] Badan Meteorologi, Klimatologi dan Geofisika – The Indonesian Meteorological, Climatological and Geophysical Agency

[3] Servicio Meteorológico Nacional de México – The Mexican National Meteorological Service

data separate from the rest of the study, which is particularly important when calculating the decorrelation length scale, which is on the whole larger for these gridded data.

Country	**Region box** (red dashed boxes in Fig. 1 and on each map at beginning of chapter)	**Data source** (T = temperature, P = precipitation)	**Period of data coverage** (T = temperature, P = precipitation)	**Indices included** (see Table 4 for details)	**Temporal resolution available**	**Notes**
Argentina	73.125 to 54.375 ^{o} W, 21.25 to 56.25 ^{o} S	Matilde Rusticucci (T,P)	1960-2010 (T,P)	TN10p, TN90p, TX10p, TX90p, PRCPTOT, CDD, CWD	annual	
Australia	114.375 to 155.625 ^{o} E, 11.25 to 43.75 ^{o} S	GHCND (T,P)	1960-2010 (T,P)	TN10p, TN90p, TX10p, TX90p, PRCPTOT, CDD, CWD	monthly, seasonal and annual	Land-sea mask has been adapted to include Tasmania and the area around Brisbane
Bangladesh	88.125 to 91.875 ^{o} E, 21.25 to 26.25 ^{o} N	Indian Gridded data (T,P)	1960-2007 (P), 1970-2009 (T)	TN10p, TN90p, TX10p, TX90p, PRCPTOT, CDD, CWD	monthly, seasonal and annual	Interpolated from Indian Gridded data
Brazil	73.125 to 31.875 ^{o} W, 6.25 ^{o} N to 33.75 ^{o} S	HadEX (T,P)	1960-2000 (P) 2002 (T)	TN10p, TN90p, TX10p, TX90p, PRCPTOT, CDD, CWD	annual	Spatial coverage is poor
China	73.125 to 133.125 ^{o} E, 21.25 to 53.75 ^{o} N	GHCND (T,P)	1960-1997 (P) 1960-2003 (T_{min}) 1960-2010 (T_{max})	TN10p, TN90p, TX10p, TX90p, PRCPTOT, CDD, CWD	monthly, seasonal and annual	Precipitation has very poor coverage beyond 1997 except in 2003-04, and no data at all in 2000-02, 2005-11
Egypt	24.375 to 35.625 ^{o} E, 21.25 to 31.25 ^{o} N	HadEX (T,P)	No data	TN10p, TN90p, TX10p, TX90p, PRCPTOT,	annual	There are no data for Egypt so all grid-box values have been interpolated from stations in Jordan, Israel, Libya and Sudan
France	5.625 ^{o} W to 9.375 ^{o} E, 41.25 to 51.25 ^{o} N	ECA&D (T,P)	1960-2010 (T,P)	TN10p, TN90p, TX10p, TX90p, PRCPTOT, CDD, CWD	monthly, seasonal and annual	

Germany	5.625 to 16.875 ^{o} E, 46.25 to 56.25 ^{o} N	ECA&D (T,P)	1960-2010 (T,P)	TN10p, TN90p, TX10p, TX90p, PRCPTOT, CDD, CWD	monthly, seasonal and annual	
India	69.375 to 99.375 ^{o} E, 6.25 to 36.25 ^{o} N	Indian Gridded data (T,P)	1960-2003 (P), 1970-2009 (T)	TN10p, TN90p, TX10p, TX90p, PRCPTOT, CDD, CWD	monthly, seasonal and annual	
Indonesia	95.625 to 140.625 ^{o} E, 6.25 ^{o} N to 11.25 ^{o} S	HadEX (T,P)	1968-2003 (T,P)	TN10p, TN90p, TX10p, TX90p, PRCPTOT,	annual	Spatial coverage is poor
Italy	5.625 to 16.875 ^{o} E, 36.25 to 46.25 ^{o} N	ECA&D (T,P)	1960-2010 (T,P)	TN10p, TN90p, TX10p, TX90p, PRCPTOT, CDD, CWD	monthly, seasonal and annual	Land-sea mask has been adapted to improve coverage of Italy
Japan	129.375 to 144.375 ^{o} E, 31.25 to 46.25 ^{o} N	HadEX (P) GHCND (T)	1960-2003 (P) 1960-2000 (T_{min}) 1960-2010 (T_{max})	TN10p, TN90p, TX10p, TX90p, PRCPTOT,	monthly, seasonal and annual (T), annual (P)	
Kenya	31.875 to 43.125 ^{o} E, 6.25 ^{o} N to 6.25 ^{o} S	HadEX (T,P)	1960-1999 (P)	TN10p, TN90p, TX10p, TX90p, PRCPTOT	annual	There are no temperature data for Kenya and so grid-box values have been interpolated from neighbouring Uganda and the United Republic of Tanzania. Regional averages include grid-boxes from outside Kenya that enable continuation to 2003
Mexico	118.125 to 88.125 ^{o} W, 13.75 to 33.75 ^{o} N	Raw station data from the Servicio Meteorológico Nacional (SMN) (T,P)	1960-2009 (T,P)	TN10p, TN90p, TX10p, TX90p, PRCPTOT, CDD, CWD	monthly, seasonal and annual	237/5298 stations selected. Non uniform spatial coverage. Drop in T and P coverage in 2009.
Peru	84.735 to 65.625 ^{o} W, 1.25 ^{o} N to 18.75 ^{o} S	HadEX (T,P)	1960-2002 (T,P)	TN10p, TN90p, TX10p, TX90p, PRCPTOT, CDD, CWD	annual	Intermittent coverage in TX90p, CDD and CWD

Russia	West Russia 28.125 to 106.875 ° E, 43.75 to 78.75 ° N, East Russia 103.125 to 189.375 ° E, 43.75 to 78.75 ° N	ECA&D (T,P)	1960-2010 (T,P)	TN10p, TN90p, TX10p, TX90p, PRCPTOT, CDD, CWD	monthly, seasonal and annual	Country split for presentation purposes only.
Saudi Arabia	31.875 to 54.375 ° E, 16.25 to 33.75 ° N	HadEX (T,P)	1960-2000 (T,P)	TN10p, TN90p, TX10p, TX90p, PRCPTOT	annual	Spatial coverage is poor
South Africa	13.125 to 35.625 ° W, 21.25 to 36.25 ° S	HadEX (T,P)	1960-2000 (T,P)	TN10p, TN90p, TX10p, TX90p, PRCPTOT, CDD, CWD	annual	---
Republic of Korea	125.625 to 129.375 ° E, 33.75 to 38.75 ° N	HadEX (T,P)	1960-2003 (T,P)	TN10p, TN90p, TX10p, TX90p, PRCPTOT, CDD	annual	There are too few data points for CWD to calculate trends or regional timeseries
Spain	9.375 ° W to 1.875 ° E, 36.25 to 43.75 ° N	ECA&D (T,P)	1960-2010 (T,P)	TN10p, TN90p, TX10p, TX90p, PRCPTOT, CDD, CWD	monthly, seasonal and annual	
Turkey	24.375 to 46.875 ° E, 36.25 to 43.75 ° N	HadEX (T,P)	1960-2003 (T,P)	TN10p, TN90p, TX10p, TX90p, PRCPTOT, CDD, CWD	annual	Intermittent coverage in CWD and CDD with no regional average beyond 2000
United Kingdom	9.375 ° W to 1.875 ° E, 51.25 to 58.75 ° N	ECA&D (T,P)	1960-2010 (T,P)	TN10p, TN90p, TX10p, TX90p, PRCPTOT, CDD, CWD	monthly, seasonal and annual	
United States of America	125.625 to 65.625 ° W, 23.75 to 48.75 ° N	GHCND (T,P)	1960-2010 (T,P)	TN10p, TN90p, TX10p, TX90p, PRCPTOT, CDD, CWD	monthly, seasonal and annual	

Table 5. *Summary of data used for each country.*

Quality control and gridding procedure used for updates to the HadEX analysis of extremes

In order to perform some basic quality control checks on the index data, we used a two-step process on the indices. Firstly, internal checks were carried out, to remove cases where the 5 day rainfall value is less than the 1 day rainfall value, the minimum T_min is greater than the minimum T_max and the maximum T_min is greater than the maximum T_max. Although these are physically impossible, they could arise from transcription errors when creating the daily dataset, for example, a misplaced minus sign, an extra digit appearing in the record or a column transposition during digitisation. During these tests we also require that there are at least 20 years of data in the period of record for the index for that station, and that some data is found in each decade between 1961 and 1990, to allow a reasonable estimation of the climatology over that period.

Weather conditions are often similar over many tens of kilometres and the indices calculated in this work are even more coherent. The correlation coefficient between each station-pair combination in all the data obtained is calculated for each index (and month where appropriate), and plotted as a function of the separation. An exponential decay curve is fitted to the data, and the distance at which this curve has fallen by a factor $1/e$ is taken as the decorrelation length scale (DLS). A DLS is calculated for each dataset separately. For the GHCND, a separate DLS is calculated for each hemisphere. We do not force the fitted decay curve to show perfect correlation at zero distance, which is different to the method employed when creating HadEX. For some of the indices in some countries, no clear decay pattern was observed in some data sets or the decay was so slow that no value for the DLS could be determined. In these cases a default value of 200km was used.

We then perform external checks on the index data by comparing the value for each station with that of its neighbours. As the station values are correlated, it is therefore likely that if one station measures a high value for an index for a given month, its neighbours will also be measuring high. We exploit this coherence to find further bad values or stations as follows. Although raw precipitation data shows a high degree of localisation, using indices which have monthly or annual resolution improves the coherence across wider areas and so this neighbour checking technique is a valid method of finding anomalous stations.

We calculate a climatology for each station (and month if appropriate) using the mean value for each index over the period 1961-1990. The values for each station are then anomalised using this climatology by subtracting this mean value from the true values, so that it is clear if the station values are higher or lower than normal. This means that we do not need to take

differences in elevation or topography into account when comparing neighbours, as we are not comparing actual values, but rather deviations from the mean value.

All stations which are within the DLS distance are investigated and their anomalised values noted. We then calculate the weighted median value from these stations to take into account the decay in the correlation with increasing distance. We use the median to reduce the sensitivity to outliers.

If the station value is greater than 7.5 median-absolute-deviations away from the weighted median value (this corresponds to about 5 standard deviations if the distribution is Gaussian, but is a robust measure of the spread of the distribution), then there is low confidence in the veracity of this value and so it is removed from the data.

To present the data, the individual stations are gridded on a 3.75^{o} x 2.5^{o} grid, matching the output from HadCM3. To determine the value of each grid box, the DLS is used to calculate which stations can reasonably contribute to the value. The value of each station is then weighted using the DLS to obtain a final grid box value. At least three stations need to have valid data and be near enough (within 1 DLS of the gridbox centre) to contribute in order for a value to be calculated for the grid point. As for the original HadEX, the HadCM3 land-sea mask is used. However, in three cases the mask has been adjusted as there are data over Tasmania, eastern Australia and Italy that would not be included otherwise (Figure 6).

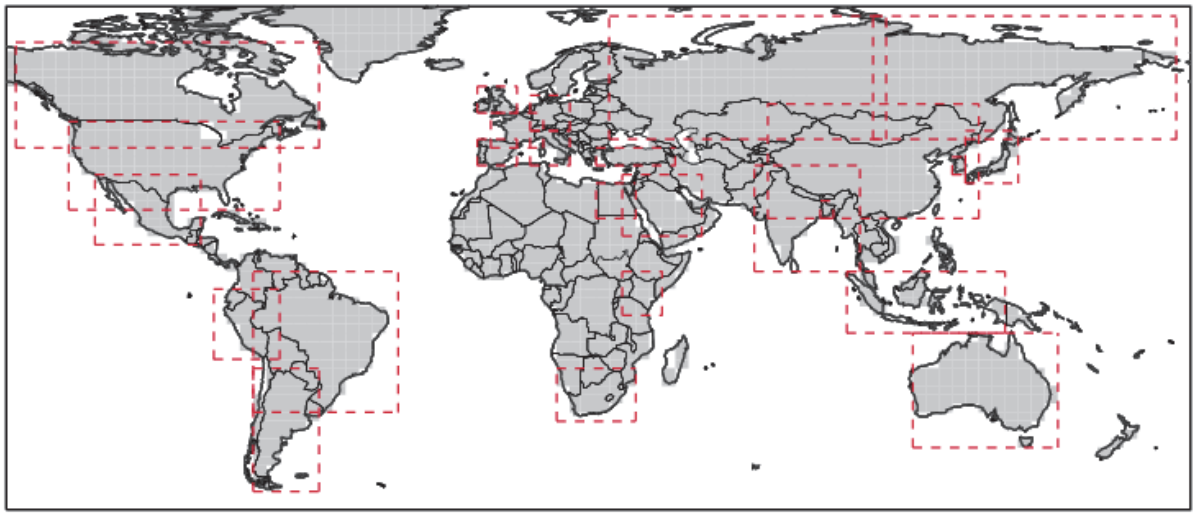

Figure 6. *Land-sea mask used for gridding the station data and regional areas allocated to each country as described in Table 5.*

Presentation of extremes of temperature and precipitation

Indices are displayed as regional gridded maps of decadal trends and regional average time-series with decadal trends where appropriate. Trends are fitted using the median of pairwise slopes method (Sen 1968, Lanzante 1996). Trends are considered to be significantly different from a zero trend if the 5th to 95th percentiles of the pairwise slopes do not encompass zero. This is shown by a black dot in the centre of the grid-box or by a solid line on time-series plots. This infers that there is high confidence in the sign (positive or negative) of the sign. Confidence in the trend magnitude can be inferred by the spread of the 5th to 95th percentiles of the pairwise slopes which is given for the regional average decadal trends. Trends are only calculated when there are data present for at least 50% of years in the period of record and for the updated data (not HadEX) there must be at least one year in each decade.

Due to the practice of data-interpolation during the gridding stage (using the DLS) there are values for some grid boxes when no actually station lies within the grid box. There is more confidence in grid boxes for which there are underlying data. For this reason, we identify those grid boxes which contain at least 3 stations by a black contour line on the maps. The DLS differs with region, season and index which leads to large differences in the spatial coverage. The indices, by their nature of being largely threshold driven, can be intermittent over time which also effects spatial and temporal coverage (see Table 4).

Each index (and each month for the indices for which there is monthly data) has a different DLS, and so the coverage between different indices and datasets can be different. The restrictions on having at least 20 years of data present for each input station, at least 50% of years in the period of record and at least one year in each decade for the trending calculation, combined with the DLS, can restrict the coverage to only those regions with a dense station network reporting reliably.

Each country has a rectangular region assigned as shown by the red dashed box on the map in Figure 1 and listed in Table 2, which is used for the creation of the regional average. This is sometimes identical to the attribution region shown in grey on the map in Figure 1. This region is again shown on the maps accompanying the time series of the regional averages as a reminder of the region and grid boxes used in the calculation. Regional averages are created by weighting grid box values by the cosine of their grid box centre latitude. To ensure consistency over time a regional average is only calculated when there are a sufficient number of grid boxes present. The full-period median number of grid-boxes present is calculated. For regions with a median of more than six grid-boxes there must be at least 80%

of the median number of grid boxes present for any one year to calculate a regional average. For regions with six or fewer median grid boxes this is relaxed to 50%. These limitations ensure that a single station or grid box which has a longer period of record than its neighbours cannot skew the timeseries trend. So sometimes there may be grid-boxes present but no regional average time series. The trends for the regional averages are calculated in the same way as for the individual grid boxes, using the median of pairwise slopes method (Sen 1968, Lanzante 1996). Confidence in the trend is also determined if the 5^{th} to 95^{th} percentiles of the pairwise slopes are of the same sign and thus inconsistent with a zero trend. As well as the trend in quantity per decade, we also show the full change in the quantity from 1960 to 2010 that this fitted linear trend implies.

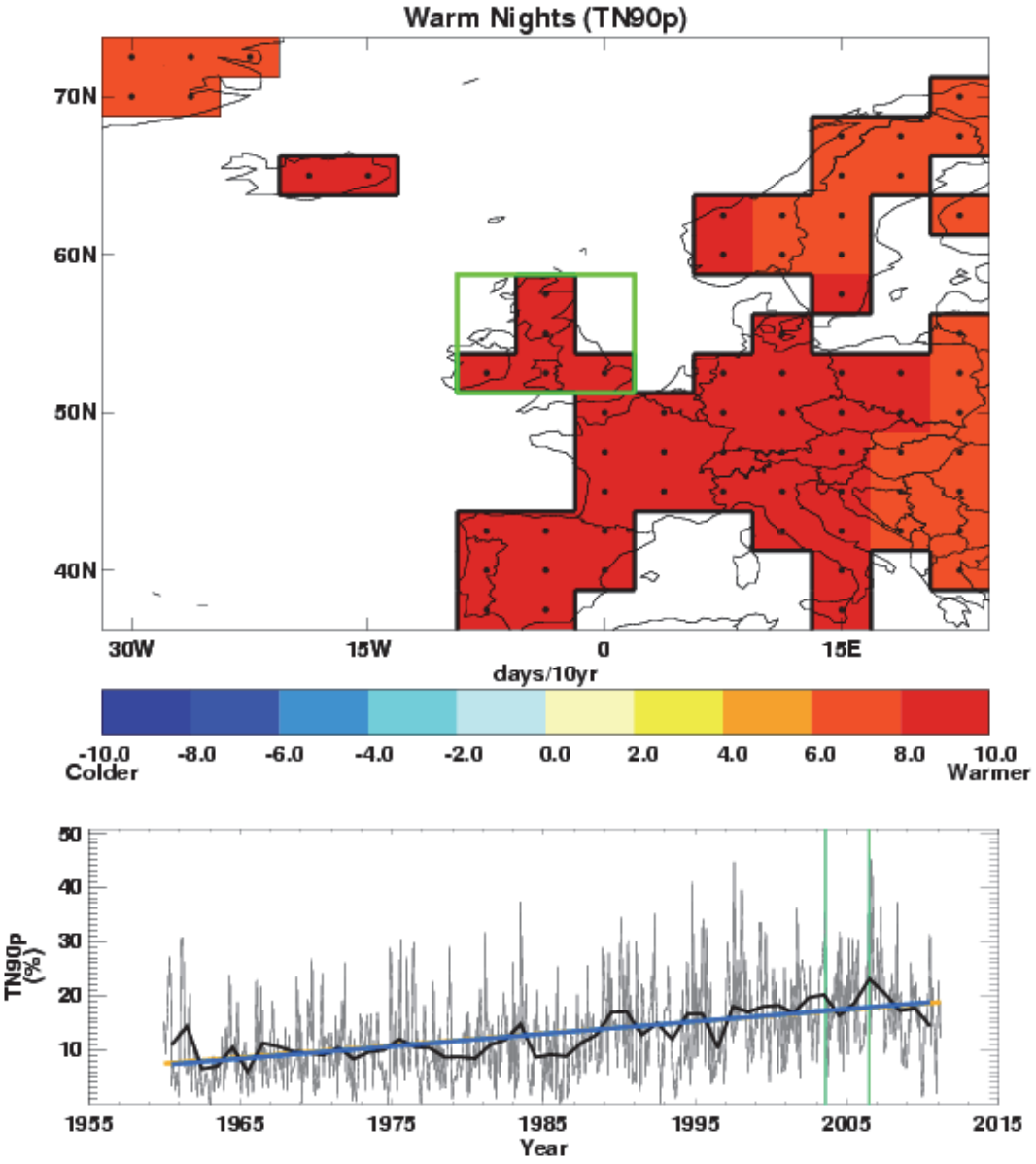

Monthly: 2.20% per decade (1.80 to 2.61)
Total change of 11.02% from 1960 to 2011 (9.00% to 13.06%)

Annual: 2.28% per decade (1.69 to 2.86)
Total change of 11.41% from 1960 to 2010 (8.43% to 14.28%)

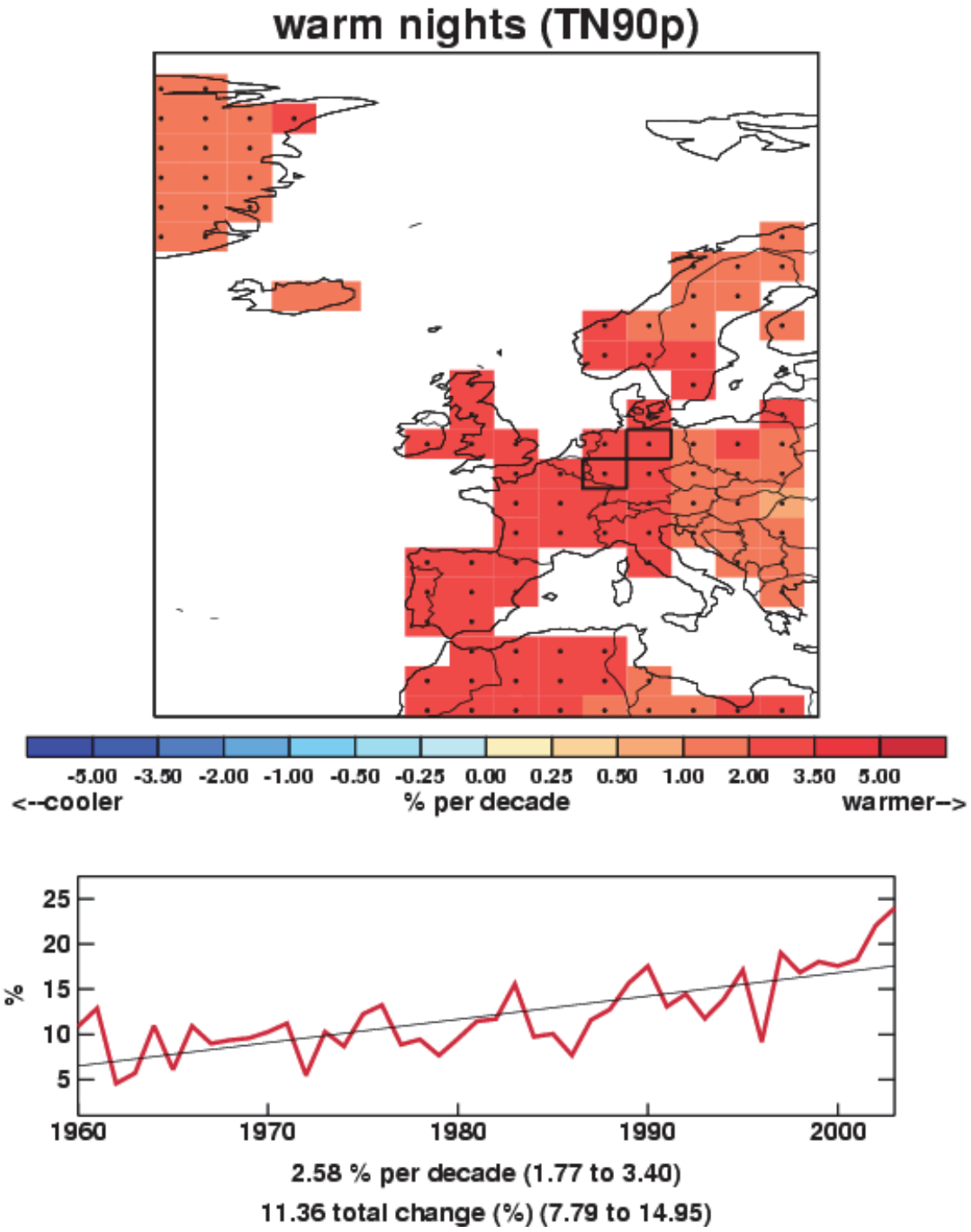

Figure 7. *Examples of the plots shown in the data section. Left: From ECA&D data between 1960-2010 for the number of warm nights, and Right: from HadEX data (1960-2003) for the total precipitation. A full explanation of the plots is given in the text below.*

The results are presented in the form of a map and a time series for each country and index. The map shows the grid box decadal trend in the index over the period for which there are data. High confidence, as determined above, is shown by a black dot in the grid box centre. To show the variation over time, the values for each year (and month if available) are shown in a time series for a regional average. The values of the indices have been normalised to a

base period of 1961-1990 (except the Indian gridded data which use a 1971 to 1990 period), both in HadEX and in the new data acquired for this project. Therefore, for example, the percentage of nights exceeding the 90th percentile for a temperature is 10% for that period.

There are two influences on whether a grid box contains a value or not – the land-sea mask, and the decorrelation length scale. The land-sea mask is shown in Figure 6. There are grid boxes which contain some land but are mostly sea and so are not considered. The decorrelation length scale sets the maximum distance a grid box can be from stations before no value is assigned to it. Grid boxes containing three or more stations are highlighted by a thick border. This indicates regions where the value shown is likely to be more representative of the grid box area mean as opposed to a single station location.

On the maps for the new data there is a box indicating which grid boxes have been extracted to calculate the area average for the time series. This box is the same as shown in Figure 1 at the beginning of each country's document. These selected grid boxes are combined using area (cosine) weighting to calculate the regional average (both annual [thick lines] and monthly [thin lines] where available). Monthly (orange) and annual (blue) trends are fitted to these time series using the method described above. The decadal trend and total change over the period where there are data are shown with 5th to 95th percentile confidence intervals in parentheses. High confidence, as determined above, is shown by a solid line as opposed to a dotted one. The green vertical lines on the time series show the dates of some of the notable events outlined in each section.

Attribution

Regional distributions of seasonal mean temperatures in the 2000s are computed with and without the effect of anthropogenic influences on the climate. The analysis considers temperatures averaged over the regions shown in Figure 8. These are also identified as grey boxes on the maps in Figure 1. The coordinates of the regions are given in Table 6. The methodology combines information from observations and model simulations using the approach originally introduced in Christidis et al., 2010 and later extended in Christidis et al., 2011, where more details can be found. The analysis requires spatial scales greater than about 2,500 km and for that reason the selected regions (Fig.8 and Table 6) are often larger than individual countries, or include several smaller countries in a single region (for example UK, Germany and France are grouped in one region).

Observations of land temperature come from the CRUTEM3 gridded dataset (Brohan et al., 2006) and model simulations from two coupled GCMs, namely the Hadley Centre HadGEM1 model (Martin et al., 2006) and version 3.2 of the MIROC model (K-1 Developers, 2004). The use of two GCMs helps investigate the sensitivity of the results to the model used in the analysis. Ensembles of model simulations from two types of experiments are used to partition the temperature response to external forcings between its anthropogenic and natural components. The first experiment (ALL) simulates the combined effect of natural and anthropogenic forcings on the climate system and the second (ANTHRO) includes anthropogenic forcings only. The difference of the two gives an estimate of the effect of the natural forcings (NAT). Estimates of the effect of internal climate variability are derived from long control simulations of the unforced climate. Distributions of the regional summer mean temperature are computed as follows:

A global optimal fingerprinting analysis (Allen and Tett, 1999; Allen and Stott, 2003) is first carried out that scales the global simulated patterns (fingerprints) of climate change attributed to different combinations of external forcings to best match them to the observations. The uncertainty in the scaling that originates from internal variability leads to samples of the scaled fingerprints, i.e. several realisations that are plausibly consistent with the observations. The 2000-2009 decade is then extracted from the scaled patterns and two samples of the decadal mean temperature averaged over the reference region are then computed with and without human influences, which provide the Probability Density Functions (PDFs) of the decadal mean temperature attributable to ALL and NAT forcings.

Model-derived estimates of noise are added to the distributions to take into account the uncertainty in the simulated fingerprints.

In the same way, additional noise from control model simulations is introduced to the distributions to represent the effect of internal variability in the annual values of the seasonal mean temperatures. The result is a pair of estimated distributions of the annual values of the seasonal mean temperature in the region with and without the effect of human activity on the climate. The temperatures throughout the analysis are expressed as anomalies relative to period 1961-1990.

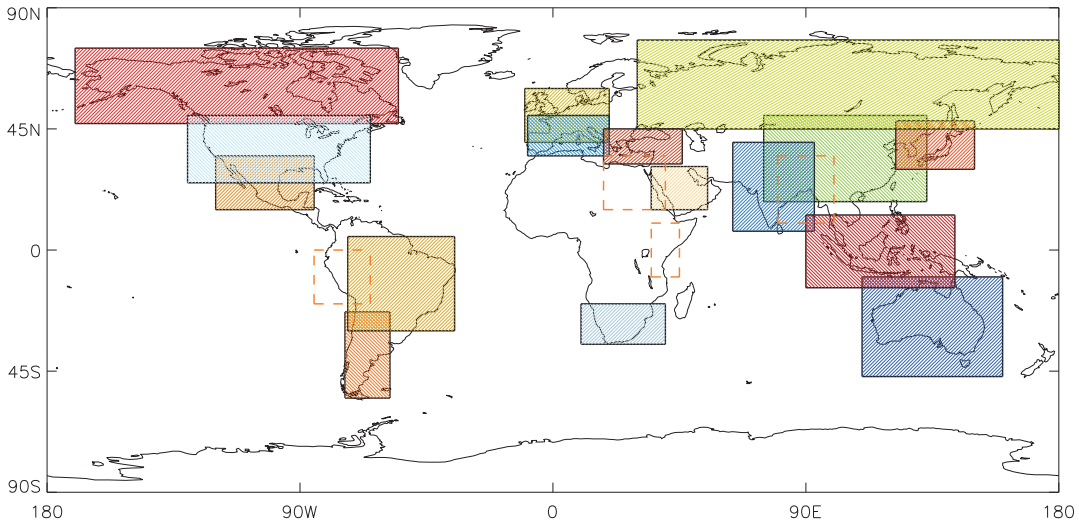

Figure 8. *The regions used in the attribution analysis. Regions marked with dashed orange boundaries correspond to non-G20 countries that were also included in the analysis.*

Region	Region Coordinates
Argentina	74-58W, 55-23S
Australia	110-160E, 47-10S
Bangladesh	80-100E, 10-35N
Brazil	73-35W, 30S-5N
Canada-Alaska	170-55W, 47-75N
China	75-133E, 18-50N
Egypt	18-40E, 15-35N
France-Germany-UK	10W-20E, 40-60N
India	64-93E, 7-40N
Indonesia	90-143E, 14S-13N
Italy-Spain	9W-20E, 35-50N
Japan-Republic of Korea	122-150E, 30-48N
Kenya	35-45E, 10S-10N
Mexico	120-85W, 15-35N
Peru	85-65W, 20-0S
Russia	30-185E, 45-78N
Saudi Arabia	35-55E, 15-31N
South Africa	10-40E, 35-20S
Turkey	18-46E, 32-45N

Table 6. *The coordinates of the regions used in the attribution analysis.*

References

ALEXANDER, L. V., ZHANG. X., PETERSON, T. C., CAESAR, J., GLEASON, B., KLEIN TANK, A. M. G., HAYLOCK, M., COLLINS, D., TREWIN, B., RAHIMZADEH, F., TAGIPOUR, A., RUPA KUMAR, K., REVADEKAR, J., GRIFFITHS, G., VINCENT, L., STEPHENSON, D. B., BURN, J., AGUILAR, E., BRUNET, M., TAYLOR, M., NEW, M., ZHAI, P., RUSTICUCCI, M. and VAZQUEZ-AGUIRRE, J. L. 2006. Global observed changes in daily climate extremes of temperature and precipitation. *J. Geophys. Res.* 111, D05109. doi:10.1029/2005JD006290.

ALLEN, M. R., TETT S. F. B. 1999. Checking for model consistency in optimal fingerprinting. Clim Dyn 15: 419-434

ALLEN M. R., STOTT P. A. 2003. Estimating signal amplitudes in optimal fingerprinting, part I: theory. Clim Dyn 21: 477-491

AMADOR, J. A. 2011. Socioeconomic impacts associated with meteorological systems and tropical cyclones in Central America in 2010 in State of the Climate in 2009. *Bulletin of the American Meteorological Society* 92, S184

BROHAN, P., KENNEDY, J.J., HARRIS, I., TETT, S.F.B. and JONES, P.D. 2006. Uncertainty estimates in regional and global observed temperature changes: a new dataset from 1850. *J. Geophys. Res.* 111, D12106. doi:10.1029/2005JD006548.

CHRISTIDIS N., STOTT. P A., ZWIERS, F. W., SHIOGAMA, H., NOZAWA, T. 2010. Probabilistic estimates of recent changes in temperature: a multi-scale attribution analysis. Clim Dyn 34: 1139-1156

CHRISTIDIS, N., STOTT, P. A., ZWIERS, F. W., SHIOGAMA, H., NOZAWA, T. 2011. The contribution of anthropogenic forcings to regional changes in temperature during the last decade. *Climate Dynamics* in press.

COMPO, G. P., J.S. WHITAKER, P.D. SARDESHMUKH, N. MATSUI, R.J. ALLAN, X. YIN, B.E. GLEASON, R.S. VOSE, G. RUTLEDGE, P. BESSEMOULIN, S. BRÖNNIMANN, M. BRUNET, R.I. CROUTHAMEL, A.N. GRANT, P.Y. GROISMAN, P.D. JONES, M.C. KRUK, A.C. KRUGER, G.J. MARSHALL, M. MAUGERI, H.Y. MOK, Ø. NORDLI, T.F. ROSS, R.M. TRIGO, X.L. WANG, S.D. WOODRUFF and S.J. WORLEY. 2011. The Twentieth Century Reanalysis Project. *Q. J. R.Met.S.* 137, 1-28, doi: 10.1002/qj.776

CORNES, R. C., and P. D. JONES. 2011. An examination of storm activity in the northeast Atlantic region over the 1851–2003 period using the EMULATE gridded MSLP data series. J. Geophys. Res. 116, D16110, doi:10.1029/2011JD016007.

DAVYDOVA-BELITSKAYA, V. and F. ROMERO-CRUZ. 2010. México in State of the Climate in 2009. *Bulletin of the American Meteorological Society* 91, S142-143

DAVYDOVA-BELITSKAYA, V. and F. J. ROMERO-CRUZ. 2011. México in State of the Climate in 2009. *Bulletin of the American Meteorological Society* 92, S181-182

K-1 MODEL DEVELOPERS (2004) K-1 coupled GCM (MIROC) description, K-1 Tech Rep, H Hasumi and S Emori (eds), Centre for Clim Sys Res, Univ of Tokyo.

LANZANTE, J. R. 1996. Resistant, robust and non-parametric techniques for the analysis of climate data: theory and examples, including applications to historical radiosonde station data. *Int. J. Clim*. 16, 1197–226.

LYON, B. & A. M. WAPLE. 2003. Pacific Tropical Storms in State of the Climate in 2009. *Bulletin of the American Meteorological Society* 84, S29

MARTIN G.M., RINGER. M. A., POPE V. D., JONES, A., DEARDEN, C., HINTON, T. 2006. The physical properties of the atmosphere in the new Hadley Centre Global Environmental Model (HadGEM1). Part I: Model description and global climatology. J Clim 19: 1274-1301

NOAA. 2009. State of the Climate Global Hazards Report August 2009. Available online: http://www.ncdc.noaa.gov/sotc/hazards/2009/8 accessed 14 October 2011.

PETERSON, T.C., VAUTARD, R., McVICAR, T.R., THÉPAUT, J-N. and BERRISFORD, P. 2011. Global Climate, Surface Winds over Land in State of the Climate 2010. *Bulletin of the American Meteorological Society* 92 (6), S57.

SANCHEZ-LUGO, A., KENNEDY, J.J. and BERRISFORD, P. 2011. Global Climate, Surface Temperatures in State of the Climate 2010. *Bulletin of the American Meteorological Society* 92 (6), S36-S37.

SEN, P. K. 1968. Estimates of the regression coefficient based on Kendall's tau. *J. Am. Stat. Assoc*. 63, 1379–89.

WMO WORLD METEOROLOGICAL ORGANIZATION. 2001. Statement on Status of the Global Climate in 2000, WMO-No. 920.
http://www.wmo.int/pages/prog/wcp/wcdmp/statement/wmostatement_en.html

WMO WORLD METEOROLOGICAL ORGANIZATION. 2002. Statement on Status of the Global Climate in 2001, WMO-No. 940.
http://www.wmo.int/pages/prog/wcp/wcdmp/statement/wmostatement_en.html

WMO WORLD METEOROLOGICAL ORGANIZATION. 2003. Statement on Status of the Global Climate in 2002, WMO-No. 949.
http://www.wmo.int/pages/prog/wcp/wcdmp/statement/wmostatement_en.html

WMO WORLD METEOROLOGICAL ORGANIZATION. 2004. Statement on Status of the Global Climate in 2003, WMO-No. 966.
http://www.wmo.int/pages/prog/wcp/wcdmp/statement/wmostatement_en.html

WMO WORLD METEOROLOGICAL ORGANIZATION. 2005. Statement on Status of the Global Climate in 2004, WMO-No. 983.
http://www.wmo.int/pages/prog/wcp/wcdmp/statement/wmostatement_en.html

WMO WORLD METEOROLOGICAL ORGANIZATION. 2006. Statement on Status of the Global Climate in 2005, WMO-No. 998.
http://www.wmo.int/pages/prog/wcp/wcdmp/statement/wmostatement_en.html

WMO WORLD METEOROLOGICAL ORGANIZATION. 2007. Statement on Status of the Global Climate in 2006, WMO-No. 1016.
http://www.wmo.int/pages/prog/wcp/wcdmp/statement/wmostatement_en.html

WMO WORLD METEOROLOGICAL ORGANIZATION. 2008. Statement on Status of the Global Climate in 2007, WMO-No. 1031.
http://www.wmo.int/pages/prog/wcp/wcdmp/statement/wmostatement_en.html

WMO WORLD METEOROLOGICAL ORGANIZATION. 2009. Statement on Status of the Global Climate in 2008, WMO-No. 1039.
http://www.wmo.int/pages/prog/wcp/wcdmp/statement/wmostatement_en.html

WMO WORLD METEOROLOGICAL ORGANIZATION. 2010. Statement on Status of the Global Climate in 2009, WMO-No. 1055.
http://www.wmo.int/pages/prog/wcp/wcdmp/statement/wmostatement_en.html

WMO WORLD METEOROLOGICAL ORGANIZATION. 2011. Statement on Status of the Global Climate in 2010, WMO-No. 1074.
http://www.wmo.int/pages/prog/wcp/wcdmp/statement/wmostatement_en.html

Acknowledgements

Data for this work were kindly provided by Jorge Vazquez and the staff of the Servicio Meteorológico Nacional (SMN) of Comisión Nacional del Agua (CNA). We thank Lisa Alexander and Markus Donat (University of New South Wales) for their help and advice.

Chapter 2 – Climate Change Projections

Introduction

Climate models are used to understand how the climate will evolve over time and typically represent the atmosphere, ocean, land surface, cryosphere, and biogeochemical processes, and solve the equations governing their evolution on a geographical grid covering the globe. Some processes are represented explicitly within climate models, large-scale circulations for instance, while others are represented by simplified parameterisations. The use of these parameterisations is sometimes due to processes taking place on scales smaller than the typical grid size of a climate model (a Global Climate Model (GCM) has a typical horizontal resolution of between 250 and 600km) or sometimes to the current limited understanding of these processes. Different climate modelling institutions use different plausible representations of the climate system, which is why climate projections for a single greenhouse gas emissions scenario differ between modelling institutes. This gives rise to "climate model structural uncertainty".

In response to a proposed activity of the World Climate Research Programme's (WCRP's; http://www.wcrp-climate.org/) Working Group on Coupled Modelling (WGCM), the Program for Climate Model Diagnosis and Intercomparison (PCMDI; http://www-pcmdi.llnl.gov/) volunteered to collect model output contributed by leading climate modelling centres around the world. Climate model output from simulations of the past, present and future climate was collected by PCMDI mostly during the years 2005 and 2006, and this archived data constitutes phase 3 of the Coupled Model Intercomparison Project (CMIP3). In part, the WGCM organised this activity to enable those outside the major modelling centres to perform research of relevance to climate scientists preparing the IPCC Fourth Assessment Report (AR4). This unprecedented collection of recent model output is commonly known as the "CMIP3 multi-model dataset". The GCMs included in this dataset are referred to regularly throughout this review, although not exclusively.

The CMIP3 multi-model ensemble has been widely used in studies of regional climate change and associated impacts. Each of the constituent models was subject to extensive testing by the contributing institute, and the ensemble has the advantage of having been constructed from a large pool of alternative model components, therefore sampling alternative structural assumptions in how best to represent the physical climate system. Being assembled on an opportunity basis, however, the CMIP3 ensemble was not designed to represent model uncertainties in a systematic manner, so it does not, in isolation, support robust estimates of the risk of different levels of future climate change, especially at a regional level.

Since CMIP3, a new (CMIP5) generation of coupled ocean-atmosphere models has been developed, which is only just beginning to be available and is being used for new projections for the IPCC Fifth Assessment Report (AR5).

These newer models typically feature higher spatial resolution than their CMIP3 counterparts, including in some models a more realistic representation of stratosphere-troposphere interactions. The CMIP5 models also benefit from several years of development in their parameterisations of small scale processes, which, together with resolution increases, are expected to result in a general improvement in the accuracy of their simulations of historical climate, and in the credibility of their projections of future changes. The CMIP5 programme also includes a number of comprehensive Earth System Models (ESMs) which explicitly simulate the earth's carbon cycle and key aspects of atmospheric chemistry, and also contain more sophisticated representations of aerosols compared to CMIP3 models.

The CMIP3 results should be interpreted as a useful interim set of plausible outcomes. However, their neglect of uncertainties, for instance in carbon cycle feedbacks, implies that higher levels of warming outside the CMIP3 envelope cannot be ruled out. In future, CMIP5 coupled model and ESM projections can be expected to produce improved advice on future regional changes. In particular, ensembles of ESM projections will be needed to provide a more comprehensive survey of possible future changes and their relative likelihoods of occurrence. This is likely to require analysis of the CMIP5 multi-model ESM projections, augmented by larger ensembles of ESM simulations in which uncertainties in physical and biogeochemical feedback processes can be explored more systematically, for example via ensembles of model runs in which key aspects of the climate model are slightly adjusted. Note that such an exercise might lead to the specification of wider rather than narrower uncertainties compared to CMIP3 results, if the effects of representing a wider range of earth system processes outweigh the effects of refinements in the simulation of physical atmosphere-ocean processes already included in the CMIP3 models.

Climate projections

The Met Office Hadley Centre is currently producing perturbed parameter ensembles of a single model configuration known as HadCM3C, to explore uncertainties in physical and biogeochemical feedback processes. The results of this analysis will become available in the next year and will supplement the CMIP5 multi-model ESM projections, providing a more comprehensive set of data to help progress understanding of future climate change. However, many of the studies covered in the chapter on climate impacts have used CMIP3 model output. For this reason, and because it is still the most widely used set of projections available, the CMIP3 ensemble output for temperature and precipitation, for the A1B emission scenario, for Mexico and the surrounding region is shown below.

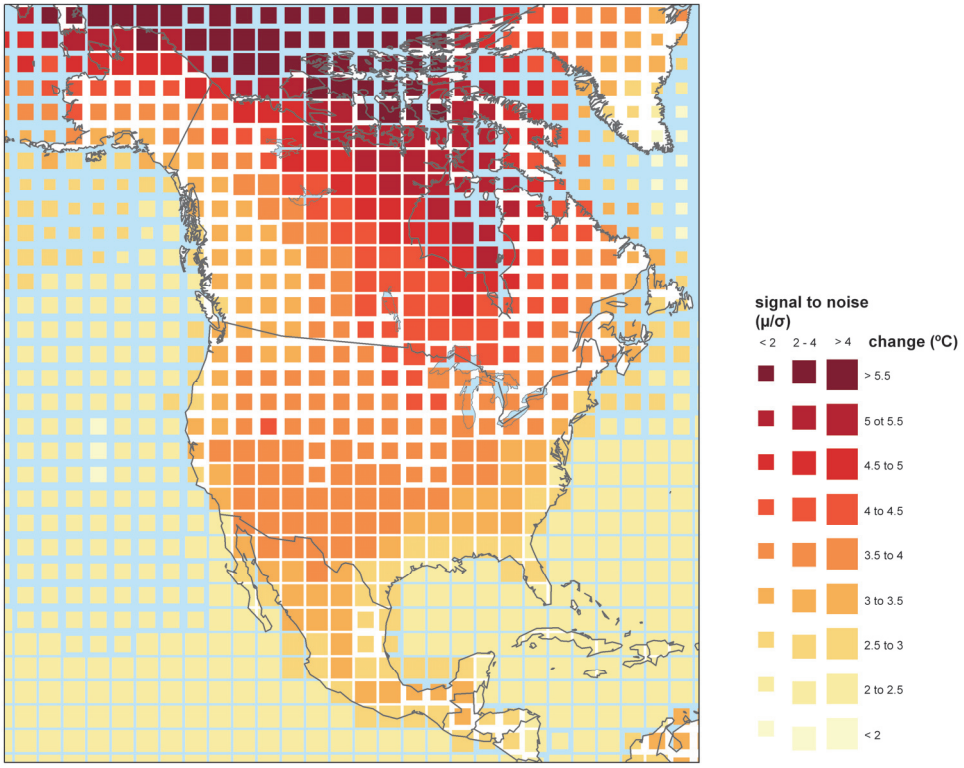

Figure 1. *Percentage change in average annual temperature by 2100 from 1960-1990 baseline climate, averaged over 21 CMIP3 models. The size of each pixel represents the level of agreement between models on the magnitude of the change.*

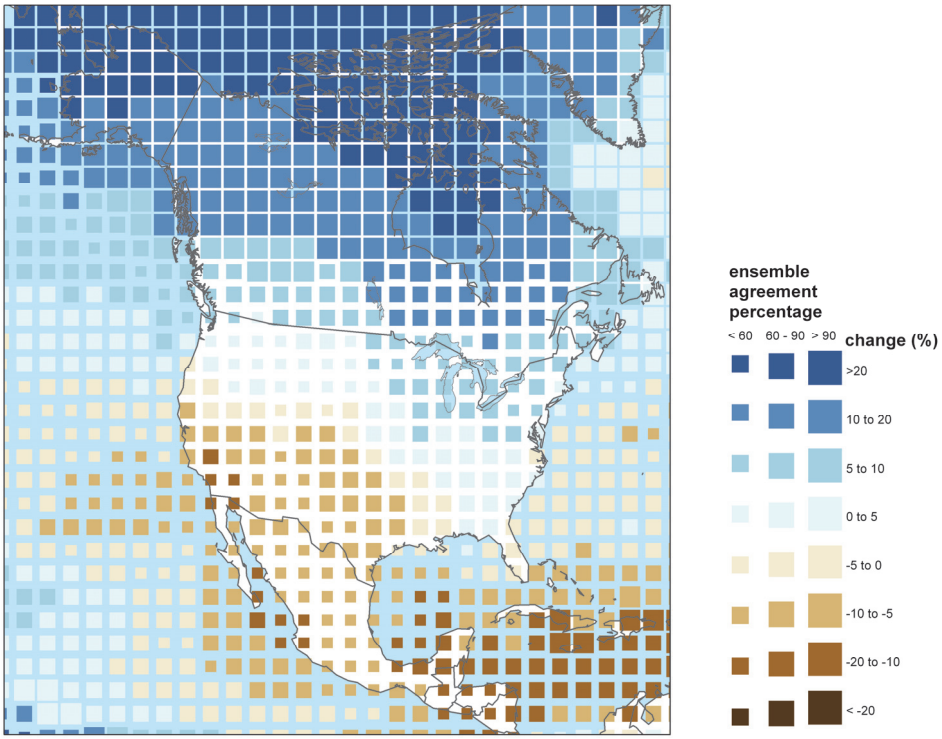

Figure 2. *Percentage change in average annual precipitation by 2100 from 1960-1990 baseline climate, averaged over 21 CMIP3 models. The size of each pixel represents the level of agreement between models on the sign of the change.*

Summary of temperature change in Mexico

Figure 1 shows the percentage change in average annual temperature by 2100 from 1960-1990 baseline climate, averaged over 21 CMIP3 models. All of the models in the CMIP3 ensemble project increased temperatures in the future, but the size of each pixel indicates how well the models agree over the magnitude of the increase.

Projected temperature increases over Mexico are up to around 4°C close to the US border, with the rest of the country showing increases of around 2.5- 3.5°C. Agreement between models is generally high.

Summary of precipitation change in Mexico

Figure 2 shows the percentage change in average annual precipitation by 2100 from 1960-1990 baseline climate, averaged over 21 CMIP3 models. Unlike for temperature, the models sometimes disagree over whether precipitation is increasing or decreasing over a region, so

in this case the size of each pixel indicates the percentage of the models in the ensemble that agree on the sign of the change in precipitation.

Mexico is located in a region of projected decreased precipitation with typical decreases of around 5 to 10%. However, ensemble agreement is generally quite low.

Chapter 3 - Climate Change Impact Projections

Introduction

Aims and approach

This chapter looks at research on a range of projected climate change impacts, with focus on results for the Mexico. It includes projections taken from the AVOID programme, for some of the impact sectors.

The aim of this work is to take a 'top down' approach to assessing global impacts studies, both from the literature and from new research undertaken by the AVOID programme. This project covers 23 countries, with summaries from global studies provided for each of these. This global approach allows some level of comparison between countries, whilst presenting information on a scale most meaningful to inform international policy.

The literature covered in this chapter focuses on research published since the Fourth Assessment Report (AR4) of the Intergovernmental Panel on Climate Change (IPCC) and should be read in conjunction with IPCC AR4 WG1 and WG2 reports. For some sectors considered, an absence of research developments since the IPCC AR4, means earlier work is cited as this helps describe the current level of scientific understanding. This report focuses on assessing scientific research about climate change impacts within sectors; it does not present an integrated analysis of climate change adaptation policies.

Some national and sub-national scale literature is reported to a limited extent to provide some regional context.

Impact sectors considered and methods

This report reviews the evidence for the impact of climate change on a number of sectors, for Mexico. The following sectors are considered in turn in this report:

- Crop yields
- Food security
- Water stress and drought
- Pluvial flooding and rainfall
- Fluvial flooding

- Tropical cyclones (where applicable)
- Coastal regions

Supporting literature

Literature searches were conducted for each sector with the Thomson Reuters Web of Science (WoS., 2011) and Google Scholar academic search engines respectively. Furthermore, climate change impact experts from each of the 23 countries reviewed were contacted. These experts were selected through a combination of government nomination and from experts known to the Met Office. They were asked to provide literature that they felt would be of relevance to this review. Where appropriate, such evidence has been included. A wide range of evidence was considered, including; research from international peer-reviewed journal papers; reports from governments, non-governmental organisations, and private businesses (e.g. reinsurance companies), and research papers published in national journals.

For each impact sector, results from assessments that include a global- or regional-scale perspective are considered separately from research that has been conducted at the national- or sub-national-scale. The consideration of global- and regional-scale studies facilitates a comparison of impacts across different countries, because such studies apply a consistent methodology for each country. While results from national- and sub-national-scale studies are not easily comparable between countries, they can provide a level of detail that is not always possible with larger-scale studies. However, the national- and sub-national scale literature included in this project does not represent a comprehensive coverage of regional-based research and cannot, and should not, replace individual, detailed impacts studies in countries. The review aims to present an up-to-date assessment of the impact of climate change on each of the sectors considered.

AVOID programme results

Much of the work in this report is drawn from modelling results and analyses coming out of the AVOID programme. The AVOID programme is a research consortium funded by DECC and Defra and led by the UK Met Office and also comprises the Walker Institute at the University of Reading, the Tyndall Centre represented through the University of East Anglia,

and the Grantham Institute for Climate Change at Imperial College. The expertise in the AVOID programme includes climate change research and modelling, climate change impacts in natural and human systems, socio-economic sciences, mitigation and technology. The unique expertise of the programme is in bringing these research areas together to produce integrated and policy-relevant results. The experts who work within the programme were also well suited to review the literature assessment part of this report. In this report the modelling of sea level rise impacts was carried out for the AVOID programme by the University of Southampton.

The AVOID programme uses the same emissions scenarios across the different impact sectors studied. These are a business as usual (IPCC SRES A1B) and an aggressive mitigation (the AVOID A1B-2016-5-L) scenario. Model output for both scenarios was taken from more than 20 GCMs and averaged for use in the impact models. The impact models are sector specific, and frequently employ further analytical techniques such as pattern scaling and downscaling in the crop yield models.

Data and analysis from AVOID programme research is provided for the following impact sectors:

- Crop yields
- Water stress and drought
- Fluvial flooding
- Coastal regions

Uncertainty in climate change impact assessment

There are many uncertainties in future projections of climate change and its impacts. Several of these are well-recognised, but some are not. One category of uncertainty arises because we don't yet know how mankind will alter the climate in the future. For instance, uncertainties in future greenhouse gas emissions depends on the future socio-economic pathway, which, in turn, depends on factors such as population, economic growth, technology development, energy demand and methods of supply, and land use. The usual approach to dealing with this is to consider a range of possible future scenarios.

Another category of uncertainties relate to our incomplete understanding of the climate system, or an inability to adequately model some aspects of the system. This includes:

- Uncertainties in translating emissions of greenhouse gases into atmospheric concentrations and radiative forcing. Atmospheric CO_2 concentrations are currently rising at approximately 50% of the rate of anthropogenic emissions, with the remaining 50% being offset by a net uptake of CO_2 into the oceans and land biosphere. However, this rate of uptake itself probably depends on climate, and evidence suggests it may weaken under a warming climate, causing the CO_2 rise to be larger proportion of emissions. The extent of this feedback is highly uncertain, but it not considered in most studies. The 3rd Coupled Model Intercomparison Project (CMIP3), which provided the future climate projections for the IPCC 4th Assessment Report, used a single estimate of CO_2 concentration rise for each emissions scenario, so the CMIP3 projections (which were used in most studies presented here, including AVOID) do not account for this uncertainty.

- Uncertainty in climate response to the forcing by greenhouse gases and aerosols. One aspect of this is the response of global mean temperature ("climate sensitivity"), but a more relevant aspect for impacts studies is the response of regional climates, including temperature, precipitation and other meteorological variables. Different climate models can give very different results in some regions, while giving similar results in other regions. Confidence in regional projections requires more than just agreement between models: physical understanding of the relevant atmospheric, ocean and land surface processes is also important, to establish whether the models are likely to be realistic.

- Additional forcings of regional climate. Greenhouse gas changes are not the only anthropogenic driver of climate change; atmospheric aerosols and land cover change are also important, and unlike greenhouse gases, the strength of their influence varies significantly from place to place. The CMIP3 models used in most impacts studies generally account for aerosols but not land cover change.

- Uncertainty in impacts processes. The consequences of a given changes in weather or climatic conditions for biophysical impacts such as river flows, drought, flooding, crop yield or ecosystem distribution and functioning depend on many other processes which are often poorly-understood, especially at large scales. In particular, the extent to which different biophysical impacts interact with each other has been hardly studied, but may be crucial; for example, impacts of climate change on crop yield may depend not only on local climate changes affecting rain-fed crops, but also remote climate changes affecting river flows providing water for irrigation.

- Uncertainties in non-climate effects of some greenhouse gases. As well as being a greenhouse gas, CO_2 exerts physiological influences on plants, affecting photosynthesis and transpiration. Under higher CO_2 concentrations, and with no other limiting factors, photosynthesis can increase ,while the requirements of water for transpiration can decrease. However, while this has been extensively studied under experimental conditions, including in some cases in the free atmosphere, the extent to which the ongoing rise in ambient CO_2 affects crop yields and natural vegetation functioning remains uncertain and controversial. Many impacts projections assume CO_2 physiological effects to be significant, while others assume it to be non-existent. Studies of climate change impacts on crops and ecosystems should therefore be examined with care to establish which assumptions have been made.

In addition to these uncertainties, the climate varies significantly through natural processes from year-to-year and also decade-to-decade, and this variability can be significant in comparison to anthropogenic forcings on shorter timescales (the next few decades) particularly at regional scales. Whilst we can characterise the natural variability it will not be possible to give a precise forecast for a particular year decades into the future.

A further category of uncertainty in projections arises as a result of using different methods to correct for uncertainties and limitations in climate models. Despite being painstakingly developed in order to represent current climate as closely as possible, current climate models are nevertheless subject to systematic errors such as simulating too little or too much rainfall in some regions. In order to reduce the impact of these, '*bias correction*' techniques are often employed, in which the climate model as a source of information on the *change* in climate which is then applied to the observed present-day climate state (rather than using the model's own simulation of the present-day state). However, these bias-corrections typically introduce their own uncertainties and errors, and can lead to inconsistencies between the projected impacts and the driving climate change (such as river flows changing by an amount which is not matched by the original change in precipitation). Currently, this source of uncertainty is rarely considered

When climate change projections from climate models are applied to climate change impact models (e.g. a global hydrological model), the climate model structural uncertainty carries through to the impact estimates. Additional uncertainties include changes in future emissions and population, as well as parameterisations within the impact models (this is rarely considered). Figure 1 highlights the importance of considering climate model structural uncertainty in climate change impacts assessment. Figure 1 shows that for 2°C prescribed

global-mean warming, the magnitude of, and sign of change in average annual runoff from present, simulated by an impacts model, can differ depending upon the GCM that provides the climate change projections that drive the impact model. This example also shows that the choice of impact model, in this case a global hydrological model (GHM) or catchment-scale hydrological model (CHM), can affect the magnitude of impact and sign of change from present (e.g. see IPSL CM4 and MPI ECHAM5 simulations for the Xiangxi). To this end, throughout this review, the number of climate models applied in each study reviewed, and the other sources of uncertainty (e.g. emissions scenarios) are noted. Very few studies consider the application of multiple impacts models and it is recommended that future studies address this.

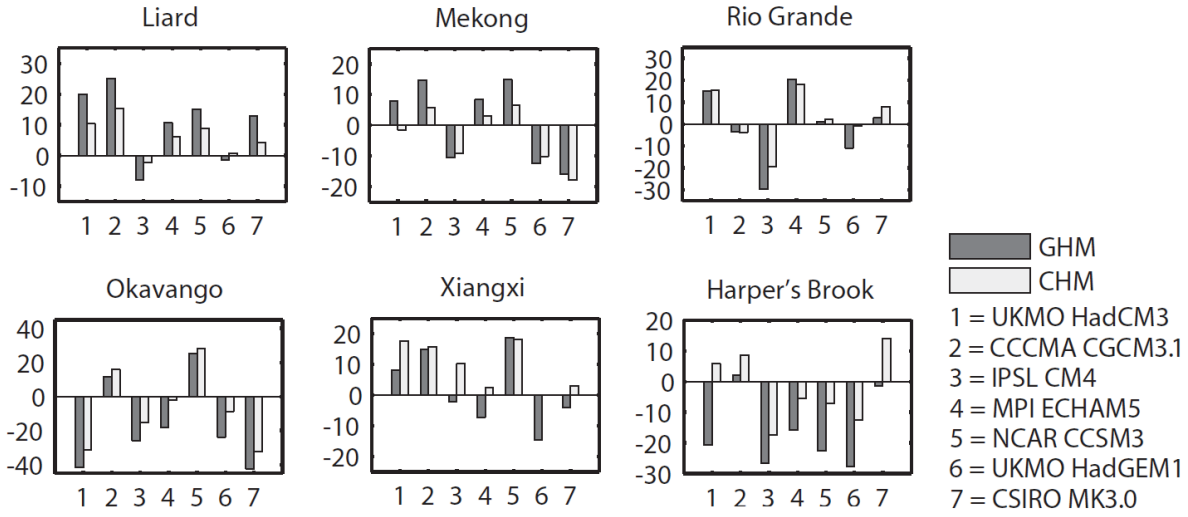

***Figure 1**. Change in average annual runoff relative to present (vertical axis; %), when a global hydrological model (GHM) and a catchment-scale hydrological model (CHM) are driven with climate change projections from 7 GCMs (horizontal axis), under a 2°C prescribed global-mean warming scenario, for six river catchments. The figure is from Gosling et al. (2011).*

Uncertainties in the large scale climate relevant to Mexico include changes in the El Niño-Southern Oscillation (ENSO) which could undergo rapid change with climate change. This could have a serious impact on large-scale atmospheric circulation, rainfall and seasonality in many parts of the world. Latif and Keenlyside (2009) concluded that, at this stage of understanding, it is not known how climate change might affect the tropical Pacific climate system. None of the global climate models (GCMs) they analysed showed rapid changes in behaviour. However, a threshold of abrupt change cannot be ruled out because whilst the GCMs that Latif and Keenlyside (2009) analysed (the CMIP3 multi-model dataset) are better than the previous generation of models (Reichler and Kim, 2008), these same models all show large biases in simulating the contemporary tropical Pacific, with no consensus on the sign of change in ENSO-like response.

Country summary

Crop yields

- Quantitative crop yield projections for Mexico under climate change scenarios vary across studies due to the application of different models, assumptions and emissions scenarios.

- Results from the AVOID programme for Mexico show that under both emissions scenarios, no models project an increase in suitability for cultivation for current Mexican croplands. For both scenarios, between 40% and 70% of current Mexican croplands are projected to undergo declining suitability by 2030. By 2100 this rises to 50%-80% under the mitigation scenario and 60%-100% under A1B.

- Important knowledge gaps and key uncertainties include the quantification of yield increases due to CO_2 fertilisation, quantification of yield declines due to ozone damage and the extent to which crop diseases may affect crop yields with climate change.

Food security

- Mexico is currently a country of extremely low undernourishment. Global- and regional-scale studies suggest a mixed outlook for food security issues under climate change, although the majority of these studies suggest that the country is not likely to face severe food security issues in the next 40 years.

- However, research by the AVOID programme indicates that adaptation measures, such as reducing food for exports, may be required to avoid major food security issues in Mexico with climate change.

- One study concluded that the national economy of Mexico presents a moderate vulnerability to climate change impacts on fisheries by the 2050s. Another suggests that the 10-year averaged maximum fish catch potential from 2005 to 2055 could decrease by 4% under SRES A1B. This is a small decline relative to some other countries across the globe.

Water stress and drought

- Global-scale studies included here concur that Mexico is currently highly vulnerable to water security threats.
- There is large uncertainty in how climate change could affect water stress in Mexico, which partly arises from climate modelling uncertainty. However, the majority of global-scale studies included here project that that the population exposed to water stress could increase substantially with climate change.
- Recent simulations by the AVOID programme support this.

Pluvial flooding and rainfall

- The IPCC AR4 reported a general decrease in mean precipitation with climate change for Mexico. Recent studies confirm this and add further detail.
- However, studies of extreme precipitation suggest the possibility of increases, but with a large uncertainty attached to future projections of tropical cyclone occurrence.

Fluvial flooding

- Few studies have investigated changes in flood hazard in Mexico under climate change scenarios. However, at least one global-scale assessments suggests that flood frequency and magnitude may decrease with climate change.
- Simulations by the AVOID programme showed a greater tendency among models towards decreasing flood risk early in the 21st century. Later in the century the balance shifted towards an increase in flood risk under the A1B scenario, while under a mitigation scenario the majority of the models still showed a decrease.
- A regional analysis of changes in precipitation intensity, together with a better understanding of how climate change may affect the frequency and intensity of land-falling hurricanes is required to further improve understanding of flood risk in Mexico.

Tropical cyclones

- There remains large uncertainty in the current understanding of how tropical cyclones might be affected by climate change, including in the Gulf of Mexico and the East Pacific as conclusions are based upon a limited number of studies whose projections are from either coarse-resolution global models or from statistical or dynamical downscaling techniques. To this end, caution should be applied in interpreting model-based results, even where the models are in agreement.
- The majority of studies reviewed here suggest that tropical cyclone intensities could increase in both the Gulf of Mexico and East Pacific basins with climate change.

Coastal regions

- Two global-scale studies suggest that Mexico's population is not highly vulnerable to sea level rise (SLR), relative to other countries across the globe.
- One of these studies suggests that SLR could have little or no affect on Mexico's population.
- However, another study found that out of 84 developing countries considered, Mexico was ranked the 7th highest with respect to the amount of agricultural land that could be submerged with a simulated 1m SLR.

Crop yields

Headline

The majority of studies that assess the impact of climate change on crop yields in Mexico focus on maize, as one of Mexico's most important crops. However, maize yield projections vary greatly across studies, due to the application of different models, assumptions, emissions scenarios.

Results from the AVOID programme for Mexico show that under both emissions scenarios, no models project an increase in suitability for cultivation for current Mexican croplands. For both scenarios, between 40% and 70% of current Mexican croplands are projected to undergo declining suitability by 2030. By 2100 this rises to 50%-80% under the mitigation scenario and 60%-100% under A1B.

Supporting literature

Introduction

The impacts of climate change on crop productivity are highly uncertain due to the complexity of the processes involved. Most current studies are limited in their ability to capture the uncertainty in regional climate projections, and often omit potentially important aspects such as extreme events and changes in pests and diseases. Importantly, there is a lack of clarity on how climate change impacts on drought are best quantified from an agricultural perspective, with different metrics giving very different impressions of future risk. The dependence of some regional agriculture on remote rainfall, snowmelt and glaciers adds to the complexity - these factors are rarely taken into account, and most studies focus solely on the impacts of local climate change on rain-fed agriculture. However, irrigated agricultural land produces approximately 40-45 % of the world's food (Doll and Siebert 2002), and the water for irrigation is often extracted from rivers which can depend on climatic conditions far from the point of extraction. Hence, impacts of climate change on crop productivity often need to take account of remote as well as local climate changes. Indirect impacts via sea-level rise, storms and diseases have also not been quantified. Perhaps most seriously, there is high uncertainty in the extent to which the direct effects of CO_2 rise on plant physiology will

interact with climate change in affecting productivity. Therefore, at present, the aggregate impacts of climate change on large-scale agricultural productivity cannot be reliably quantified (Gornall et al, 2010). This section summarises findings from a range of post IPCC AR4 assessments to inform and contextualise the analysis performed by AVOID programme for this project. The results from the AVOID work are discussed in the next section.

Maize is the main food crop in Mexico and other important food crops include sorghum, beans and wheat (see Table 1) (FAO, 2008). In monetary terms, sugar cane takes a second place after maize.

Harvested area (ha)		Quantity (Metric ton)		Value ($1000)	
Maize	7350000	Sugar cane	51100000	Maize	1290000
Sorghum	1830000	Maize	24300000	Sugar cane	1060000
Beans, dry	1500000	Oranges	4300000	Oranges	756000
Wheat	801000	Wheat	4010000	Avocados	722000
Coffee, green	755000	Tomatoes	2930000	Chillies and peppers, green	709000
Sugar cane	669000	Lemons and limes	2220000	Tomatoes	695000
Oranges	331000	Bananas	2150000	Wheat	601000

Table 1. *The top 7 crops by harvested area, quantity and value according to the FAO (2008) in Mexico. Crops that feature in all lists are shaded green; crops that feature in two top 7 lists are shaded amber. Data is from FAO (2008) and has been rounded down to three significant figures.*

A number of impact model studies looking at crop yield which include results for some of the main crops in Mexico have been conducted. They apply a variety of methodological approaches, including using different climate model inputs and treatment of other factors that might affect yield, such as impact of increased CO_2 in the atmosphere on plant growth and adaption of agricultural practises to changing climate conditions. These different models, assumptions and emissions scenarios mean that there are a range of crop yield projections for Mexico.

Important knowledge gaps and key uncertainties, which are applicable to Mexico as well as at the global-scale, include: the way crops might respond to changes in the frequency and magnitude of ENSO events with climate change (projections of ENSO are highly uncertain), the quantification of yield increases due to CO_2 fertilisation and yield reductions due to ozone damage (Ainsworth and McGrath, 2010, Iglesias et al., 2009, Avnery et al., 2011), and the extent crop diseases could affect crop yields with climate change (Luck et al., 2011).

Most crop simulation models do not include the direct effect of extreme temperatures on crop development and growth, thus only changes in mean climate conditions are considered to affect crop yields for the studies included here.

Assessments that include a global or regional perspective

Recent past

Crop yield changes could be due to a variety of factors, which might include, but not be confined to, a changing climate. In order to assess the impact of recent climate change (1980-2008) on wheat, maize, rice and soybean, Lobell et al. (2011) looked at how the overall yield trend in these crops changed in response to changes in climate over the period studied. The study was conducted at the global-scale but national estimates for Mexico were also calculated. Lobell et all. (2011) divided the climate-induced yield trend by the overall yield trend for 1980–2008, to produce a simple metric of the importance of climate relative to all other factors. The ratio produced indicates the influence of climate on the productivity trend. So for example a value of –0.1 represents a 10% reduction in yield gain due to climate change, compared to the increase that could have been achieved without climate change, but with technology and other gains. This can also be expressed as 10 years of climate trend being equivalent to the loss of roughly 1 year of technology gains. For Mexico, a negative effect on wheat yield was estimated relative to what could have been achieved without the climate trends (see Table 2).

Crop	Trend
Maize	n/a
Rice	0.0 to 0.1
Wheat	-0.4 to -0.3
Soybean	0.0 to 0.1

Table 2. *The estimated net impact of climate trends for 1980-2008 on crop yields in Mexico. Climate-induced yield trend divided by overall yield trend. 'n/a' infers zero or insignificant crop production or unavailability of data. Data is from Lobell et al. (2011).*

Climate change studies

Several recent studies have applied climate projections from Global Climate Models (GCMs) to crop yield models to assess the global-scale impact of climate change on crop yields. At least one of these studies (Iglesias and Rosenzweig, 2009) includes impact estimates at the national-scale for Mexico which are presented in this section. Most other studies report projections for a geographic or climatic area larger than Mexico alone and it is not always clear to what extent the crop yield projections are representative for this country only in these cases. The process of CO_2 fertilisation of some crops is usually included in most

climate impact studies of yields. However, other gases can influence crop yield and are not always included in impacts models. An example of this is ozone (O_3) and so a study which attempts to quantify the potential impact on crop yield of changes in ozone in the atmosphere is also included (Avnery et al. 2011). In addition to these studies, the AVOID programme analysed the patterns of climate change for 21 GCMs, to establish an index of 'climate suitability' of agricultural land. Climate suitability is not directly equivalent to crop yields, but is a means of looking at a standard metric across all the countries including in this project, and of assessing the level of agreement on variables that affect crop production, between all 21 GCMs.

Iglesias and Rosenzweig (2009) repeated an earlier study presented by Parry et al. (2004) by applying climate projections from the HadCM3 GCM (instead of HadCM2, which was applied by Parry et al. (2004)), under seven SRES emissions scenarios and for three future time periods. This study used a globally consistent crop simulation methodologies and climate change scenarios, and weighted the model site results by their contribution to regional and national, and rain-fed and irrigated production. The study also applied a quantitative estimation of physiological CO_2 effects on crop yields and considered the affect of adaptation by assessing the country or regional potential for reaching optimal crop yield. The results from the study for Mexico are presented in Table 3 and Table 4. The simulations showed that wheat yield decreased steadily with climate change. Maize yield was projected to decrease until 2050 after which it increased slightly. Projected maize yield losses relative to baseline yield level were larger than wheat yield loss by 2020 and 2050 but not always by 2080.

Scenario	Year	Wheat	Maize
	2020	-0.09	-5.78
	2050	-7.05	-10.21
A1FI	2080	-17.14	-2.81
	2020	-0.57	-5.37
	2050	0.05	-7.09
A2a	2080	-4.34	-4.37
	2020	-2.78	-5.51
	2050	-4.72	-8.35
A2b	2080	-10.36	-9.26
	2020	-1.23	-4.74
	2050	-3.83	-7.74
A2c	2080	-11.21	2.39
	2020	-4.39	-6.22
	2050	-5.74	-8.96
B1a	2080	-6.77	-8.11
	2020	-4.70	-7.38
	2050	-3.97	-9.25
B2a	2080	-3.35	-6.70
	2020	-4.22	-7.26
	2050	-2.94	-9.10
B2b	2080	-8.11	-7.46

***Table 3**. Wheat and maize yield changes (%) in Mexico relative to baseline scenario (1970-2000) for different emission scenarios and future time periods. Some emissions scenarios were run in an ensemble simulation (e.g. A2a, A2b, A2c). Data is from Iglesias and Rosenzweig (2009).*

	Wheat		Maize	
	Up	Down	Up	Down
Baseline to 2020	0	7	0	7
Baseline to 2050	1	6	0	7
Baseline to 2080	0	7	1	6
2020 to 2050	3	4	0	7
2050 to 2080	1	6	5	2

***Table 4.** The number of emission scenarios that predict yield gains ("Up") or yield losses ("Down") for wheat and maize in Mexico between two points in time. Data is from Iglesias and Rosenzweig (2009).*

Several other recent studies have assessed the impact of climate change on a global-scale and include impact estimates for regions that include Mexico, e.g. Central America or Latin America and the Caribbean (Arnell et al., 2010a, Nelson et al., 2009, Tatsumi et al., 2011, Lobell et al., 2008, Fischer et al., 2009). Whilst these studies provide a useful indicator of crop yields under climate change for the region, it should be noted that the crop yields presented in such cases are not definitive national estimates. This is because the yields are averaged over the entire region, which includes other countries as well as Mexico.

Nelson et al. (2009) applied two GCMs in combination with the DSSAT crop model under the SRES A2 emissions scenario to project future yields of rice, maize, soybean, wheat and groundnut with and without CO_2 enrichment, and for rain-fed and irrigated lands, for several regions across the globe. Table 5 represents the results for Latin America and the Caribbean, the IFPRI regional grouping in which Mexico is included. When the effect of CO_2 fertilisation was included, a general increase in yield was projected for most crops, with the exception of irrigated rice and maize. Without this effect, yields of both rain-fed and irrigated maize, as well as irrigated rice and soybean were also projected to decline under both GCMs.

GCM and CO_2 fertilisation	Rice		Maize		Soybean		Wheat		Groundnut	
	Rf.	Irr.	Rf.	Irr.	Rf.	Irr.	Rf.	Irr.	Rf.	Irr.
CSIRO NoCF	5.3	-6.4	-0.4	-2.8	-2.6	-1.2	2.3	0.3	0.9	0.0
NCAR NoCF	-1.8	-0.8	-1.9	-3.0	4.2	-2.5	4.2	-5.6	7.1	0.0
CSIRO CF	12.7	-1.2	2.2	-2.3	19.1	19.5	12.2	6.5	18.1	0.0
NCAR CF	6.7	7.0	0.4	-2.5	19.1	18.2	11.8	0.9	17.9	0.0

Table 5. *Projected yield changes (%) in Latin America and the Caribbean by 2050 compared to baseline (yields with 2000 climate) using two GCMs with (CF) and without CO_2 fertilisation effect (NoCF). Rain-fed (Rf.) and Irrigated (Irr.) crop lands were assessed separately. Data is from Nelson et al. (2009).*

Tatsumi et al. (2011) applied an improved version of the GAEZ crop model (iGAEZ) to simulate crop yields on a global scale for wheat, potato, cassava, soybean, rice, sweet potato, maize, green beans. The impact of global warming on crop yields from the 1990s to 2090s was assessed by projecting five GCM outputs under the SRES A1B scenario and comparing the results for crop yields as calculated using the iGAEZ model for the period of 1990-1999. The results for Central America, which includes Mexico, are displayed in Table 6 and suggest a general increase in yield for wheat, maize, soybean and green beans, but a decline for potato, cassava and rice.

Wheat	Potato	Cassava	Soybean	Rice	Sweet potato	Maize	Green beans
6.85	-5.56	-4.94	25.95	-5.89	-0.58	19.39	20.79

Table 6. *Average change in yield (%), during 1990s-2090s in Central America. Data is from Tatsumi et al. (2011).*

Arnell et al. (2010a) used 5 GCMs to assess the effects of climate scenarios on crop productivity. Specifically, the crop simulation model GLAM-maize was used to simulate the

effect of climate change on maize productivity. For Meso-America a loss of between approximately 35% and 48% of yield by 2050 was simulated relative to the baseline (1961-1990) in the absence of adaptation and mitigation strategies. Implementing the mitigation strategy A1B-2016-5-L (a 5%/year reduction in emissions from 2016 onwards to a low emissions floor) reduced the negative impact by approximately 20% and 30% in 2050 and 2100 respectively.

Fischer (2009) projected global 'production potential' changes for 2050 using the GAEZ (Global Agro-Ecological Zones) crops model with climate change scenarios from the HadCM3 and CSIRO GCMs respectively, under SRES A2 emissions. The impact of future climate on crop yields of rain-fed cereals in Central America and the Carribean, relative to yield realised under current climate, are presented in Table 7. In contrast to Nelson et al. (2009) and Tatsumi et al. (2011) the results indicated a strong decrease in yields of rain-fed wheat, even when the effect of CO_2 fertilisation was included. Yields of rain-fed maize were projected to increase or remain more or less unchanged.

	CO_2 fert.	2020s		2050s		2080s	
		CSIRO	HADCM3	CSIRO	HADCM3	CSIRO	HADCM3
Rain-fed wheat	Yes	-19	-33	-36	-54	-53	-76
	No	-21	n/a	-39	n/a	-57	n/a
Rain-fed maize	Yes	2	6	7	9	13	-1
	No	0	n/a	3	n/a	7	n/a
Rain-fed cereals	Yes	n/a	-1	n/a	-2	n/a	-15
	No	n/a	n/a	n/a	n/a	n/a	n/a
Rain-fed sorghum	Yes	3	n/a	10	n/a	17	n/a
	No	1	n/a	6	n/a	11	n/a

***Table 7**. Impacts of climate change on the production potential in Central America and the Carribean of rain-fed cereals in current cultivated land (% change with respect to yield realised under current climate), with two GCMs and with and without CO_2 fertilisation ("CO_2 fert.") under SRES A2 emissions. Data is from Fischer (2009).*

Lobell et al. (2008) conducted an analysis of climate risks for the major crops in 12 food-insecure regions to identify adaptation priorities. Statistical crop models were used in combination with climate projections for 2030 from 20 GCMs that have contributed to the World Climate Research Programme's Coupled Model Intercomparison Project phase 3. The results from the study for Central America and the Caribbean are presented in Figure 2. Lobell et al. (2008) found that in this region, climate change had an adverse impact in 2030 on wheat and rice yield. However, sugarcane, cassava and maize yield were projected to increase.

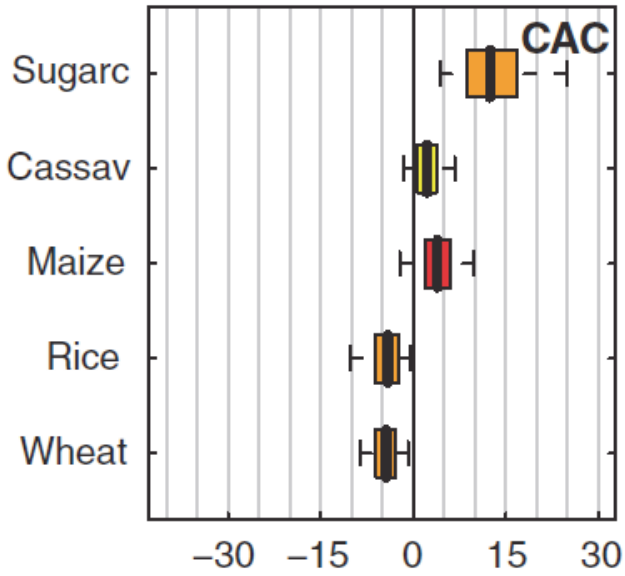

Figure 2. *Probabilistic projections of production impacts in 2030 from climate change (expressed as a percentage of 1998 to 2002 average yields) for Central America and the Caribbean. Red, orange, and yellow indicate a Hunger Importance Ranking of 1 to 30 (more important), 31 to 60 (important), and 61 to 94 (less important), respectively. Dashed lines extend from 5th to 95th percentile of projections, boxes extend from 25th to 75th percentile, and the middle vertical line within each box indicates the median projection. Figure is from Lobell et al. (2008).*

In addition to the studies looking at the effect of changes in climate and CO_2 concentrations on crop yield, Avnery et al. (2011) investigated the effects of ozone surface exposure on crop yield losses for soybeans, maize and wheat under the SRES A2 and B1 scenarios respectively. Two metrics of ozone exposure were investigated; seasonal daytime (08:00-19:59) mean O_3 ("M12") and accumulated O_3 above a threshold of 40 ppbv ("AOT40"). The effect of the ozone exposure was considered in isolation from climate and other changes. The results for Mexico are presented in Table 8.

	A2		B1	
	M12	**AOT40**	**M12**	**AOT40**
Soybeans	-	-	-	-
Maize	8-10	4-6	4-6	0-2
Wheat	6-8	20-25	4-6	10-15

Table 8. *National relative crop yield losses (%) for 2030 under A2 and B1 emission scenarios according to the M12 (seasonal daytime (08:00–19:59) mean) and AOT40 (accumulated O_3 above a threshold of 40 ppbv) metrics of O_3 exposure. Data is from Avnery et al. (2011).*

National-scale or sub-national scale assessments

Castillo-Alvarez et al. (2007) applied two GCMs to estimate rain-fed maize and wheat yield by 2100, assuming a doubling of CO_2 relative to baseline (2000), and accounted for changes in soil fertility and water availability. Their results suggest that a reduction in soil fertility can cause crop yield changes of up to 20%, indicating its importance for crop productivity predictions. The results further estimate maize yield increases of up to 463kg·ha^{-1} in arid and semiarid zones with climate change, but decreases up to 392kg·ha^{-1} in humid and semi-humid zones. For wheat, a crop yield increase of up to 1100kg·ha^{-1} was simulated.

Monterroso-Rivas et al. (2011) estimated the potential area suitable for cropping of rain-fed maize with climate change in the 2050s by applying climate projections from three GCMs (ECHAM5/MPI, UKHADGEM1 and GFDL-CM2.0) under SRES A2 and B2 emissions scenarios. Under the baseline scenario (1950-2000), 6.2% of total land area indicated suitable conditions, while 25.1% and 31.6% had moderated and limited conditions, respectively. Each of the GCMs simulated that the area best suited for maize growing decreased under both the A2 and B2 emissions scenarios by more than 50%. This implies that mean yield could decrease with climate change in Mexico. One GCM, however, simulated large decreases of the area 'not suitable' for maize production in both the A2 and B2 scenarios and in these cases, average yield may slightly increase.

AVOID programme results

To further quantify the impact of climate change on crops, the AVOID programme simulated the effect of climate change on the suitability of land for crop cultivation for all countries reviewed in this literature assessment based upon the patterns of climate change from 21 GCMs (Warren et al., 2010). This ensures a consistent methodological approach across all countries and takes consideration of climate modelling uncertainties.

Methodology

The effect of climate change on the suitability of land for crop cultivation is characterised here by an index which defines the percentage of cropland in a region with 1) a decrease in suitability or 2) an increase in suitability. A threshold change of 5% is applied here to characterise decrease or increase in suitability. The crop suitability index is calculated at a spatial resolution of 0.5°x0.5°, and is based on climate and soil properties (Ramankutty et al., 2002). The baseline crop suitability index, against which the future changes are measured, is

representative of conditions circa 2000. The key features of the climate for the crop suitability index are temperature and the availability of water for plants. Changes in these were derived from climate model projections of future changes in temperature and precipitation, with some further calculations then being used to estimate actual and potential evapotranspiration as an indicator of water availability. It should be noted that changes in atmospheric CO_2 concentrations can decrease evapotranspiration by increasing the efficiency of water use by plants (Ramankutty et al., 2002), but that aspect of the index was not included in the analysis here. Increased CO_2 can also increase photosynthesis and improve yield to a small extent, but again these effects are not included. Exclusion of these effects may lead to an overestimate of decreases in suitability.

The index here is calculated only for grid cells which contain cropland circa 2000, as defined in the global crop extent data set described by Ramankutty et al. (2008) which was derived from satellite measurements. It is assumed that crop extent does not change over time. The crop suitability index varies significantly for current croplands across the world (Ramankutty et al., 2002), with the suitability being low in some current cropland areas according to this index. Therefore, while climate change clearly has the potential to decrease suitability for cultivation if temperature and precipitation regimes become less favourable, there is also scope for climate change to increase suitability in some existing cropland areas if conditions become more favourable in areas where the suitability index is not at its maximum value of 1. It should be noted that some areas which are not currently croplands may already be suitable for cultivation or may become suitable as a result of future climate change, and may become used a croplands in the future either as part of climate change adaptation or changes in land use arising for other reasons. Such areas are not included in this analysis.

Results

Crop suitability was estimated under the pattern of climate change from 21 GCMs with two emissions scenarios; 1) SRES A1B and 2) an aggressive mitigation scenario where emissions follow A1B up to 2016 but then decline at a rate of 5% per year thereafter to a low emissions floor (denoted A1B-2016-5-L). The application of 21 GCMs is an attempt to quantify the uncertainty due to climate modelling, although it is acknowledged that only one crop suitability impacts model is applied. Simulations were performed for the years 2030, 2050, 2080 and 2100. The results for Mexico are presented in Figure 3.

Under both emissions scenarios, almost no models project an increase in suitability for cultivation for current Mexican croplands. For both scenarios, between 40% and 70% of

current Mexican croplands are projected to undergo declining suitability by 2030. By 2100 this rises to around 50%-80% under the mitigation scenario and 60%-100% under A1B.

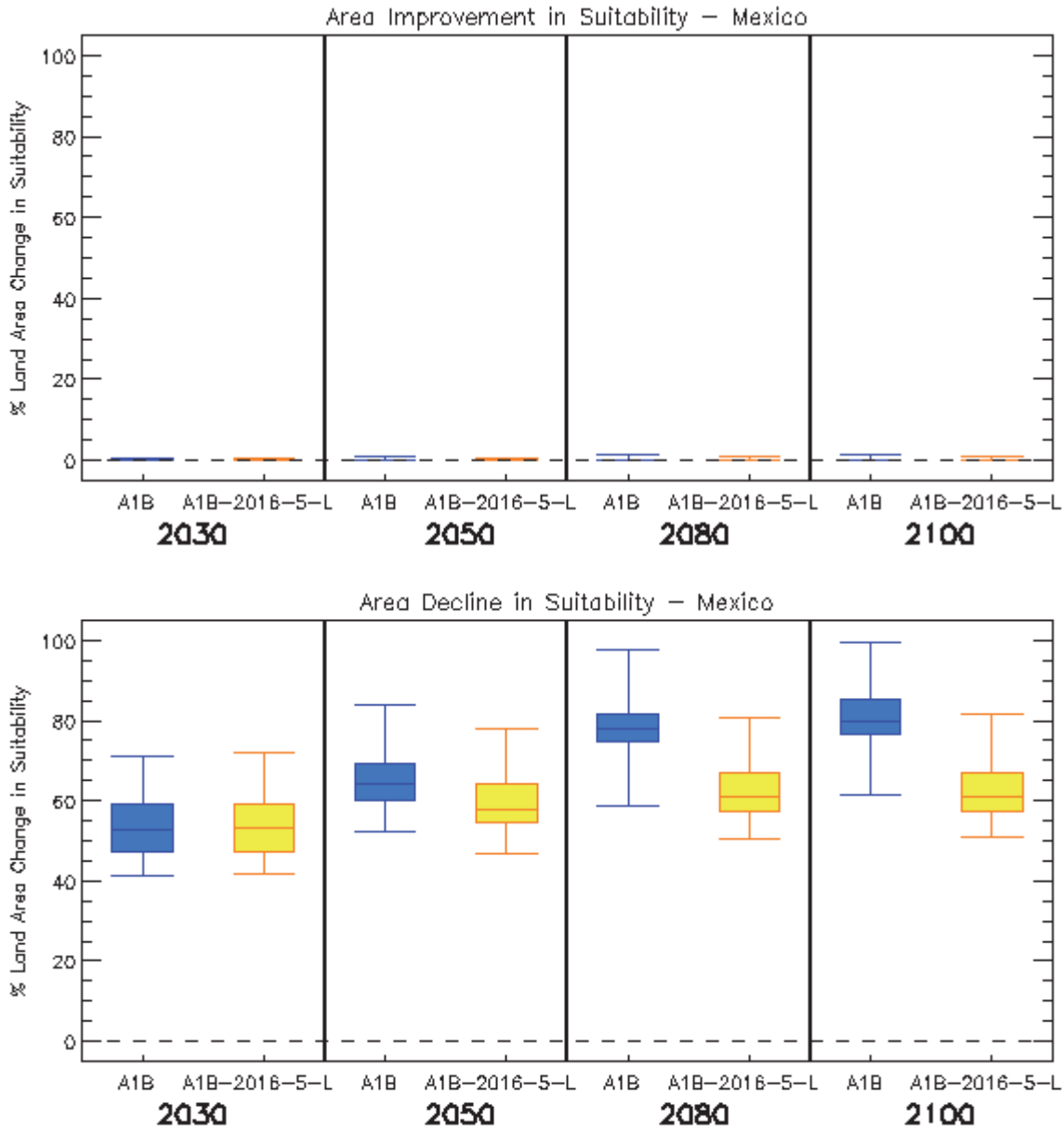

Figure 3. *Box and whisker plots for the impact of climate change on increased crop suitability (top panel) and decreased crop suitability (bottom panel) for Mexico, from 21 GCMs under two emissions scenarios (A1B and A1B-2016-5-L), for four time horizons. The plots show the 25th, 50th, and 75th percentiles (represented by the boxes), and the maximum and minimum values (shown by the extent of the whiskers).*

Food security

Headline

Studies show a mixed outlook for food security issues under climate change for Mexico. One study suggests that Mexico may be a food exporting country in 2050. However, research by the AVOID programme indicates that adaptation measures, such as reducing food for exports, may be required to avoid major food security issues in Mexico with climate change. There is no consensus across studies upon whether climate change could have a beneficial or negative impact on food security for Mexico.

Introduction

Food security is a concept that encompasses more than just crop production, but is a complex interaction between food availability and socio-economic, policy and health factors that influence access to food, utilisation and stability of food supplies. In 1996 the World Food Summit defined food security as existing 'when all people, at all times, have physical and economic access to sufficient, safe and nutritious food to meet their dietary needs, and their food preferences are met for an active and healthy life'. As such this section cannot be a comprehensive analysis of all the factors that are important in determining food security, but does attempt to assess a selection of the available literature on how climate change, combined with projections of global and regional population and policy responses, may influence food security.

With regards to food security Mexico is presently a country of low concern, relative to other countries across the globe. According to FAO statistics (FAO, 2010) Mexico has extremely low levels of undernourishment (less than 5% of the population). However, a number of global studies disagree on whether climate change will have a positive or negative impact on food security in Mexico.

Assessments that include a global or regional perspective

Several recent studies have analysed food security under climate change across the globe. Wu et al. (2011) applied the GIS-based Environmental Policy Integrated Climate (EPIC) model. This was combined with crop areas simulated by a crop choice decision model to calculate total food production and per capita food availability across the globe, which was used to represent the status of food availability and stability. The study focussed on the

SRES A1 scenario and applied climate change simulations for the 2000s (1991–2000) and 2020s (2011–2020). The climate simulations were performed by MIROC (Model for Interdisciplinary Research on Climate) version 3.2., which means the effects of climate model uncertainty were not considered. Downscaled population and GDP data from the International Institute for Applied Systems Analysis (IIASA) were applied in the simulations. Wu et al. (2011) conclude that Mexico is not likely to face severe food insecurity in the next 20 years.

Falkenmark et al. (2009) also present a positive outlook for Mexico. The study presents a global analysis of food security under climate change scenarios for the 2050s that considers the importance of water availability for ensuring global food security. Falkenmark et al. (2009) perform an analysis of water constraints and opportunities for global food production on current croplands and assesses five main factors:

1) how far improved land and water management might go towards achieving global food security,

2) the water deficits that would remain in regions currently experiencing water scarcity and which are aiming at food self-sufficiency,

3) how the water deficits above may be met by importing food,

4) the cropland expansion required in low income countries without the needed purchasing power for such imports, and

5) the proportion of that expansion pressure which will remain unresolved due to potential lack of accessible land.

Similar to the study presented by Wu et al. (2011), there is no major treatment of modelling uncertainty; simulations were generated by only the LPJml dynamic global vegetation and water balance model (Gerten et al. 2004) with population growth and climate change under the SRES A2 emission scenario. Falkenmark et al. (2009) summarise the impacts of future improvements (or lack thereof) in water productivity for each country across the globe and show that this generates either a deficit or a surplus of water in relation to food water requirements in each country. These can be met either by trade or by horizontal expansion (by converting other terrestrial ecosystems to crop land). The study estimated that in 2050 around one third of the world's population will live in each of three regions: those that export food, those that import food, and those that have to expand their croplands at the expense of

other ecosystems because they do not have enough purchasing power to import their food. The simulations demonstrated that Mexico was a food exporting country in 2050.

The International Food Policy Research Institute (IFPRI) have produced a report and online tool that describes the possible impact of climate change on two major indicators of food security; 1) the number of children aged 0-5 malnourished, and 2) the average daily kilocalorie availability (Nelson et al., 2010, IFPRI, 2010)**.** The study considered three broad socio-economic scenarios; 1) a 'pessimistic' scenario, which is representative of the lowest of the four GDP growth rate scenarios from the Millennium Ecosystem Assessment GDP scenarios and equivalent to the UN high variant of future population change, 2) a 'baseline' scenario, which is based on future GDP rates estimated by the World Bank and a population change scenario equivalent to the UN medium variant, and 3) an 'optimistic' scenario that is representative of the highest of the four GDP growth rate scenarios from the Millennium Ecosystem Assessment GDP scenarios and equivalent to the UN low variant of future population change. Nelson et al. (2010) also considered climate modelling and emission uncertainty and included a factor to account for CO_2 fertilisation in their work. The study applied two GCMs, the CSIRO GCM and the MIROC GCM, and forced each GCM with two SRES emissions scenarios (A1B and B1). They also considered a no climate change emissions scenario, which they called 'perfect mitigation' (note that in most other climate change impact studies that this is referred to as the baseline). The perfect mitigation scenario is useful to compare the effect of climate change against what might have happened without, but is not a realistic scenario itself. Estimates for both indicators of food security from 2010 to 2050, for Mexico, are presented in Table 9 and Table 10. Figure 4 displays the effect of climate change, calculated by comparing the 'perfect mitigation' scenario with each baseline, optimistic and pessimistic scenario. The results show that average kilocalorie availability declines during 2010-2050 under the baseline and pessimistic scenarios. Only under the optimistic scenario does this increase by 2050, relative to 2010. It is noteworthy that by 2050, the additional affect of climate change (relative to no climate change) is to reduce kilocalorie availability by around at least 200 kilocalories; the decline attributable to climate change can be up to around 10%. All three socioeconomic scenarios are associated with large reductions in the number of malnourished children, although this is partially off set by climate change, e.g. by 2050, climate change is attributable for up to around a 50% of malnourishment level, relative to malnourishment in the absence of climate change. Figure 5 and Figure 6 show how the changes projected for Mexico compare with the projections for the rest of the globe (IFPRI, 2010).

Scenario	2010	2050
Baseline CSI A1B	2907	2777
Baseline CSI B1	2914	2806
Baseline MIR A1B	2878	2674
Baseline MIR B1	2901	2753
Baseline Perfect Mitigation	2955	2986
Pessimistic CSI A1B	2968	2792
Pessimistic CSI B1	2976	2821
Pessimistic MIR A1B	2939	2682
Pessimistic MIR B1	2952	2730
Pessimistic Perfect Mitigation	3018	3001
Optimistic CSI A1B	2913	3126
Optimistic CSI B1	2918	3145
Optimistic MIR A1B	2882	2999
Optimistic MIR B1	2894	3048
Optimistic Perfect Mitigation	2959	3347

Table 9. *Average daily kilocalorie availability simulated under different climate and socioeconomic scenarios, for Mexico (IFPRI, 2010).*

Scenario	2010	2050
Baseline CSI A1B	0.91	0.46
Baseline CSI B1	0.91	0.44
Baseline MIR A1B	0.94	0.52
Baseline MIR B1	0.92	0.47
Baseline Perfect Mitigation	0.87	0.33
Pessimistic CSI A1B	0.86	0.52
Pessimistic CSI B1	0.85	0.5
Pessimistic MIR A1B	0.89	0.6
Pessimistic MIR B1	0.87	0.57
Pessimistic Perfect Mitigation	0.82	0.37
Optimistic CSI A1B	0.91	0.21
Optimistic CSI B1	0.9	0.2
Optimistic MIR A1B	0.93	0.27
Optimistic MIR B1	0.92	0.25
Optimistic Perfect Mitigation	0.87	0.11

Table 10*. Number of malnourished children (aged 0-5; millions) simulated under different climate and socioeconomic scenarios, for Mexico (IFPRI, 2010).*

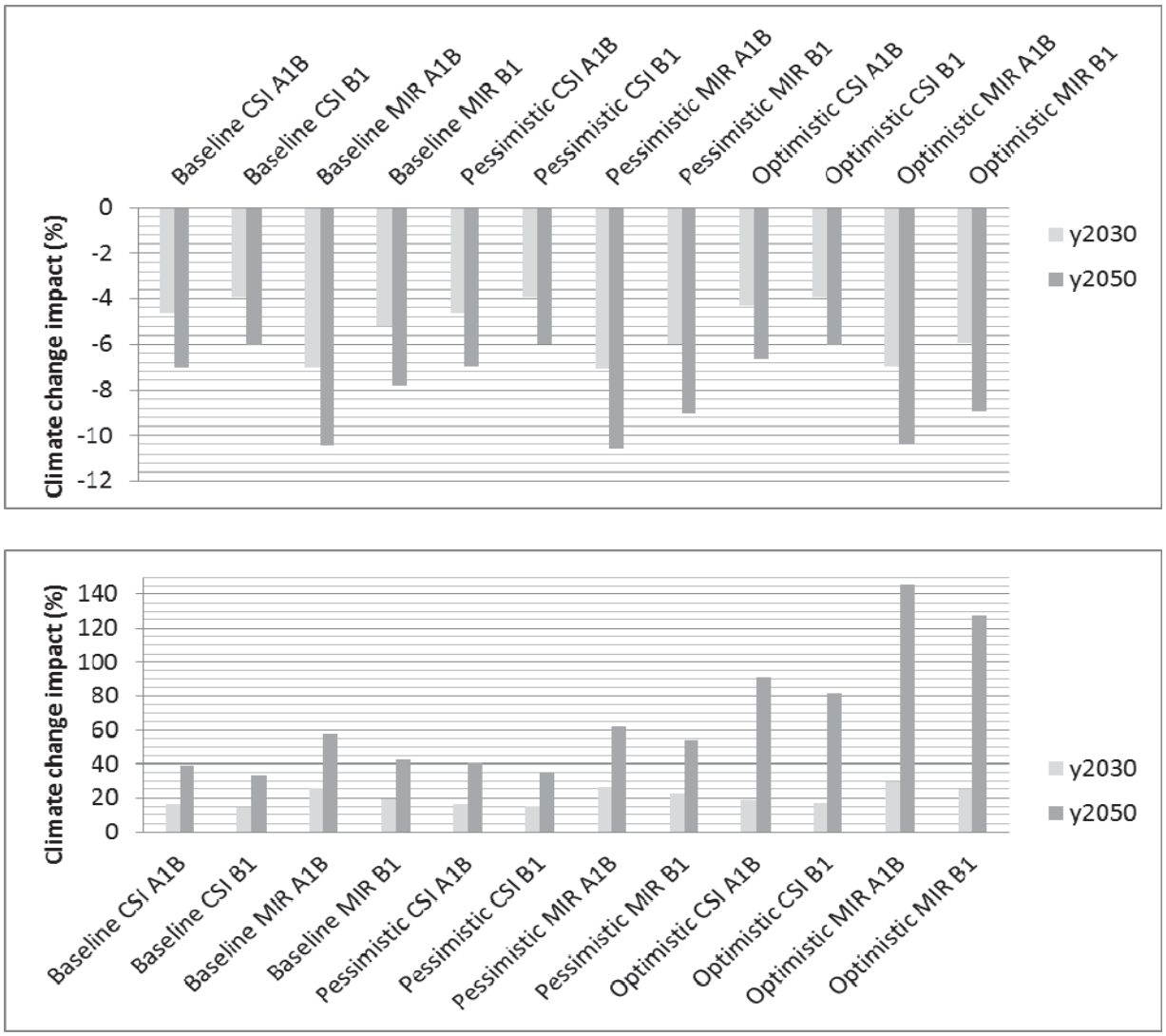

Figure 4. *The impact of climate change on average daily kilocalorie availability (top panel) and number of malnourished children (bottom) (IFPRI, 2010).*

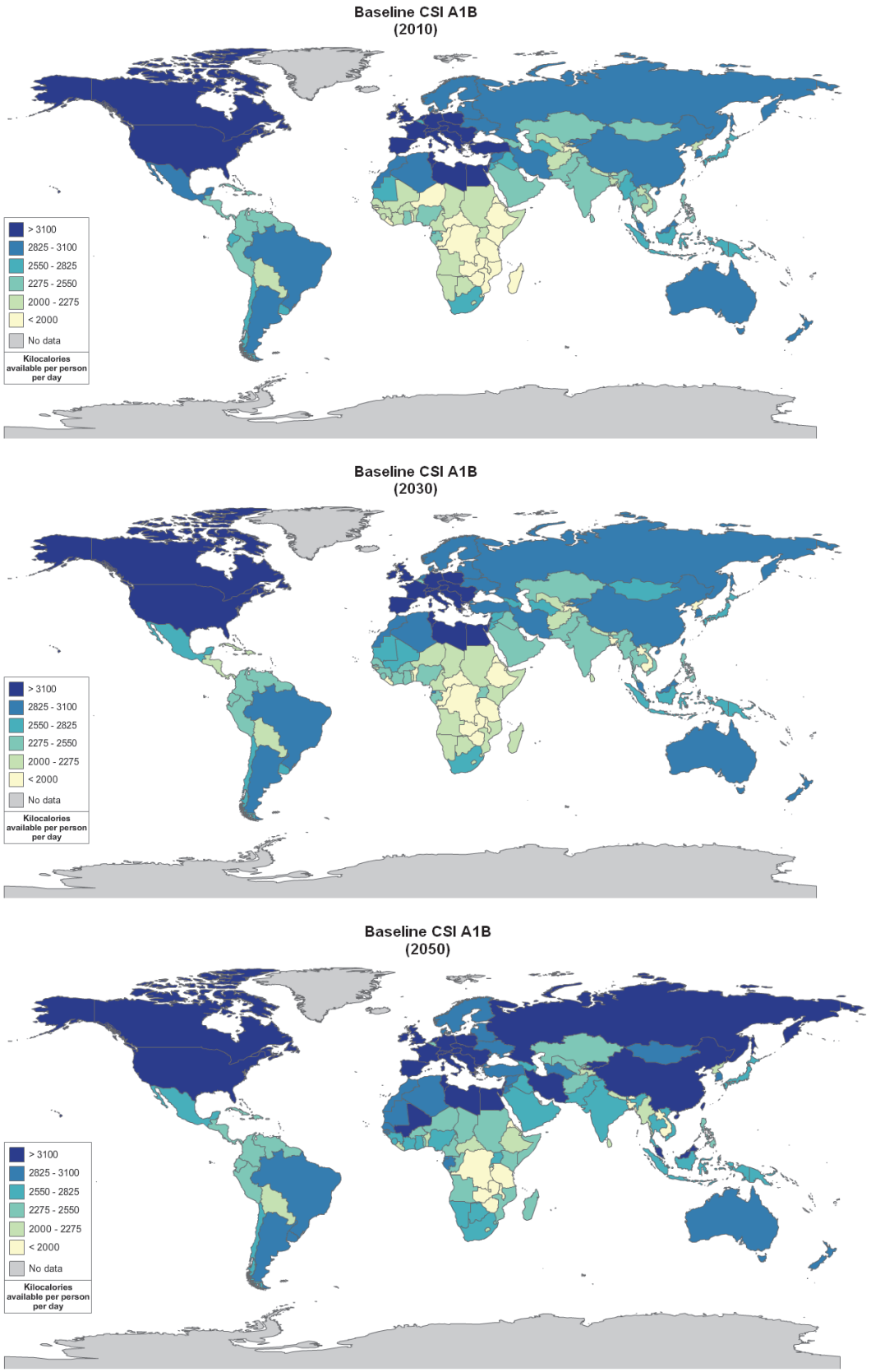

Figure 5. *Average daily kilocalorie availability simulated by the CSIRO GCM (CSI) under an A1B emissions scenario and the baseline socioeconomic scenario, for 2010 (top panel), 2030 (middle panel) and 2050 (bottom panel). The figure is from IFPRI (IFPRI, 2010). The changes show the combination of both climate change and socio-economic changes.*

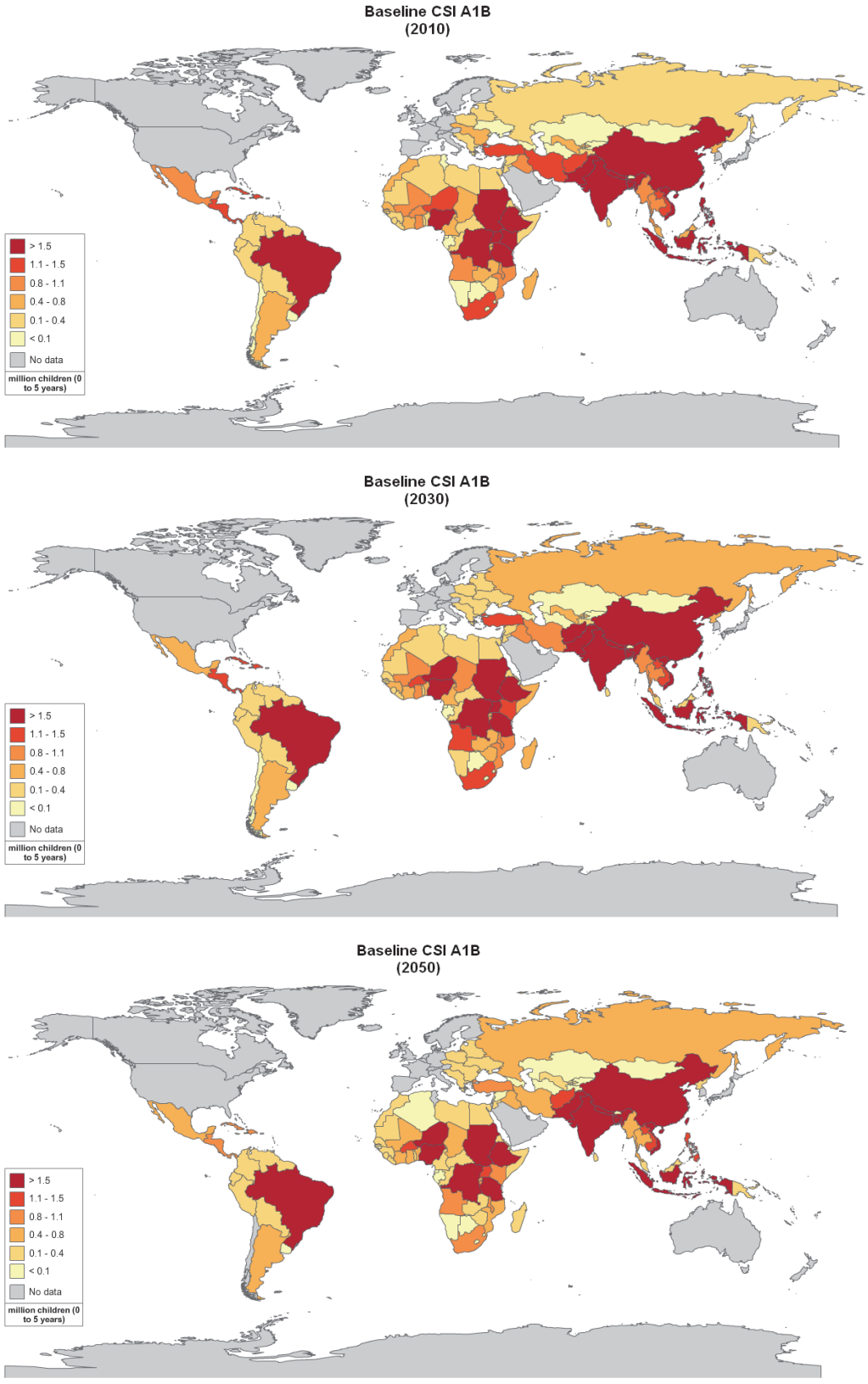

Figure 6. *Number of malnourished children (aged 0-5; millions) simulated by the CSIRO GCM (CSI) under an A1B emissions scenario and the baseline socioeconomic scenario, for 2010 (top panel), 2030 (middle panel) and 2050 (bottom panel). The figure is from IFPRI (IFPRI, 2010). The changes shown the combination of both climate change and socio-economic changes.*

Arnell et al. (2010b) considered the impacts of global climate change and mitigation scenario on food security for eleven countries. The study applied climate change patterns from the HadCM3 GCM and explored food security under two emissions scenarios; a business as usual scenario (SRES A1B) and four mitigations scenarios where emissions peak in 2030 and subsequently reduce at 2% per year to a high emissions floor (referred to as 2030-2-H) or 5% per year to a low emissions floor (2030-5-L), or where they peak in 2016 and subsequently reduce at 2% per year to a high emissions floor (referred to as 2016-2-H) or 5% per year to a low emissions floor (2016-5-L). The study also considered a a series of structural adjustments that could be made in the future to adapt to food security issues, including that 1) if there is a shortfall of any per-capita food availability due to crop yield and/or population changes, then original (baseline) food amounts are made up by reducing or removing export amounts; and 2) if, after the above adjustments, there is still a shortfall, then the amount of crops going to animal feed is reduced or removed to try to make up to the original (baseline) food amounts. The model simulations presented by Arnell et al. (2010b) characterise the numbers of people exposed to undernourishment in the absence of increased crop production and imports, not actual numbers of undernourished people. The results are presented in Figure 7. The results presented by Arnell et al. (2010b) highlight the importance of potential adaptation methods in Mexico. Mexico's population is expected to increase by 34% by 2050 under an A1B scenario, and when this is coupled with a 30% decrease in crop yields, this leads to a major increase in undernourishment from 5% of the population at present, to 83% by 2050, when no structural adjustments are considered. Undernourishment is somewhat lower under the 2016-5-L and 2030-5-L mitigation scenarios (without structural adjustment), at 71% and 76% of the population respectively. However, when structural adjustments are incorporated into the simulations, Arnell et al. (2010b) estimate that in 2050, undernourishment in Mexico is around 17- 18% of the total population, for any given emissions scenario. Beyond 2050, crop yields generally continue to decrease but population declines mean that exposure to undernourishment also declines towards 2100.

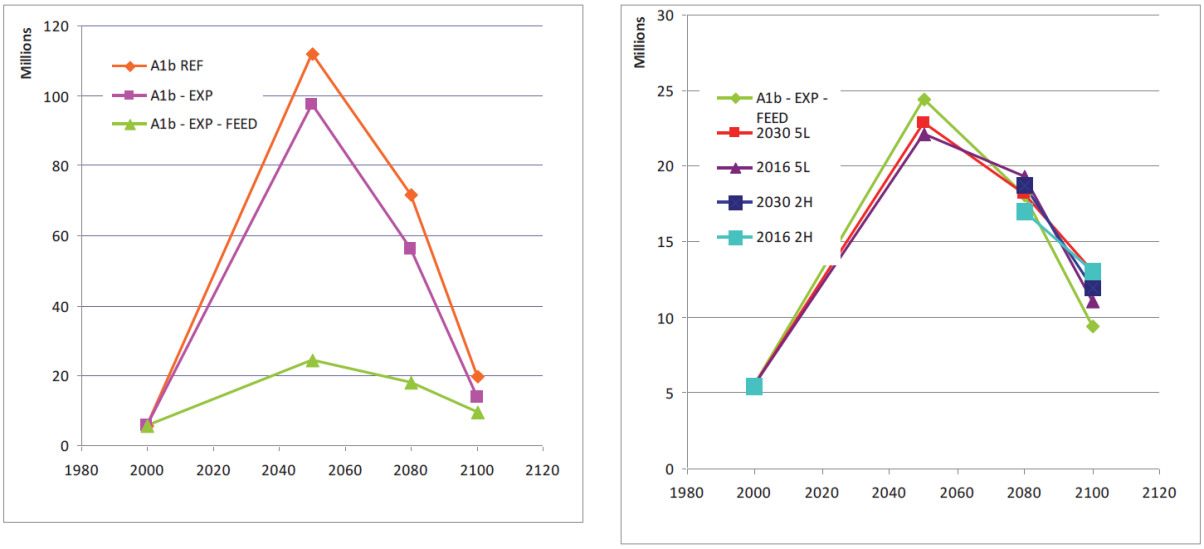

Figure 7. *Total projected population exposed to undernourishment in Mexico. The left panel shows total exposure under the A1B emissions scenario ("A1b REF"), plus the A1B scenario with exports reduced or removed ("A1b–EXP") and the A1B scenario with exports removed and allocation to feed reduced or removed ("A1b–EXP–FEED"). The right panel shows the total exposure under the A1b–EXP–FEED and three mitigation scenarios. The figure is from Arnell et al. (2010b).*

It is important to note that up until recently, projections of climate change impacts on global food supply have tended to focus solely on production from terrestrial biomes, with the large contribution of animal protein from marine capture fisheries often ignored. However, recent studies have addressed this knowledge gap (Allison et al., 2009, Cheung et al., 2010). In addition to the direct affects of climate change, changes in the acidity of the oceans, due to increases in CO_2 levels, could also have an impact of marine ecosystems, which could also affect fish stocks. However, this relationship is complex and not well understood, and studies today have not been able to begin to quantify the impact of ocean acidification on fish stocks.

Allison et al. (2009) present a global analysis that compares the vulnerability of 132 national economies to potential climate change impacts on their capture fisheries. The study considered a country's vulnerability to be a function of the combined effect of projected climate change, the relative importance of fisheries to national economies and diets, and the national societal capacity to adapt to potential impacts and opportunities. Climate change projections from a single GCM under two emissions scenarios (SRES A1FI and B2) were used in the analysis. Allison et al. (2009) concluded that the national economy of Mexico presented a moderate vulnerability to climate change impacts on fisheries. In contrast, countries in Central and Western Africa (e.g. Malawi, Guinea, Senegal, and Uganda), Peru and Colombia in north-western South America, and four tropical Asian countries (Bangladesh, Cambodia, Pakistan, and Yemen) were identified as most vulnerable (see Figure 8). It should be noted, however, that results from studies that have applied only a

single climate model or climate change scenario should be interpreted with caution. This is because they do not consider other possible climate change scenarios which could result in a different impact outcome, in terms of magnitude and in some cases sign of change.

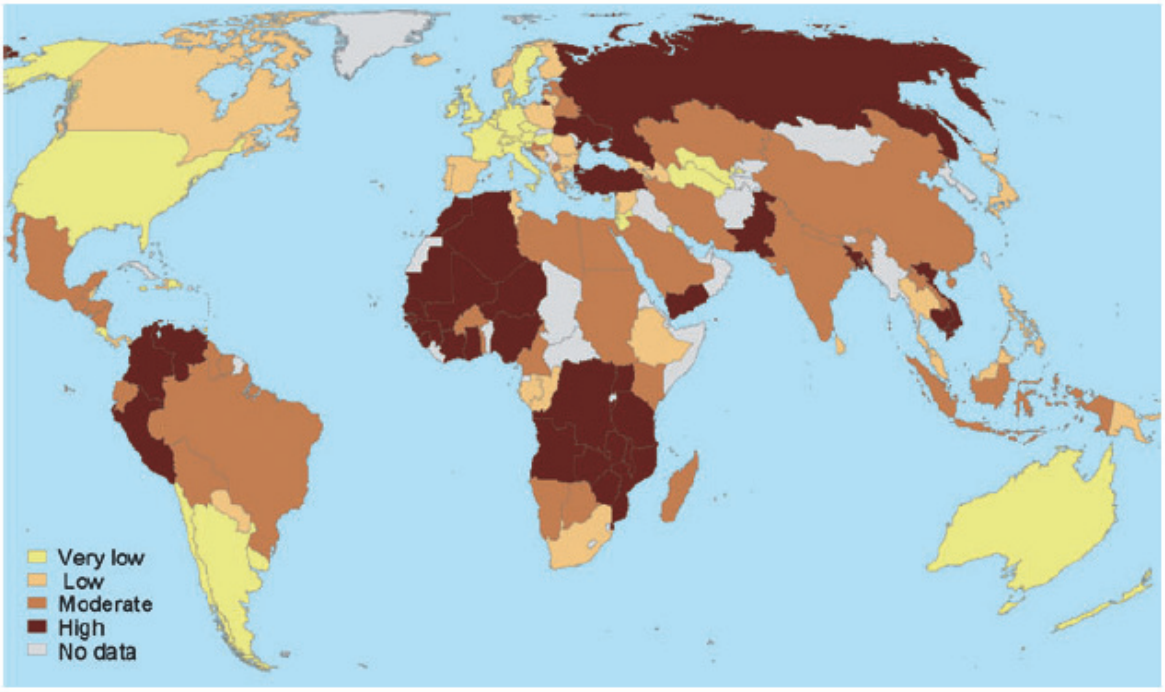

Figure 8. *Vulnerability of national economies to potential climate change impacts on fisheries under SRES B2* (Allison et al., 2009). Colours represent quartiles with dark brown for the upper quartile (highest index value), yellow for the lowest quartile, and grey where no data were available.

Cheung et al. (2010) also consider marine capture fisheries at the global scale for several countries. The study projected changes in global catch potential for 1066 species of exploited marine fish and invertebrates from 2005 to 2055 under climate change scenarios. Cheung et al. (2010) found that climate change may lead to large-scale redistribution of global catch potential, with an average of 30–70% increase in high-latitude regions and a decline of up to 40% in the tropics. The simulations were based climate simulations from a single GCM (GFDL CM2.1) under a SRES A1B emissions scenario (CO_2 concentration at 720ppm in 2100) and a stable-2000 level scenario (CO_2 concentration maintains at year 2000 level of 365ppm). The limitations of applying a single GCM have been noted previously. For Mexico, the projected change in the 10-year averaged maximum catch potential from 2005 to 2055 was around a 4% reduction under the A1B scenario. Climate change mitigation scenario had no effect on changing this. Figure 9 demonstrates how this compares with projected changes for other countries across the globe.

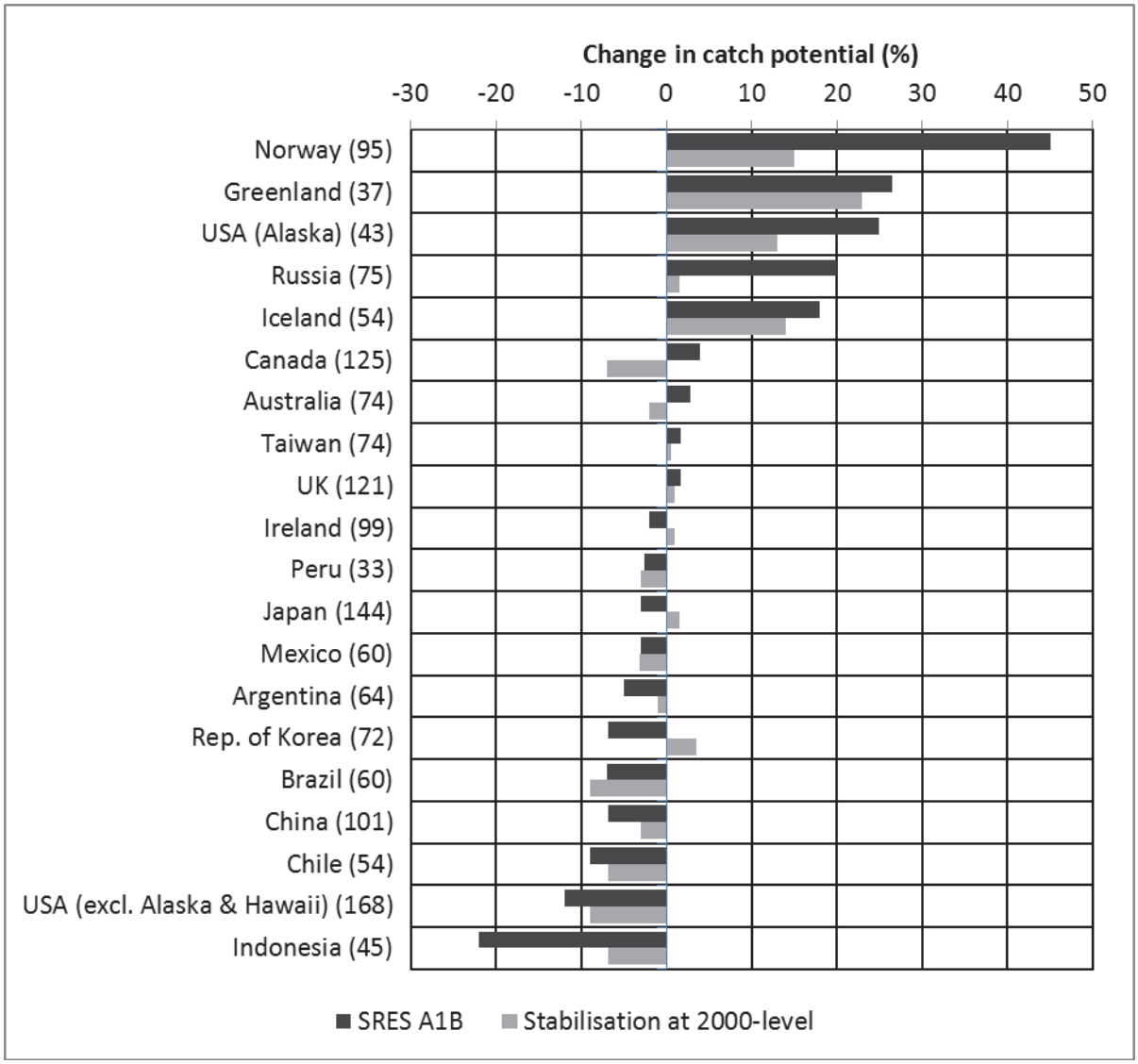

Figure 9. *Projected changes in the 10-year averaged maximum catch potential from 2005 to 2055. The numbers in parentheses represent the numbers of exploited species included in the analysis. Adapted from Cheung et al. (2010).*

National-scale or sub-national scale assessments

Literature searches yielded no results for national-scale or sub-national scale studies for this impact sector.

Water stress and drought

Headline

There is large uncertainty in how climate change could affect water stress in Mexico, which arises in part from climate modelling uncertainty. However, the majority of studies suggest that Mexico is highly vulnerable to water security threats and that the population exposed to water stress could increase substantially with climate change. Recent simulations by the AVOID programme support this. A recent study suggests that severe drought conditions could be the 'normal state' in Southern Mexico by 2100 under an A1B emissions scenario.

Supporting literature

Introduction

For the purposes of this report droughts are considered to be extreme events at the lower bound of climate variability; episodes of prolonged absence or marked deficiency of precipitation. Water stress is considered as the situation where water stores and fluxes (e.g. groundwater and river discharge) are not replenished at a sufficient rate to adequately meet water demand and consumption.

A number of impact model studies looking at water stress and drought for the present (recent past) and future (climate change scenario) have been conducted. These studies are conducted at global or national scale and include the application of global water 'availability' or 'stress' models driven by one or more climate change scenario from one or more GCM. The approaches variously include other factors and assumptions that might affect water availability, such as the impact of changing demographics and infrastructure investment, etc. These different models (hydrological and climate), assumptions and emissions scenarios mean that there are a range of water stress projections for Mexico. This section summarises findings from these studies to inform and contextualise the analysis performed by the AVOID programme for this project. The results from the AVOID work and discussed in the next section.

Important knowledge gaps and key uncertainties which are applicable to Mexico as well as at the global-scale, include; the appropriate coupling of surface water and groundwater in hydrological models, including the recharge process, improved soil moisture and evaporation dynamics, inclusion of water quality, inclusion of water management (Wood et al. 2011) and further refinement of the down-scaling methodologies used for the climate driving variables (Harding et al. 2011).

Assessments that include a global or regional perspective

Recent past

Recent research presented by Vörösmarty et al. (2010) describes the calculation of an '*Adjusted Human Water Security Threat'* (HWS) indicator. The indicator is a function of the cumulative impacts of 23 biophysical and chemical drivers simulated globally across 46,517 grid cells representing 99.2 million km^2. With a digital terrain model at its base, the calculations in each of the grid boxes of this model take account of the multiple pressures on the environment, and the way these combine with each other, as water flows in river basins. The level of investment in water infrastructure is also considered. This infrastructure measure (the *investment benefits factor*) is based on actual existing built infrastructure, rather than on the financial value of investments made in the water sector, which is a very unreliable and incomplete dataset. The analysis described by Vörösmarty et al. (2010) represents the current state-of-the-art in applied policy-focussed water resource assessment. In this measure of water security, the method reveals those areas where this is lacking, which is a representation of human water stress. One drawback of this method is that no analysis is provided in places where there is 'no appreciable flow', where rivers do not flow, or only do so for such short periods that they cannot be reliably measured. This method also does not address places where water supplies depend wholly on groundwater or desalination, being piped in, or based on wastewater reuse. It is based on what is known from all verified peer reviewed sources about surface water resources as generated by natural ecosystem processes and modified by river and other hydraulic infrastructure (Vörösmarty et al., 2010).

Here, the present day HWS is mapped for Mexico. The model applied operates at 50km resolution, so, larger countries appear to have smoother coverage than smaller countries, but all are mapped and calculated on the same scale, with the same data and model, and thus comparisons between places are legitimate. It is important to note that this analysis is a comparative one, where each place is assessed *relative* to the rest of the globe. In this way, this presents a realistic comparison of conditions across the globe. As a result of this,

however, some places may seem to be less stressed than may be originally considered. One example is Australia, which is noted for its droughts and long dry spells, and while there are some densely populated cities in that country where water stress is a real issue, for most of the country, *relative to the rest of the world*, the measure suggests water stress (as measured by HWS defined by Vörösmarty et al. (2010)), is not a serious problem.

Figure 10 presents the results of this analysis for Mexico. For all of Mexico where rivers flow, the threats to human water security is found to be high or moderately high. Around Mexico City in particular, water stress is very high. Those areas where there is no appreciable flow rely on rainwater collection, groundwater, and trucked or piped water.

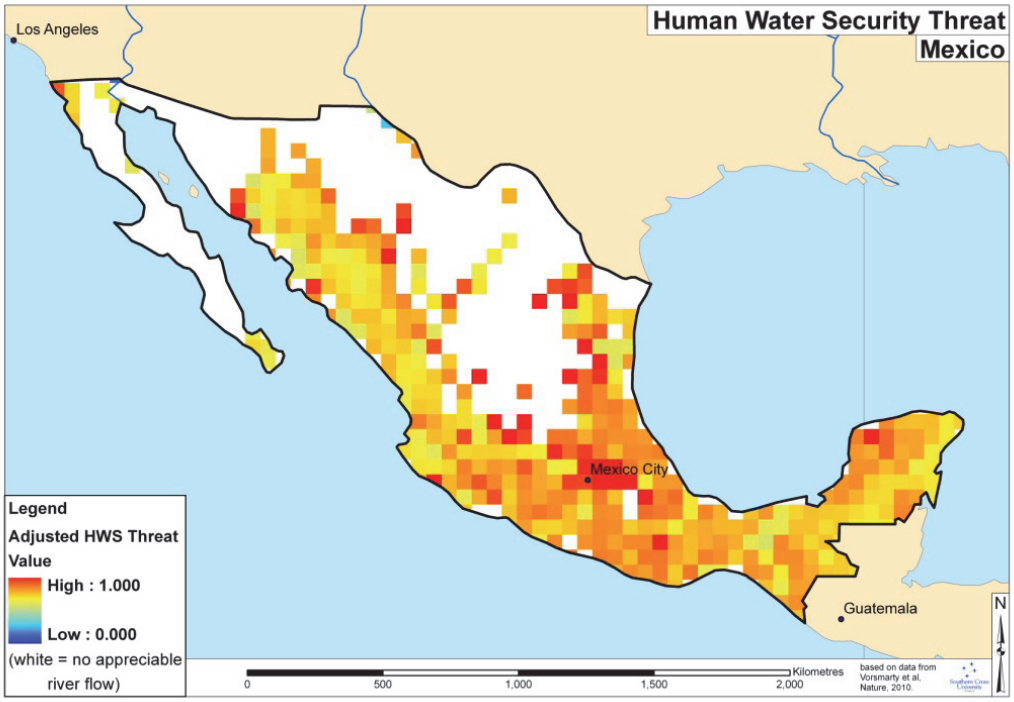

Figure 10. *Present Adjusted Human Water Security Threat (HWS) for Mexico, calculated following the method described by Vörösmarty et al. (2010).*

Smakhtin et al. (2004) present a first attempt to estimate the volume of water required for the maintenance of freshwater-dependent ecosystems at the global scale. This total environmental water requirement (EWR) consists of ecologically relevant low-flow and high-flow components. The authors argue that the relationship between water availability, total use and the EWR may be described by the water stress indicator (WSI). If WSI exceeds 1.0, the basin is classified as “environmentally water scarce”. In such a basin, the discharge has already been reduced by total withdrawals to such levels that the amount of water left in the basin is less than EWR. Smaller index values indicate progressively lower water resources

exploitation and lower risk of “environmental water scarcity.” Basins where WSI is greater than 0.6 but less than 1.0 are arbitrarily defined as heavily exploited or “environmentally water stressed” and basins where WSI is greater than 0.3 but less than 0.6 are defined as moderately exploited. In these basins, 0-40% and 40-70% of the utilizable water respectively is still available before water withdrawals come in conflict with the EWR. Environmentally “safe” basins are defined as those where WSI is less than 0.3. The global distribution of WSI for the 1961-1990 time horizon is shown in Figure 11. The results show that for the basins considered in Mexico, environmental water stress is high.

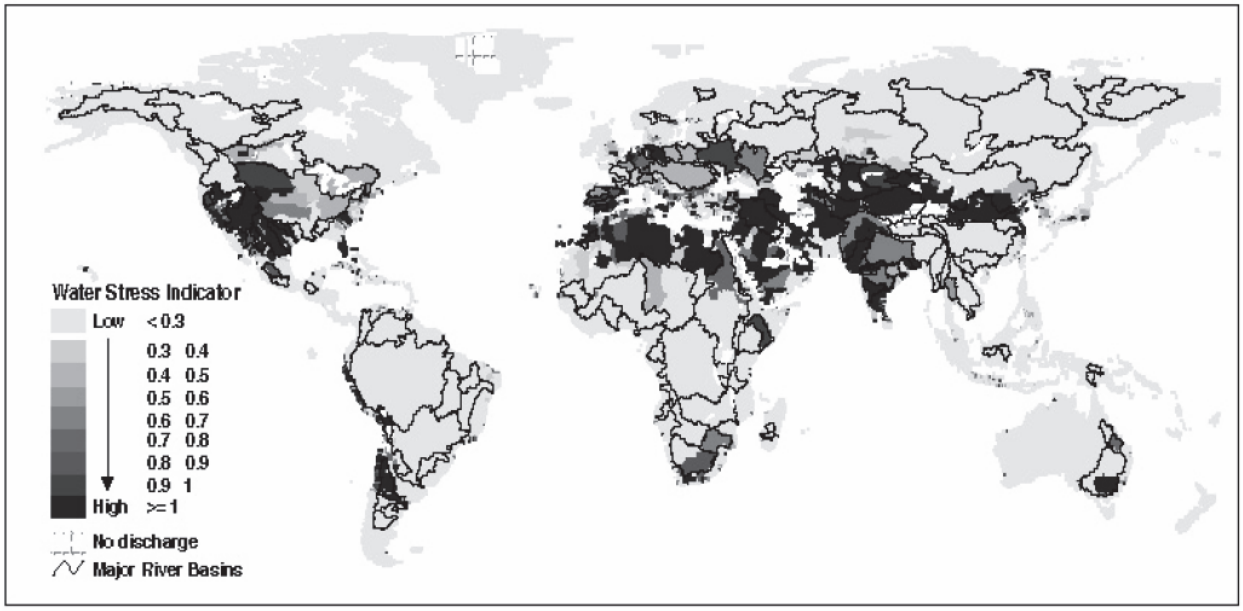

Figure 11. *A map of the major river basins across the globe and the water stress indicator (WSI) for the 1961-1990 time horizon. The figure is from Smakhtin et al. (2004).*

Climate Change Studies

Rockstrom et al. (2009) applied the LPJml vegetation and water balance model (Gerten et al. 2004) to assess green-blue water (irrigation and infiltrated water) availability and requirements. The authors applied observed climate data from the CRU TS2.1 gridded dataset for a present-day simulation, and climate change projections from the HadCM2 GCM under the SRES A2 scenario to represent the climate change scenario for the year 2050. The study assumed that if water availability was less than 1,300m^3/capita/year, then the country was considered to present insufficient water for food self-sufficiency. The simulations presented by Rockstrom et al. (2009) should not be considered as definitive, however, because the study only applied one climate model, which means climate modelling uncertainty was overlooked. The results from the two simulations are presented in Figure 12. Rockstrom et al. (2009) found that globally in 2050 and under the SRES A2 scenario, around

59% of the world's population could be exposed to "blue water shortage" (i.e. irrigation water shortage), and 36% exposed to "green water shortages" (i.e. infiltrated rain shortage). For Mexico, Rockstrom et al. (2009) found that blue-green water availability was well above the 1,300m^3/capita/year threshold in present conditions and under climate change, but it should be noted that this is based upon climate projections from a single GCM.

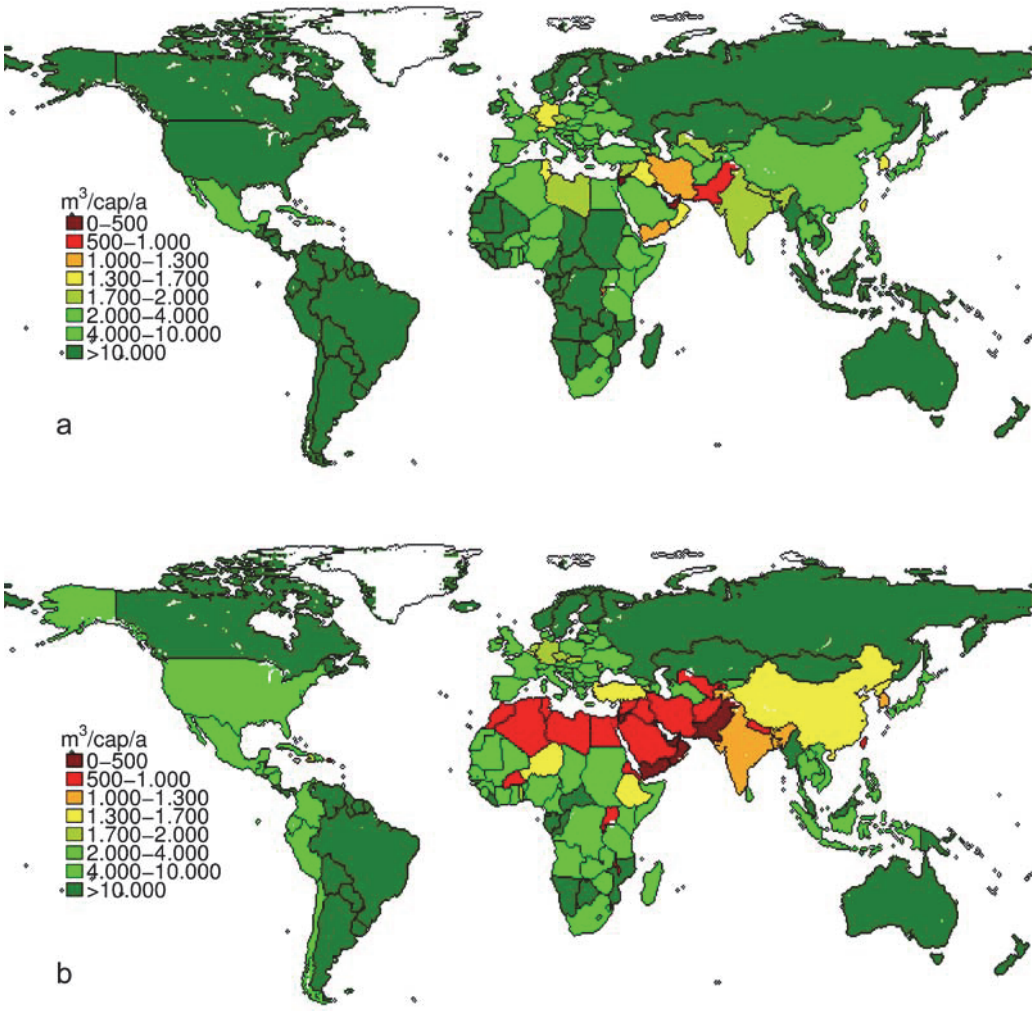

***Figure 12**. Simulated blue-green water availability (m^3/capita/year) for present climate (top panel) and including both demographic and climate change under the SRES A2 scenario in 2050 (bottom panel). The study assumed that if water availability was less than 1,300m^3/capita/year, then the country was considered to present insufficient water for food self-sufficiency. The figure is from Rockstrom et al. (2009).*

Doll (2009) presents updated estimates of the impact of climate change on groundwater resources by applying a new version of the WaterGAP hydrological model. The study accounted for the number of people affected by changes in groundwater resources under climate change relative to present (1961-1990). To this end, the study provides an assessment of the vulnerability of humans to decreases in available groundwater resources

(GWR). This indicator was termed the “Vulnerability Index” (VI), defined as; VI = -% change GWR * Sensitivity Index (SI). The SI component was a function of three more specific sensitivity indicators that include an indicator of water scarcity (calculated from the ratio between consumptive water use to low flows), an indicator for the dependence upon groundwater supplies, and an indicator for the adaptive capacity of the human system. Doll (2009) applied climate projections from two GCMs (ECHAM4 and HadCM3) to WaterGAP, for two scenarios (SRES A2 and B2), for the 2050s. Figure 13 presents each of these four simulations respectively. There is variation across scenarios and GCMs. For Mexico, the HadCM3 simulations demonstrate a medium to high VI in southern and eastern Mexico whereas ECHAM4 did not simulate decreases in GWR for much of the country.

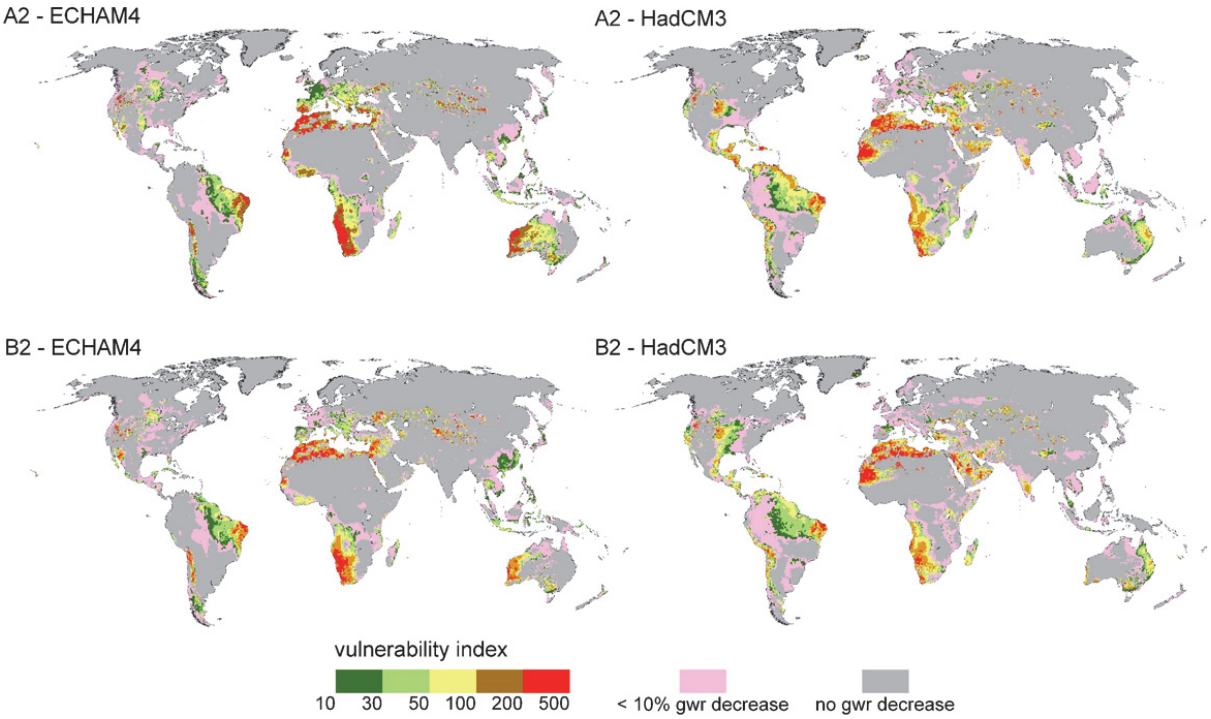

***Figure 13**. Vulnerability index (VI) showing human vulnerability to climate change induced decreases of renewable groundwater resources (GWR) by the 2050s under two emissions scenarios for two GCMs. VI is only defined for areas with a GWR decrease of at least 10% relative to present (1961-1990). The figure is from Doll (2009).*

Wehner et al. (2011) presented multi-model mean projections of the Palmer Drought Severity Index (PDSI) over North America at the end of the 21st Century under the SRES A1B emissions scenario. The authors showed that what is currently considered severe to extreme drought conditions could be normal climatology by 2100. Widespread drying was projected over much of North America at the point in time when the global mean temperature increases by 2.5°C. Severe drought conditions were projected to be the ‘normal state’ in

Southern Mexico. For the continental United States and Mexico, about 35% of the region's climatology was moderate drought and about 5% was extreme drought in this projection.

National-scale or sub-national scale assessments

Mexico's fourth national communication to the United Nations Framework on Climate Change (2009) has incorporated national-scale and sub-national scale studies published in the Spanish literature including institutional reports. In the English summary (main report not yet available in English) the Mexican government reports that studies on climate change impacts, vulnerability and adaptation have highlighted three main areas of concern: the lack of water in some states, the increase in distribution areas and number of dengue cases, as well as the gradual reduction of biodiversity in large areas of central and northern Mexico. The Third National Communication (2007) suggested that both Baja California and Sonora would face critical water shortages by 2020.

AVOID Programme Results

To further quantify the impact of climate change on water stress and the inherent uncertainties, the AVOID programme calculated water stress indices for all countries reviewed in this literature assessment based upon the patterns of climate change from 21 GCMs, following the method described by Gosling et al. (2010) and Arnell (2004). This ensures a consistent methodological approach across all countries and takes consideration of climate modelling uncertainties.

Methodology

The indicator of the effect of climate change on exposure to water resources stress has two components. The first is the number of people within a region with an *increase in exposure to stress*, calculated as the sum of 1) people living in water-stressed watersheds with a significant reduction in runoff due to climate change and 2) people living in watersheds which become water-stressed due to a reduction in runoff. The second is the number of people within a region with a *decrease in exposure to stress*, calculated as the sum of 1) people living in water-stressed watersheds with a significant increase in runoff due to climate change and 2) people living in watersheds which cease to be water-stressed due to an increase in runoff. It is not appropriate to calculate the net effect of "increase in exposure" and "decrease in exposure", because the consequences of the two are not equivalent. A water-stressed watershed has an average annual runoff less than $1000m^3$/capita/year, a

widely used indicator of water scarcity. This indicator may underestimate water stress in watersheds where per capita withdrawals are high, such as in watersheds with large withdrawals for irrigation.

Average annual runoff (30-year mean) is simulated at a spatial resolution of 0.5x0.5^{o} using a global hydrological model, MacPDM (Gosling and Arnell, 2011), and summed to the watershed scale. Climate change has a "significant" effect on average annual runoff when the change from the baseline is greater than the estimated standard deviation of 30-year mean annual runoff: this varies between 5 and 10%, with higher values in drier areas.

The pattern of climate change from 21 GCMs was applied to MacPDM, under two emissions scenarios; 1) SRES A1B and 2) an aggressive mitigation scenario where emissions follow A1B up to 2016 but then decline at a rate of 5% per year thereafter to a low emissions floor (denoted A1B-2016-5-L). Both scenarios assume that population changes through the 21st century following the SRES A1 scenario as implemented in IMAGE 2.3 (van Vuuren et al., 2007). The application of 21 GCMs is an attempt to quantify the uncertainty due to climate modelling, although it is acknowledged that only one impacts model is applied (MacPDM). Simulations were performed for the years 2030, 2050, 2080 and 2100. Following Warren et al. (2010), changes in the population affected by increasing or decreasing water stress represent the additional percentage of population affected due to climate change, not the absolute change in the percentage of the affected population relative to present day.

Results

The results for Mexico are presented in Figure 14. All the models in the study show some percentage of the population of Mexico experiencing increased water stress as a result of climate change. By 2080, under the A1B scenario, the median result shows around 95% of the population undergoing an increase in water stress, although the uncertainty is high (the full range of the models is 1-100%). The median result is the same under the aggressive mitigation scenario, but more of the models indicate lower levels of increased water stress. Declines in population by 2100 mean that exposure to increased water stress is lower in 2100 than in 2080 but the uncertainty across climate models remains large. The majority of GCMs are consistent in suggesting that climate change may be associated with little decrease in water stress in Mexico throughout the 21st century.

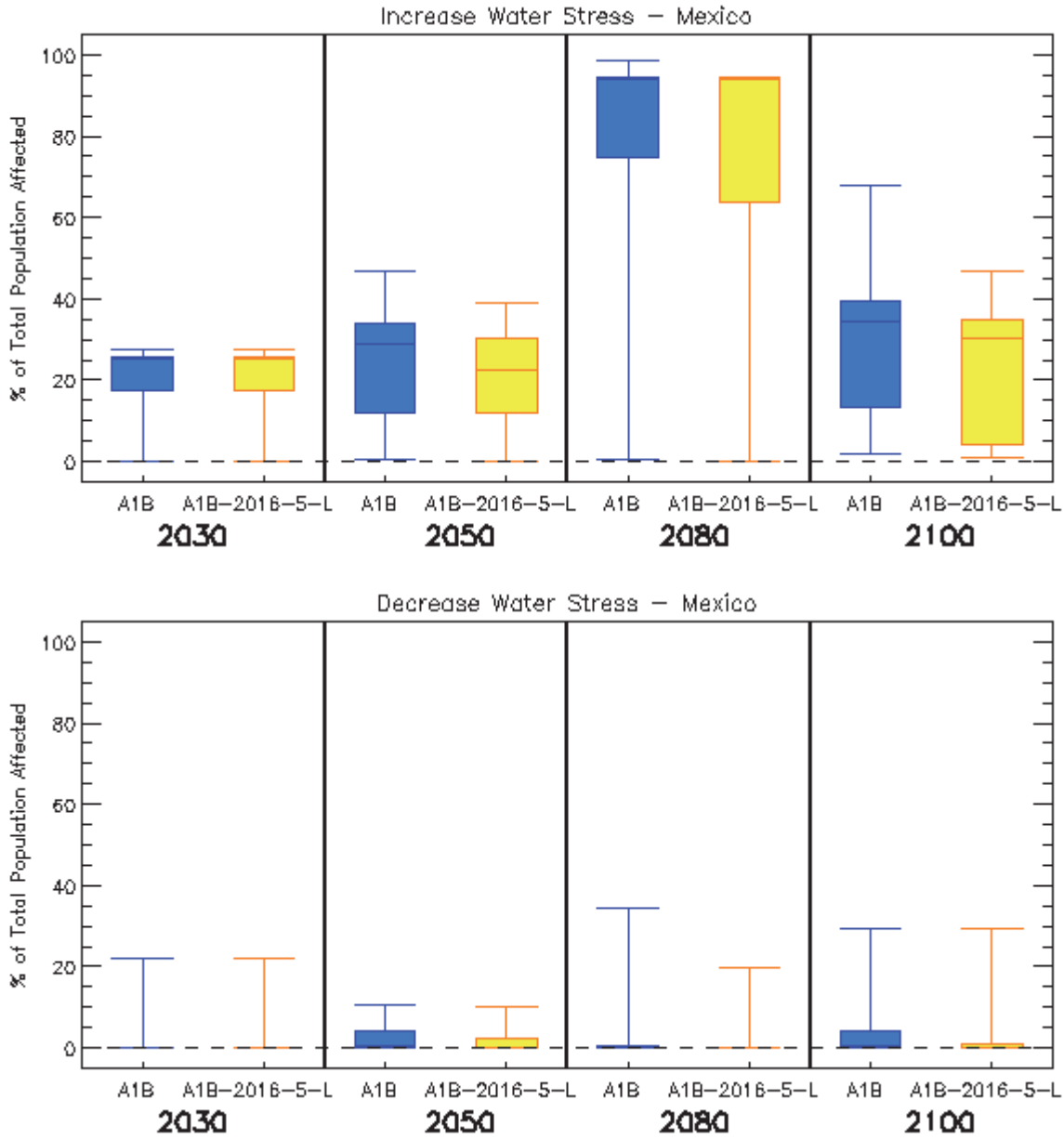

Figure 14. *Box and whisker plots for the impact of climate change on increased water stress (top panel) and decreased water stress (bottom panel) in Mexico, from 21 GCMs under two emissions scenarios (A1B and A1B-2016-5-L), for four time horizons. The plots show the 25th, 50th, and 75th percentiles (represented by the boxes), and the maximum and minimum values (shown by the extent of the whiskers).*

Pluvial flooding and rainfall

Headline

Recent studies, in common with the IPCC AR4, point towards a general decrease in mean precipitation over Mexico. However, studies of extreme precipitation suggest the possibility of increases, but with a large uncertainty attached to future projections of tropical cyclone occurrence.

Introduction

Pluvial flooding can be defined as flooding derived directly from heavy rainfall, which results in overland flow if it is either not able to soak into the ground or exceeds the capacity of artificial drainage systems. This is in contrast to fluvial flooding, which involves flow in rivers either exceeding the capacity of the river channel or breaking through the river banks, and so inundating the floodplain. Pluvial flooding can occur far from river channels, and is usually caused by high intensity, short-duration rainfall events, although it can be caused by lower intensity, longer-duration events, or sometimes by snowmelt. Changes in mean annual or seasonal rainfall are unlikely to be good indicators of change in pluvial flooding; changes in extreme rainfall are of much greater significance. However, even increases in daily rainfall extremes will not necessarily result in increases in pluvial flooding, as this is likely to be dependent on the sub-daily distribution of the rainfall as well as local factors such as soil type, antecedent soil moisture, land cover (especially urbanisation), capacity and maintenance of artificial drainage systems etc. It should be noted that both pluvial and fluvial flooding can potentially result from the same rainfall event.

Assessments that include a global or regional perspective

The IPCC AR4 (2007b) reported that the CMIP3 multi-model dataset showed a general decrease in precipitation over most of Central America where the median annual change by the end of the 21st century was -9% (compared to a 1980-1999 baseline) under the A1B emissions scenario. Half of the models projected mean changes of between -16% and -5%, although the full range of projections was between -48% and +9%. Mean precipitation for Central America decreased in most models in all seasons, with the exception of parts of NE Mexico, where increases in summer precipitation were projected. However, tropical cyclones can contribute significantly to rainfall totals during the hurricane season, and there is

therefore the possibility that rainfall could change as a result of storms which are not well captured by GCMs.

Saenz-Romero et al. (2010) examined climate change projections from three GCMs under the SRES A2 and B1 scenarios. Annual precipitation was projected to decrease by 7% by 2030, 9% by 2060, and 18% by 2090 (compared to a 1961-1990 baseline), but there was large variation between the GCMs and scenarios (see Figure 15). By 2090, all projections indicated that precipitation could decrease for Mexico, although the range was for a decrease of between 9% and 29% compared with 1961-1990. These results are consistent with those presented by the IPCC AR4 (2007b) where changes between +9% and -48% were simulated for Mexico and Central America for the 2080-2099 time horizon. Differences between the scenarios were small in the early part of the century but by 2060 the reduction was 10.9% under A1 and 5.7% under B2, whilst by 2090 the reduction of precipitation under A2 was 22%, compared with only 12.2% under B1.

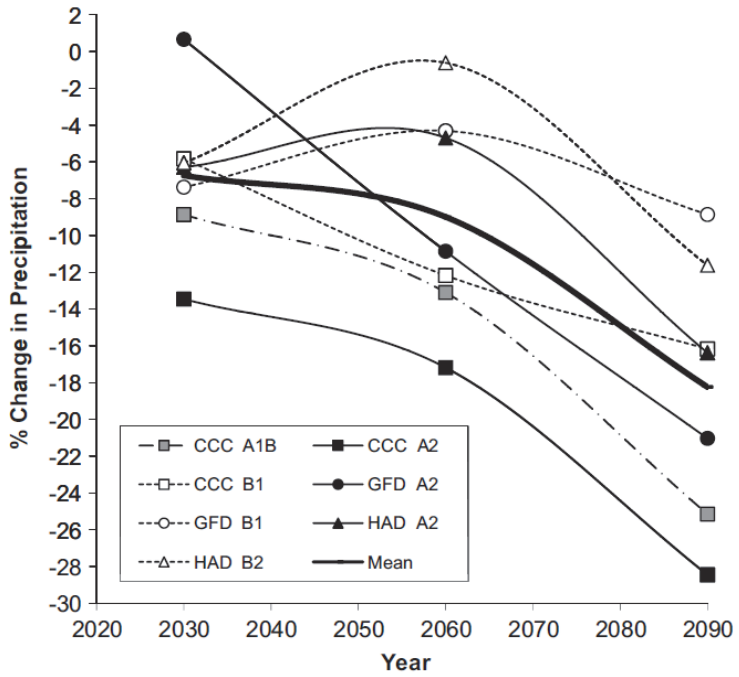

Figure 15. *Mean change in annual precipitation (%) for Mexico in comparison to contemporary climate (1961–1990) from 3,971 weather stations updated into the future using inverse distance weighted GCM grid point data from the Canadian Center for Climate Modeling and Analysis (CCC, scenarios A2, B1 and A1B), Hadley Centre (HAD, scenarios A2 and B2) and Geophysical Fluid Dynamics Laboratory (GFD, scenarios A2 and B1) for decades centred on years 2030, 2060 and 2090. The figure is from Saenz-Romero et al. (2010).*

National-scale or sub-national scale assessments

Peterson et al. (2008) investigated observed changes in precipitation and highlighted that in Mexico's northern Baja California there have been increases in heavy wintertime precipitation since 1977 (Cavazos and Rivas, 2004). Also, while heavy summer precipitation has not changed significantly over the last 30 years in central Mexico, very heavy (99th percentile) precipitation has increased (Groisman et al., 2005). Peralta-Hernandez et al. (2008) investigated observed trends in precipitation extremes at 44 stations in Southern Mexico between 1960 and 2004, a region where rainfall totals can be strongly affected by hurricane activity. They found an upward trend in the frequency and intensity of extremes, and also that they were more likely to occur during La Niña episodes. Arriaga-Ramirez and Cavazos (2010) studied observations of precipitation in northwest Mexico over the period of 1960-1997. Significant positive trends were found in extreme precipitation exceeding the 95th and 99th percentiles. There were also significant positive trends in the 95th percentile index during June-October, mainly due to tropical cyclone activity. El Niño and the Pacific Decadal Oscillation were important large-scale mechanisms underlying the trends and variability.

Fluvial Flooding

Headline

Few studies have investigated changes in flood hazard in Mexico under climate change scenarios. However, at least one-global-scale assessment suggest that flood frequency and magnitude may decrease with climate change. Simulations by the AVOID programme, based on climate change projections from 21 climate models, showed a greater tendency among models towards decreasing flood risk early in the 21st century. Later in the century the balance shifted towards an increase in flood risk under the A1B scenario, while under a mitigation scenario the majority of the models still showed a decrease. A regional analysis of changes in precipitation intensity, together with a better understanding of how climate change may affect the frequency and intensity of land-falling hurricanes, is required to further improve understanding of flood risk in Mexico.

Supporting literature

Introduction

This section summarises findings from a number of post IPCC AR4 assessments on river flooding in Mexico to inform and contextualise the analysis performed by the AVOID programme for this project. The results from the AVOID work are discussed in the next section.

Fluvial flooding involves flow in rivers either exceeding the capacity of the river channel or breaking through the river banks, and so inundating the floodplain. A complex set of processes is involved in the translation of precipitation into runoff and subsequently river flow (routing of runoff along river channels). Some of the factors involved are; the partitioning of precipitation into rainfall and snowfall, soil type, antecedent soil moisture, infiltration, land cover, evaporation and plant transpiration, topography, groundwater storage. Determining whether a given river flow exceeds the channel capacity, and where any excess flow will go, is also not straightforward, and is complicated by the presence of artificial river embankments and other man-made structures for example. Hydrological models attempt to simplify and conceptualise these factors and processes, to allow the simulation of runoff

and/or river flow under different conditions. However, the results from global-scale hydrological modelling need to be interpreted with caution, especially for smaller regions, due to the necessarily coarse resolution of such modelling and the assumptions and simplifications this entails (e.g. a 0.5^{o} grid corresponds to landscape features spatially averaged to around 50-55km for mid- to low-latitudes). Such results provide a consistent, high-level picture, but will not show any finer resolution detail or variability. Smaller-scale or catchment-scale hydrological modelling can allow for more local factors affecting the hydrology, but will also involve further sources of uncertainty, such as in the downscaling of global climate model data to the necessary scale for the hydrological models. Furthermore, the application of different hydrological models and analysis techniques often makes it difficult to compare results for different catchments.

Assessments that include a global or regional perspective

Climate change studies

A global modelling study by Hirabayashi et al. (2008), applied simulations from a single GCM under the A1B emission scenario and projected that in the next few decades (2001-2030) the return period of what was a 100-year flood event in the 20th century increases in large parts of the country, suggesting a general decrease in flood frequency. By the end of the century (2071-2100) the return period of a 100-year flood was projected to increase to more than 140 year in most of the country, with the possible exception of northern Yucatán and the northwest corner of the country where the flood hazard might increase (Hirabayashi et al., 2008). It should be noted, however, that results from studies that have applied only a single climate model or climate change scenario should be interpreted with caution. This is because they do not consider other possible climate change scenarios which could result in a different impact outcome, in terms of magnitude and in some cases sign of change.

The Rio Grande, on the US-Mexican border, was included in a global modelling study by Nohara et al. (2006) that applied climate change projections from 19 GCMs under the A1B emissions scenario for the end of the 21^{st} century (2081-2100). The results mostly showed a decrease in the high-flow season discharge of the Rio Grande. However the biases in the simulations were large as the model did not account for irrigation, dams and evaporation from open water surfaces (Nohara et al., 2006).

National-scale or sub-national scale assessments

Gratiot et al. (2010) analysed streamflow records for the Cointzio watershed (Michoacán state), a medium scale mountainous basin representative of the Central Transvolcanic Mexican Belt. They found an increase in surface runoff since the early 1970s which was attributed to changes in land use. As a consequence, the intensity of annual extreme floods has tripled over the period of survey, increasing flood risks in this region. The authors did not make projections of future changes in precipitation intensity and flood frequency. However, the projected increase in aridity in this region is likely to reduce the vegetation cover, which in itself could accentuate the contribution of surface runoff (Gratiot et al., 2010). A regional analysis of changes in precipitation intensity, together with a better understanding of how climate change may affect the frequency and intensity of land-falling hurricanes, is required to further improve understanding of flood risk in Mexico.

AVOID programme results

To quantify the impact of climate change on fluvial flooding and the inherent uncertainties, the AVOID programme calculated an indicator of flood risk for all countries reviewed in this literature assessment based upon the patterns of climate change from 21 GCMs (Warren et al., 2010). This ensures a consistent methodological approach across all countries and takes consideration of climate modelling uncertainties.

Methodology

The effect of climate change on fluvial flooding is shown here using an indicator representing the percentage change in average annual flood risk within a country, calculated by assuming a standardised relationship between flood magnitude and loss. The indicator is based on the estimated present-day (1961-1990) and future flood frequency curve, derived from the time series of runoff simulated at a spatial resolution of 0.5°x0.5° using a global hydrological model, MacPDM (Gosling and Arnell, 2011). The flood frequency curve was combined with a generic flood magnitude–damage curve to estimate the average annual flood damage in each grid cell. This was then multiplied by grid cell population and summed across a region, producing in effect a population-weighted average annual damage. Flood damage is thus assumed to be proportional to population in each grid cell, not the value of exposed assets, and the proportion of people exposed to flood is assumed to be constant across each grid cell (Warren et al., 2010).

The national values are calculated across major floodplains, based on the UN PREVIEW Global Risk Data Platform (preview.grid.unep.ch). This database contains gridded estimates, at a spatial resolution of 30 arc-seconds (0.00833°x0.00833°), of the estimated frequency of flooding. From this database the proportion of each 0.5°x0.5° grid cell defined as floodplain was determined, along with the numbers of people living in each 0.5°x0.5° grid cell in flood-prone areas. The floodplain data set does not include "small" floodplains, so underestimates actual exposure to flooding. The pattern of climate change from 21 GCMs was applied to MacPDM, under two emissions scenarios; 1) SRES A1B and 2) an aggressive mitigation scenario where emissions follow A1B up to 2016 but then decline at a rate of 5% per year thereafter to a low emissions floor (denoted A1B-2016-5-L). Both scenarios assume that population changes through the 21st century following the SRES A1 scenario as implemented in IMAGE 2.3 (van Vuuren et al., 2007). The application of 21 GCMs is an attempt to quantify the uncertainty due to climate modelling, although it is acknowledged that only one impacts model is applied (MacPDM). Simulations were performed for the years 2030, 2050, 2080 and 2100. The result represents the change in flood risk due to climate change, not the change in flood risk relative to present day (Warren et al., 2010).

Results

The results for Mexico are presented in Figure 16. By the 2030s, the models project a range of changes in mean fluvial flooding risk over Mexico in both scenarios, with some models projecting decreases and others increases. However, the balance is more towards lower flood risk, with more than 50% of the models projecting a decrease. The largest decrease projected for the 2030s is −60%, while the largest increase is +100%. The mean across all projections is a decrease in annual average flood risk of approximately 5%.

By 2100 the difference in projections from the different models and from both scenarios becomes greater. Under the mitigation scenario, a majority of the models still project a decrease in flood risk (down to −80%), but several models now project larger increases (up to almost +200%). The mean of all projections is a decrease of 10%. Under the A1B scenario, the balance has shifted towards an increase in flood risk, with less than half of the models project a decrease (down to nearly 90%). The largest increase that is projected is about 550%, but the mean over all projections is an increase of only 10%.

So for Mexico, the models show a greater tendency towards decreasing flood risk at first, but later in the century the balance shifts towards an increase under the A1B scenario, while under the mitigation scenario a majority of the models still projects lower flood risk. The differences between the model projections are greater later in the century and particularly for A1B.

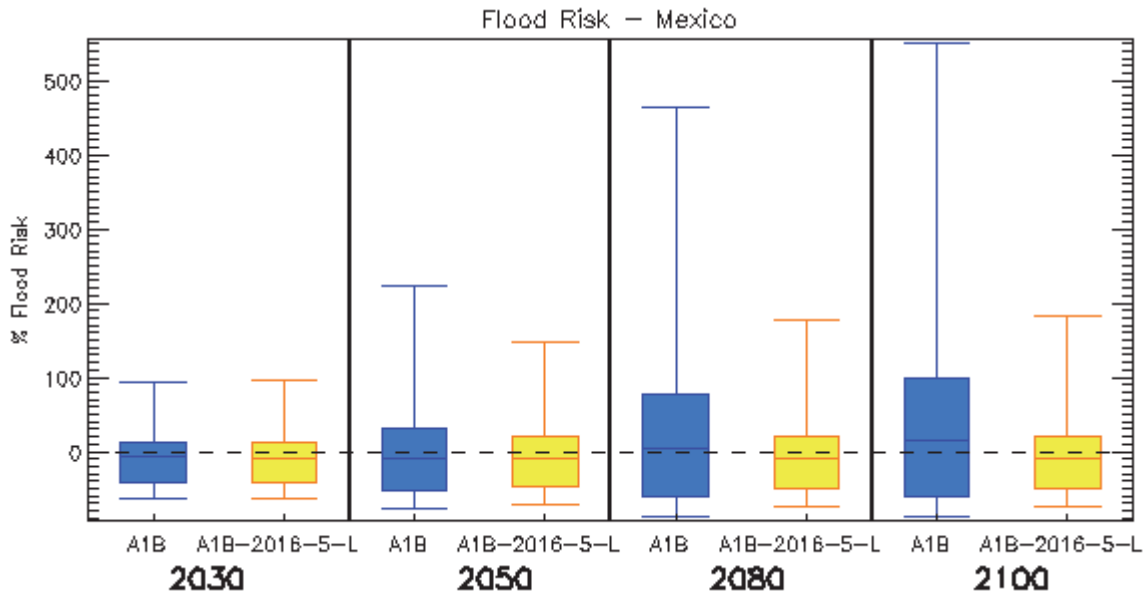

Figure 16. *Box and whisker plots for the percentage change in average annual flood risk within Mexico, from 21 GCMs under two emissions scenarios (A1B and A1B-2016-5-L), for four time horizons. The plots show the 25th, 50th, and 75th percentiles (represented by the boxes), and the maximum and minimum values (shown by the extent of the whiskers).*

Tropical cyclones

Headline

Projections of the impact of climate-change on tropical-cyclone *frequency* for Mexico are currently uncertain for both the Gulf of Mexico and the East Pacific. For the former basin, the uncertainty is due the small size of the basin and the limited resolution of the climate models. For the latter, the uncertainty is due to disagreement among models on the sign of the change in frequency in a warmer world. The majority of studies reviewed here suggest that tropical cyclone *intensities* could increase in both basins with climate change. The uncertainty in the magnitude of this change, coupled with the uncertainty in cyclone frequencies, makes estimates of future cyclone damages in Mexico due to climate change highly uncertain.

Introduction

Tropical cyclones are different in nature from those that exist in mid-latitudes in the way that they form and develop. There remains an overall large uncertainty in the current understanding of how tropical cyclones might be affected by climate change because conclusions are based upon a limited number of studies. Moreover, the majority of tropical-cyclone projections are from either coarse-resolution global models or from statistical or dynamical downscaling techniques. The former are unable to represent the most-intense storms, whereas the very patterns used for the downscaling may change under climate change. To this end, caution should be applied in interpreting model-based results, even where the models are in agreement.

Assessments that include a global or regional perspective

Tropical cyclones make landfall in Mexico from both the Gulf of Mexico and the East Pacific Ocean. Since modelling studies separate their projections of future tropical-cyclone activity by basin, the results here are organized similarly.

East Pacific

Assessment of cyclone frequency

Projections of changes in tropical-cyclone frequency in the East Pacific due to climate change are currently uncertain, even in the sign of the change, due to disagreement among modelling studies.

Bengtsson et al. (2007) conducted experiments with the atmospheric component of the ECHAM5 GCM at 60km and 40km resolutions respectively. The model was driven by sea surface temperatures (SSTs) and sea ice simulated by the lower-resolution version of the GCM under the A1B emission scenario. The study investigated the 2071-2100 time horizon for the 60km simulation and 2081-2100 for the 40km simulation. The 2081-2100 time horizon was compared with a present-day simulation using SSTs and sea ice for the 1980-2000 time horizon. The simulation results are summarised in Figure 17. The two climate-change experiments simulated an increase in eastern Pacific tropical cyclones, with a 4% increase in the 60km model and a 7% increase in the 40km model. These increases were due to an overall eastward shift in Pacific cyclogenesis (cyclone formation), due to a decrease in vertical wind shear, which is conducive to cyclogenesis, in the East Pacific and an increase in shear and in atmospheric stability in the West Pacific.

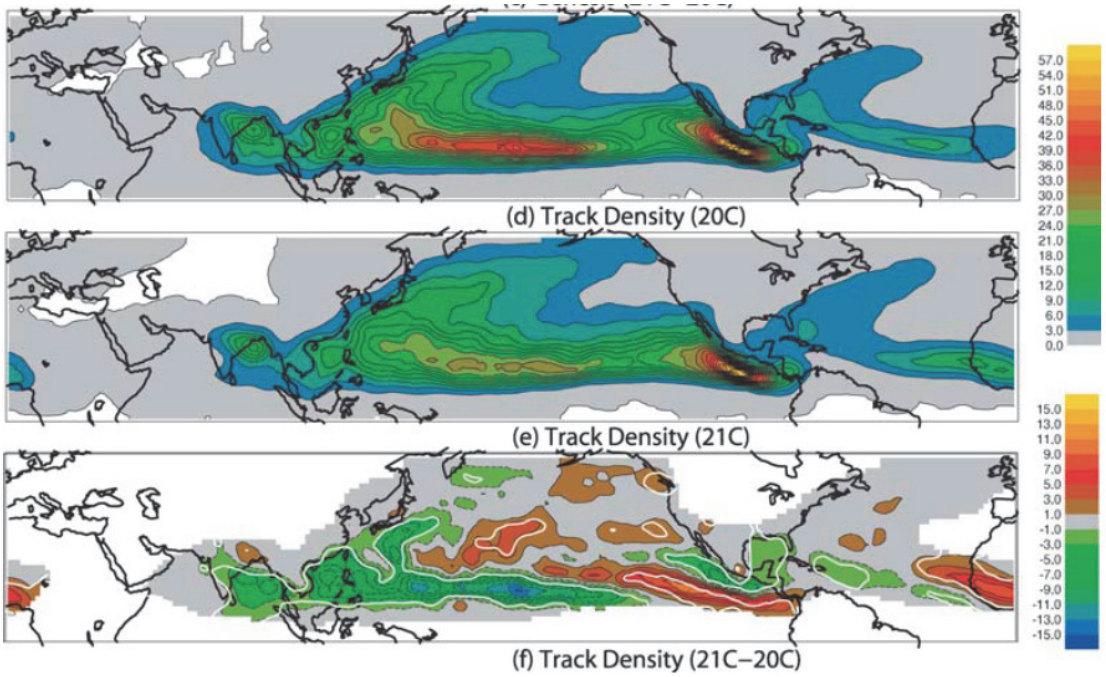

Figure 17. *Tracks of tropical cyclones simulated by the 60km resolution ECHAM5 GCM for the present-day climate (top panel; 1980-2000), under the A1B emissions scenario for the 2071-2100 time horizon (middle), and the difference between the two (bottom panel). The units are cyclones per year per unit area, where the unit area is approximately 106 km2. The prominent features are the shift in tropical-cyclone tracks away from the western coast of Mexico and the decrease in tracks in the South China Sea and near Japan. The figure is adapted from Bengtsson et al. (2007).*

McDonald et al. (2005) found large increases in East Pacific cyclone frequencies. The authors conducted an experiment with the Hadley Centre atmospheric model (HadAM3) at 100km resolution, driven by SST and sea-ice changes from the HadCM3 GCM under the IPCC IS95a greenhouse-gas scenario for the 2081-2100 time horizon. The authors compared the results of this timeslice experiment (experiments over a short period of time to enable ensemble simulations using reasonable amounts of computational power) to a similar conducted for 1979-1994, but using observed SSTs and sea-ice. The 2081-2100 simulation showed an 80% increase in the number of tropical cyclones in the East Pacific, which was statistically significant at the 5% level. There was, however, also a shift in cyclogenesis away from the Mexican coast in this simulation, which suggests that more cyclones could track out into the open ocean and fewer could strike Mexico. These sub-basin-scale results are highly uncertain, however, due to the limited resolution of this model and the use of only a single GCM (i.e., not an ensemble). It should be noted that results from studies that have applied only a single climate model or climate change scenario should be interpreted with caution. This is because they do not consider other possible climate change scenarios which could

result in a different impact outcome, in terms of magnitude and in some cases sign of change.

Zhao et al. (2009) applied the 50km GFDL GCM with four future SST and sea ice distributions; 1) the ensemble-mean from 18 GCMs included in the CMIP3 multi-model dataset, 2) the HadCM3 GCM, 3) the GFDL GCM, and 4) the ECHAM5 GCM. The SSTs distributions were for the A1B emissions scenario for the 2081-2100 time horizon. In three of the four experiments, including the one driven by the CMIP3 ensemble-mean, the frequency of cyclones in the East Pacific basin increased, with the increases ranging between 15% and 61%. However, the fourth simulation, which was with the GFDL GCM, showed a decrease in tropical cyclone frequency of 23%.

Decreases in West Pacific cyclone frequency were also reported by Oouchi et al. (2006). The authors applied the JMA climate model at 20km resolution, using the mean 2080-2099 SSTs and sea ice simulated by the MRI GCM under the A1B emissions scenario. The authors found 34% fewer cyclones in the East Pacific under the climate-change scenario, which they concluded were due to increased atmospheric stability in a warmer world; the model simulated a 10% increase in the global dry static stability, defined as the difference in potential temperature between the 250hPa level of the atmosphere and the land surface.

Further evidence for decreases in East Pacific cyclone frequency are presented by Sugi et al. (2009). The authors conducted experiments with the JMA climate model, at 60km and 20km resolutions respectively, with SSTs and sea ice from three individual GCMs as well as the CMIP3 multi-model dataset ensemble-mean. This meant eight simulations were performed, all using the A1B emissions scenario, for the end of the 21st century. In all eight experiments, the frequency of East Pacific cyclones decreased. The magnitudes of the decreases were reasonably consistent, ranging from 25% to 50% across all eight experiments.

Further complicating the evidence from projections of cyclone frequency, two studies have found roughly no change in the East Pacific relative to the present-day climate. Gualdi et al. (2008) applied the 120km resolution SINTEX-G climate model in a 30-year simulation under a 2xCO_2 emissions scenario. The authors found that East Pacific cyclones decreased by 3%, which is well inside the range of natural variability. Also, Emanuel et al. (2008) applied a hybrid statistical-dynamical downscaling method to seven GCMs under the A1B emissions scenario for the 2180-2200 time horizon. The technique they applied “seeds” large numbers of tropical-cyclone vortices into each basin, then uses the models' large-scale climate fields (e.g., SSTs, wind shear, relative humidity) to determine whether the storms grow into

cyclones or simply decay. By comparing the A1B scenario results for 2180-2200 to downscaled reanalysis data for 1980-2000, the authors concluded that East Pacific cyclone numbers could decrease by 5% with climate change. Two of the seven GCMs simulated an increase in cyclone frequencies, however, while four simulated decreases and one showed nearly no change.

Assessment of cyclone intensity

Despite uncertainty in projections of cyclone *frequency*, it is possilbe that cyclone *intensities* in the East Pacific could increase, particularly for the most intense storms. In their 60km ECHAM5 GCM simulation, Bengtsson et al. (Bengtsson et al., 2007) observed a 33% increase in the frequency of Northern Hemisphere storms with wind speeds exceeding 50 m s^{-1}, under A1B emissions by the end of the 21st century. The authors reported that "most of this increase" occurred in the East Pacific and the North Atlantic, but did not present quantitative results for each basin. Knutson and Tuleya (2004) applied nine GCMs from the CMIP2 multi-model dataset under a 1% per year CO_2 increase scenario and found that the wind speeds of East Pacific cyclones increased by 5-16% at the time of CO_2 doubling. Knutson and Tuleya (2004) also downscaled the results of the CMIP2 GCMs a using the 9 km operational GFDL hurricane model. East Pacific cyclone wind speeds strengthened by 6.6% in the mean across all models at the time of CO_2 doubling, with individual model projections ranging from 1.1% to 10.1%. Oouchi et al. (2006) found a relatively smaller intensification in their 20 km JMA model, with the mean wind speed of East Pacific cyclones increasing by just 0.6%, under A1B emissions at the end of the 21st century. Vecchi and Soden (2007) applied 18 GCMs under the A1B emissions scenario and showed that the mean model projection was a 3.5% increase in East Pacific cyclone wind speeds by 2100.

It is therefore possible that East Pacific cyclone intensities could increase with climate change, particularly for the most intense storms, in agreement with findings for global (Kitoh et al., 2009, McDonald et al., 2005, Oouchi et al., 2006).

Gulf of Mexico

Due to the small size of the Gulf of Mexico and the limited horizontal resolution of many climate models, the Gulf of Mexico has not been analysed as a separate basin in most studies on climate change and tropical cyclone activity. Therefore, results from assessments for the entire North Atlantic basin are reviewed here. Such aggregated findings may be of little use for Mexico, however, due to the potentially large intra-basin variability in Atlantic cyclone tracks. Several studies have attempted to separate projections of changes in Atlantic cyclone activity into smaller sub-basins; these are noted where applicable. It is

acknowledged that these results are highly uncertain, as even the sign of the change in aggregated Atlantic cyclone frequencies varies among the studies considered.

Note that where studies have previously been introduced for the East Pacific basin, the details of their simulations will not be repeated here, for conciseness.

Assessment of cyclone frequency

The majority of studies considered conclude that the frequency of tropical cyclones in the North Atlantic could decrease with global climate change. Knutson et al. (2008) employed an 18km resolution RCM to downscale the ensemble-mean of 18 GCMs from the CMIP3 multi-model dataset under the A1B emissions scenario. The model spontaneously generates tropical-cyclone-like disturbances, which depending on the background atmospheric conditions either develop into cyclones or decay. The model simulates observed tropical-cyclone frequencies, but its limited resolution prevents it from producing the most intense cyclones observed. When applied to the ensemble mean of the 18 GCMs, the RCM simulated a 27% decrease in tropical cyclones in the North Atlantic, with an 18% decrease in the number of hurricanes and an 8% decrease in the frequency of major hurricanes (categories 3, 4 and 5) for the 2080-2099 time horizon. Knutson et al. (2008) concluded that increasing vertical wind shear and decreases in relative humidity were the key driving factors in reducing cyclone frequencies in a warmer climate. The decreases in frequency were stronger in the western Atlantic than in the east, which suggests that the number of landfalling storms in Mexico may be reduced by more than the basin-average (27% decrease).

GCM simulations have also simulated a decrease in cyclones in the North Atlantic basin. Gualdi et al. (2008) found that cyclone frequency decreased by 14% at the point of CO_2 doubling. Bengtsson et al. (2007) found 8% and 13% decreases in North Atlantic cyclones in their 60km and 40km simulations, respectively (see Figure 17. Experiments with the Hadley Centre atmospheric model (HadAM3) at 100km resolution demonstrated a 30% reduction in cyclone frequencies (McDonald et al., 2005). Zhao et al. (2009) found considerable variability among the four experiments in their study; while the HadCM3 GCM simulated a 62% decrease in cyclone frequency, the GFDL and ECHAM5 GCMs showed nearly no change in cyclone frequency in the North Atlantic, under the A1B emissions scenario for the 2081-2100 time horizon.

Murakami and Wang (2010) applied the 20km MRI atmosphere-only GCM, driven by the ensemble-mean warming trend in SSTs simulated by the CMIP3 multi-model dataset, under the A1B emissions scenario and present-day inter-annual SST variability. A 25 year

simulation of this high-resolution model demonstrated a considerable shift in tropical-cyclone genesis regions to the north and east compared to the present-day climate. This also caused a shift in cyclone tracks, such that the model simulated fewer storms in the western North Atlantic and more in the eastern half of the basin. The reduced genesis in the western North Atlantic was due to a drying of the mid-troposphere and remotely forced anomalous descent, rather than local changes in thermodynamic forcing. The anomalous descent in the west resulted from increased ascending motion in the eastern half of the basin, itself the result of large simulated SST increases there, which supported the increased genesis in the eastern North Atlantic. These results support the conclusion of Knutson et al. (2008), that the number of land-falling storms in Mexico may be reduced as a result of climate change.

Garner et al. (2009) applied a 16km resolution RCM to downscale the ensemble-mean of 18 GCMs from the CMIP3 multi-model dataset under the A1B emissions scenario for the North Atlantic in August-October only. The ensemble-mean change in SST, wind, temperature and humidity from the CMIP3 models for the 2081-2100 time horizon was applied to reanalysis data for 1981-2000. The RCM simulated a 20-30% decrease in cyclone frequencies throughout the North Atlantic. The authors noted that the wind shear increased appreciably in the Caribbean, which would suggest a decrease in cyclones in the Gulf of Mexico that exceeded the basin average. Sugi et al. (2009) found an even greater spread among the CMIP3 multi-model dataset GCMs for the North Atlantic. Of their eight downscaling experiments with the JMA climate model, two experiments showed a decrease in North Atlantic cyclones, three simulated an increase in frequency, and the remaining three demonstrated no change from the present-day climate.

While some studies have found an increase in North Atlantic cyclone frequencies, the weight of evidence, particularly that from high-resolution simulations, lies on the side of an overall decrease in frequency.

Assessment of cyclone intensity

Whilst the overall frequency of cyclones could decrease, the intensity of North Atlantic cyclones could increase, particularly for the most-intense cyclones. Oouchi et al. (2006) concluded that the mean maximum wind speed of tropical cyclones increased by 11%, while the maximum wind speed of the most intense storm in the North Atlantic each year increased by an average of 20%, under A1B emissions at the end of the 21st century. The 18km RCM applied by Knutson et al. (2008) simulated a 3% increase in mean cyclone intensity for 2080-2099 under A1B emisions, but a doubling of the most intense storms in the model, i.e. those with wind speeds stronger than 45 m s^{-1}. Applying the GFDL hurricane

model at 9km resolution, Bender et al. (2010) downscaled the CMIP3 multi-model dataset ensemble mean and four individual GCMs, all using the A1B emissions scenario. The results are presented in Figure 18. The authors concluded that the frequency of category 4 and category 5 storms could double by 2100, supporting the results presented by Knutson et al. (Knutson et al., 2008). Knutson and Tuleya (2004) found that North Atlantic cyclone wind speeds increased by 1-6% in the mean, at the point of atmospheric CO_2 doubling. Vecchi and Soden (2007) conducted a similar study using the CMIP3 multi-model dataset and found no change in mean intensity.

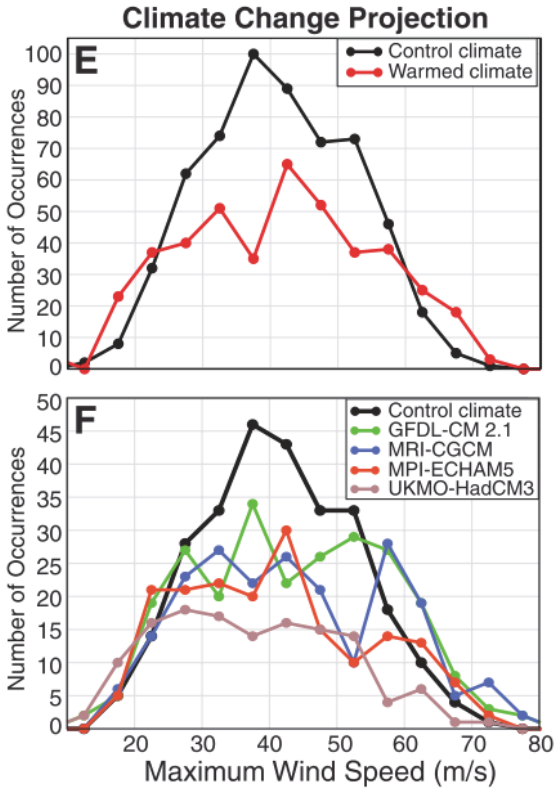

Figure 18. *The simulated maximum wind speeds of North Atlantic tropical cyclones from the GFDL operational hurricane model. The top panel displays simulations for the present-day climate (black line) and under climate change with the A1B emissions scenario (red line) using the ensemble-mean large-scale atmospheric conditions and SSTs from 18 GCMs. The bottom panel shows the same as the top panel, except here the climate change scenario is simulated by four separate GCMs. The figure is from Bender et al. (□HYPERLINK "../../../AppData/Local/Microsoft/Windows/Temporary Internet Files/Content.Outlook/Impacts/Mexico_V19.doc" \l "_ENREF_8#_ENREF_8" \o "Bender, 2010 #912"□□2010□).*

Zhao and Held (2010) also found increases in cyclone intensity, using the same 50km GFDL GCM and future SST distributions applied by Zhao et al. (2009), but with a statistical adjustment to the simulated tropical-cyclone intensities. The adjustment was calibrated by comparing modelled tropical cyclones using SSTs from the 1981-2008 period to observed cyclones, then applied to the simulated tropical-cyclones for the 2081-2100 period under the A1B emissions scenario. Using this method, Zhao and Held (2010) were able to separate simulated intensity changes into a component that was associated with a change in the frequency of storms (i.e., the authors found a positive correlation between cyclone frequency and intensity) and a purely climate-change-driven component. Zhao and Held (2010) argued that the climate-change component should be independent of the spatial pattern of SST warming simulated by the individual CMIP3 multi-model dataset GCMs, thus removing a considerable source of uncertainty. In this framework, climate change was responsible for a

5-10 m s^{-1} increase in the wind speed of strong North Atlantic storms, defined as those with wind speeds of 30-60 m s^{-1}, for approximately a 17% increase.

Assessment of precipitation change

In addition to wind-speed increases, the *intensity of precipitation* near the centre of tropical cyclones is expected to strengthen with climate change. Knutson et al. (2008) found a 37% increase in precipitation within 50km of the storm centre for North Atlantic cyclones, a 23% increase within 100km and a 10% increase within 400km. Results presented by Knutson and Tuleya (2004) support this. They applied the CMIP2 multi-model dataset GCMs and the 9km GFDL GCM, and showed that climate change was associated with a 22% increase in precipitation within 100km of the centre. Chauvin et al. (2006) also found a statistically significant, substantial increase in precipitation when downscaling the HadCM3 GCM under SRES A2 emissions. These increases in precipitation agree with global studies that did not consider specific basins (Bengtsson et al., 2007, Gualdi et al., 2008, Hasegawa and Emori, 2005, Yoshimura et al., 2006).

Assessment of cyclone damages

There remains considerable uncertainty in the projections of changes in cyclone frequency in the East Pacific and the North Atlantic, particularly in the Gulf of Mexico sub-basin. While the overall intensity of storms could increase in both basins, particularly for the most intense storms, the uncertainty in the frequency and tracks of these storms leads to high uncertainty in projections of future cyclone damages in Mexico due to climate change.

To estimate the impact of climate change on tropical cyclone damages, Mendelsohn et al. (2011) applied the cyclone "seeding" method described by Emanuel et al. (2008) to climate change projections from four GCMs under the A1B emissions scenario. They then constructed a damage model to estimate the damages from each landfalling storm. The model separates the additional damages from the impact of climate change on tropical cyclones from the additional damages due to future economic development. This is accomplished through applying the damages from both present-day and future tropical cyclones to the projected economic conditions in 2100 (the "future baseline"). Against a future baseline of $2.29 billion in damages per year in Mexico, two of the four GCMs considered simulated a decrease in cyclone damages due to climate change; the CNRM GCM ($0.37 billion) and the ECHAM5 GCM ($0.128 billion). The GFDL model simulated little change (a $0.02 billion decrease) and the MIROC model simulated a $0.55 billion increase in damages. The range of these changes indicates the high level of uncertainty in

understanding of the response of East Pacific and North Atlantic tropical cyclones to climate change.

National-scale or sub-national scale assessments

Literature searches yielded no results for national-scale or sub-national scale studies for this impact sector.

Coastal regions

Headline

Two global-scale studies suggest that Mexico's population is not highly vulnerable to sea level rise (SLR), relative to other countries across the globe. One of these studies suggests that SLR could have little or no affect on Mexico's population. However, another study found that out of 84 developing countries considered, Mexico was ranked the 7th highest with respect to the amount of agricultural land that could be submerged with a simulated 1m SLR.

Assessments that include a global or regional perspective

The IPCC AR4 concluded that at the time, understanding was too limited to provide a best estimate or an upper bound for global SLR in the twenty-first century (IPCC, 2007b). However, a range of SLR, excluding accelerated ice loss effects was published, ranging from 0.19m to 0.59m by the 2090s (relative to 1980-2000), for a range of scenarios (SRES A1FI to B1). The IPCC AR4 also provided an illustrative estimate of an additional SLR term of up to 17cm from acceleration of ice sheet outlet glaciers and ice streams, but did not suggest this is the upper value that could occur. Although there are published projections of SLR in excess of IPCC AR4 values (Nicholls et al., 2011), many of these typically use semi-empirical methods that suffer from limited physical validity and further research is required to produce a more robust estimate. Linking sea level rise projections to temperature must also be done with caution because of the different response times of these two climate variables to a given radiative forcing change.

Nicholls and Lowe (2004) previously showed that mitigation alone would not avoid all of the impacts due to rising sea levels, adaptation would likely be needed too. Recent work by van Vuuren et al. (2011) estimated that, for a world where global mean near surface temperatures reach around 2°C by 2100, global mean SLR could be 0.49m above present levels by the end of the century. Their sea level rise estimate for a world with global mean temperatures reaching 4°C by 2100 was 0.71m, suggesting around 40% of the future increase in sea level to the end of the 21st century could be avoided by mitigation. A qualitatively similar conclusion was reached in a study by Pardaens et al. (2011), which examined climate change projections from two GCMs. They found that around a third of global-mean SLR over the 21st century could potentially be avoided by a mitigation scenario

under which global-mean surface air temperature is near-stabilised at around 2°C relative to pre-industrial times. Under their baseline business-as-usual scenario the projected increase in temperature over the 21st century is around 4°C, and the sea level rise range is 0.29-0.51m (by 2090-2099 relative to 1980-1999; 5% to 95% uncertainties arising from treatment of land-based ice melt and following the methodology used by the IPCC AR4). Under the mitigation scenario, global mean SLR in this study is projected to be 0.17-0.34m.

The IPCC 4th assessment (IPCC 2007a) followed Nicholls and Lowe (2004) for estimates of the numbers of people affected by coastal flooding due to sea level rise. Nicholls and Lowe (2004) projected for the North America region that an additional 100 thousand people per year could be flooded due to sea level rise by the 2080s relative to the 1990s for the SRES A2 Scenario (note this region also includes other countries, such as USA and Canada). However, it is important to note that this calculation assumed that protection standards increased as GDP increased, although there is no additional adaptation for sea level rise. More recently, Nicholls et al. (2011) also examined the potential impacts of sea level rise in a scenario that gave around 4°C of warming by 2100. Readings from Figure 3 from Nicholls et al. (2011) for the North America Atlantic region suggest that less than an approximate 3 million additional people could be flooded for a 0.5 m SLR (assuming no additional protection), with less than an additional 3 million people flooded in the North America Pacific region. Nicholls et al. (2011) also looked at the consequence of a 2m SLR by 2100, however as we consider this rate of SLR to have a low probability we don't report these figures here.

Useful global-scale analyses of the impacts of SLR on coastal regions for several developing countries are presented by Dasgupta et al. (2009a, 2009b, 2010). Dasgupta et al. (2009a) investigated the consequences of prescribed SLR (1-5m in 1m increments) by GIS land inundation mapping but they did not consider any effects of climate change (e.g. variability in storm surges). Indeed, the authors note that there impacts estimates are conservative because of this and they note that even a small SLR can significantly magnify the impact of storm surges, which occur regularly and with devastating consequences in some coastal areas. The analysis was limited to 84 developing countries, and it was assumed that the level of coastal protection remained at present-day levels for all SLR scenarios. Out of the 84 countries that Dasgupta et al. (2009a) considered, Mexico was ranked the 7th highest with respect to the amount of agricultural land that was submerged due to a 1m SLR (see Table 11). It was estimated that 1.60% of coastal land in Mexico could be submerged under this magnitude of SLR. However, Mexico did not appear in the top 10 most impacted countries for total coastal land submerged, coastal GDP losses, coastal population affected

or urban areas affected. In a different study, Dasgupta et al. (2009b) considered the same 84 developing countries as Dasgupta et al. (2009a), but rather than investigating impacts under several magnitudes of prescribed SLR, Dasgupta et al. (2009b) considered a 10% intensification of the current 1-in-100-year storm surge combined with a 1m SLR. GIS inundation models were applied in the analysis and the method means that uncertainty associated with the climate system is inherently overlooked. Nevertheless, the projections give a useful indicator of the possible impact of SLR in Mexico. Table 12 shows that around 29% of Mexico's total coastal land area could be affected. Dasgupta et al. (2010) repeated this analysis to show that out of the 84 countries considered, Mexico presented the 5th highest percentage increase from present in agriculture affected by SLR and an intensification of storm surges; the increase from present was 209.5% (see Table 13). The results presented by Dasgupta et al. (2009a, 2009b, 2010) suggest that agriculture in Mexico is highly vulnerable to SLR, whereas other sectors are not (e.g. population exposure).

Rank	Land area	Population	GDP	Urban areas	Agricultural land	Wetlands
1	The Bahamas (11.57)	Vietnam (10.79)	Vietnam (10.21)	Vietnam (10.74)	Egypt (13.09)	Vietnam (28.67)
2	Vietnam (5.17)	Egypt (9.28)	Mauritania (9.35)	Guyana (10.02)	Vietnam (7.14)	Jamaica (28.16)
3	Qatar (2.70)	Mauritania (7.95)	Egypt (6.44)	French Guiana (7.76)	Suriname (5.60)	Belize (27.76)
4	Belize (1.90)	Suriname (7.00)	Suriname (6.35)	Mauritania (7.50)	The Bahamas (4.49)	Qatar (21.75)
5	Puerto Rico (1.64)	Guyana (6.30)	Benin (5.64)	Egypt (5.52)	Argentina (3.19)	The Bahamas (17.75)
6	Cuba (1.59)	French Guiana (5.42)	The Bahamas (4.74)	Libya (5.39)	Jamaica (2.82)	Libya (15.83)
7	Taiwan & China (1.59)	Tunisia (4.898)	Guyana (4.64)	UAE (4.80)	Mexico (1.60)	Uruguay (15.14)
8	The Gambia (1.33)	UAE (4.59)	French Guiana (3.02)	Tunisia (4.50)	Myanmar (1.48)	Mexico (14.85)
9	Jamaica (1.27)	The Bahamas (4.56)	Tunisia (2.93)	Suriname (4.20)	Guyana (1.16)	Benin (13.78)
10	Bangladesh (1.12)	Benin (4.93)	Ecuador (2.66)	The Bahamas (3.99)	Taiwan & China (1.05)	Taiwan & China (11.70)

Table 11. *The top 10 most impacted countries with a 1m SLR according to a study across 84 developing countries. Figures in parenthesis are the percentage impact for each country; e.g. 13.09% of all agricultural land in Egypt was simulated to be affected by a 1m SLR. Countries considered in this review are highlighted. Adapted from Dasgupta et al. (2009a).*

Country	**Incremental Impact: Land Area (sq. km)**	Projected Impact as a % of Coastal Total	**Incremental Impact: Population**	Projected Impact as a % of Coastal Total	**Incremental Impact: GDP (mil. USD)**	Projected Impact as a % of Coastal Total	**Incremental Impact: Agricultural Area (sq. km)**	Projected Impact as a % of Coastal Total	**Incremental Impact: Urban Extent (sq. km)**	Projected Impact as a % of Coastal Total	**Incremental Impact: Wetlands (sq. km)**	Projected Impact as a % of Coastal Total
Africa												
South Africa	607	43.09	48,140	32.91	174	30.98	70	34.48	93	48.10	132	46.23
Egypt	2,290	13.61	2,600,000	14.68	4,600	16.67	692	5.23	627	15.30	640	28.36
Kenya	274	41.93	27,400	40.23	10	32.05	40	22.13	9	38.89	177	52.51
Americas												
Argentina	2,400	18.03	278,000	19.52	2,240	16.42	157	9.93	313	27.47	459	11.30
Brazil	6,280	15.08	1,100,000	30.37	4,880	28.48	275	16.47	960	33.67	2,590	11.48
Mexico	9,130	29.04	463,000	20.56	2,570	21.22	310	10.89	701	18.35	1,760	52.25
Peru	727	36.69	61,000	46.90	177	46.18	5	26.92	54	42.72	20	37.91
Asia												
China	11,800	17.52	10,800,000	16.67	31,200	17.15	6,640	11.66	2,900	15.70	4,360	39.77
Rep. of Korea	902	61.73	863,000	50.48	10,600	47.86	237	66.75	335	48.15	77	78.81
India	8,690	29.33	7,640,000	28.68	5,170	27.72	3,740	23.64	1,290	30.04	2,510	32.31
Indonesia	14,400	26.64	5,830,000	32.75	7,990	38.71	4,110	26.12	1,280	33.25	2,680	26.97
Saudi Arabia	1,360	41.58	243,000	42.92	2,420	40.60	0	0.00	390	45.85	715	51.04
Bangladesh	4,450	23.45	4,840,000	16.01	2,220	19.00	2,710	17.52	433	18.30	3,890	24.29

Table 12. *The impact of a 1m SLR combined with a 10% intensification of the current 1-in-100-year storm surge. Impacts are presented as incremental impacts, relative to the impacts of existing storm surges. Each impact is presented in absolute terms, then as a percentage of the coastal total; e.g. 9.93% of Argentina's coastal agricultural land is impacted. The table is adapted from a study presented by Dasgupta et al. (2009b), which considered impacts in 84 developing countries. Only those countries relevant to this review are presented here and all incremental impacts have been rounded down to three significant figures.*

Rank	Land area	Population	GDP	Urban	Agriculture	Wetlands
1	Ivory Coast (285.2)	Ivory Coast (590.7)	Ivory Coast (1025.5)	Ivory Coast (500.0)	Egypt (398.3)	Algeria (400.5)
2	D.Rep.Congo (266.6)	D.Rep.Congo (285.8)	Gabon (282.5)	Gabon (300.0)	Mozambique (237.8)	Chile (400.0)
3	Sri Lanka (243.0)	Mauritania (270.2)	D.Rep.Congo (252.7)	Honduras (300.0)	Sri Lanka (218.2)	Angola (398.8)
4	Honduras (226.4)	Gabon (260.6)	Gambia (232.7)	Egypt (247.6)	Pakistan (216.7)	Nigeria (274.4)
5	Nigeria (226.3)	Gambia (204.3)	Mauritania (221/3)	Bangladesh (211.9)	Mexico (210.5)	D.Rep.Congo (220.0)
6	Nicaragua (218.6)	Egypt (190.3)	Egypt (213.7)	Cameroon (200.0)	Bangladesh (209.5)	Haiti (211.1)
7	Benin (193.3)	Sri Lanka (185.1)	Bangladesh (193.6)	Gambia (198.7)	Cuba (200.0)	Guinea (200.0)
8	Gambia (159.0)	Honduras (164.4)	Belize (192.1)	Congo (197.8)	Colombia (200.0)	Dom.Republic (198.4)
9	Guatemala (158.0)	Nicaragua (160.6)	Nicaragua (189.0)	Belize (195.2)	Cambodia (191.7)	Guatemala (197.3)
10	Haiti (147.8)	Bangladesh (154.8)	Cameroon (179.2)	Cuba (194.3)	Uruguay (175.0)	Gambia (192.3)

***Table 13**.The top 10 countries out of 84 developing countries, with largest increases in values of exposed indicators (relative to no SLR; values shown in parenthesis), under a prescribed 1m SLR and 10% intensification of storm surges. Countries considered in this review are highlighted. Data sourced from Dasgupta et al. (2010).*

This is supported by recent projections of impacts on port cities presented by Hanson et al. (2010). They investigated population exposure to global SLR, natural and human subsidence/uplift, and more intense storms and higher storm surges, for 136 port cities across the globe. Future city populations were calculated using global population and economic projections, based on the SRES A1 scenario up to 2030. The study accounted for uncertainty on future urbanization rates, but estimates of population exposure were only presented for a rapid urbanisation

scenario, which involved the direct extrapolation of population from 2030 to 2080. All scenarios assumed that new inhabitants of cities in the future will have the same relative exposure to flood risk as current inhabitants. The study is similar to a later study presented by Hanson et al. (2011) except here, different climate change scenarios were considered, and published estimates of exposure are available for more countries, including Mexico. Future water levels were generated from temperature and thermal expansion data related to greenhouse gas emissions with SRES A1B (un-mitigated climate change) and under a mitigation scenario where emissions peak in 2016 and decrease subsequently at 5% per year to a low emissions floor (2016-5-L). Table 14 shows the aspects of SLR that were considered for various scenarios and Table 15 displays regional population exposure for each scenario in the 2030s, 2050s and 2070s. The results show that climate change does not increase exposure of Mexico's port city population to coastal flooding, even under the most extreme SLR scenario that Hanson et al. (2010) considered.

Scenario		Water levels				
		Climate			Subsidence	
Code	Description	More intense storms	Sea-level change	Higher storm surges	Natural	Anthropogenic
FNC	Future city	V	x	x	X	x
FRSLC	Future City Sea-Level Change	V	V	x	V	x
FCC	Future City Climate Change	V	V	V	V	x
FAC	Future City All Changes	V	V	V	V	V

Table 14. *Summary of the aspects of SLR considered by Hanson et al. (2010). 'V' denotes that the aspect was considered in the scenario and 'x' that it was not.*

Rapid urbanisation projection																
2030						2050						2070				
Country	Ports	Water level projection				Country	Ports	Water level projection				Country	Ports	Water level projection			
		FAC	FCC	FRSLC	FNC			FAC	FCC	FRSLC	FNC			FAC	FCC	FRSLC	FNC
CHINA	15	17,100	15,500	15,400	14,600	**CHINA**	15	23,000	19,700	18,700	17,400	**CHINA**	15	27,700	22,600	20,800	18,600
INDIA	6	11,600	10,800	10,300	9,970	**INDIA**	6	16,400	14,600	13,600	12,500	**INDIA**	6	20,600	17,900	15,600	13,900
US	17	8,990	8,960	8,830	8,460	**US**	17	11,300	11,200	10,800	9,970	**US**	17	12,800	12,700	12,100	10,700
JAPAN	6	5,260	4,610	4,430	4,390	**JAPAN**	6	6,440	5,280	5,000	4,760	**JAPAN**	6	7,800	5,970	5,580	5,070
INDONESIA	4	1,420	1,200	1,200	1,170	**INDONESIA**	4	2,110	1,610	1,610	1,500	**INDONESIA**	4	2,680	1,830	1,830	1,530
BRAZIL	10	833	833	833	802	**BRAZIL**	10	929	929	929	879	**BRAZIL**	10	940	940	940	864
UK	2	497	497	478	459	**UK**	2	609	609	564	521	**UK**	2	716	716	640	569
CANADA	2	459	433	422	405	**CANADA**	2	549	512	486	457	**CANADA**	2	614	585	545	489
REP. OF KOREA	3	344	344	331	441	**REP. OF KOREA**	3	361	361	341	318	**REP. OF KOREA**	3	377	377	325	303
GERMANY	1	257	257	253	248	**GERMANY**	1	287	287	273	269	**GERMANY**	1	309	309	290	280
RUSSIA	1	177	177	177	177	**RUSSIA**	1	202	202	173	173	**RUSSIA**	1	226	226	197	169
AUSTRALIA	5	162	162	157	157	**AUSTRALIA**	5	197	197	191	181	**AUSTRALIA**	5	196	196	186	175
SOUTH AFRICA	2	30	30	30	29	**SAUDI ARABIA**	1	33	33	33	27	**SAUDI ARABIA**	1	38	38	38	29
SAUDI ARABIA	1	24	24	24	22	**SOUTH AFRICA**	2	28	28	28	27	**SOUTH AFRICA**	2	30	30	30	27
FRANCE	1	15	15	15	15	**FRANCE**	1	19	19	19	17	**FRANCE**	1	23	23	23	18
ITALY	1	2	2	2	2	**ITALY**	1	4	4	4	3	**ITALY**	1	6	6	6	4
MEXICO	0	0	0	0	0	**MEXICO**	0	0	0	0	0	**MEXICO**	0	0	0	0	0

***Table 15**. National estimates of port city population exposure (1,000s) for each water level projection (ranked according to exposure with the FAC scenario) under a rapid urbanisation projection for the 2030s, 2050s and 2070s. Estimates for present day exposure and in the absence of climate change (for 2070 only) for comparison are presented in Table 16. Data is from Hanson et al. (2010) and has been rounded down to three significant figures.*

Country	Ports	Population exposure				Exposure avoided
		Current	2070. Rapid urbanisation, FAC water level scenario			
			No climate change	A1B un-mitigated	Mitigated (2016-5-L)	
CHINA	15	8,740	18,600	27,700	26,500	1,140
UNITED STATES	17	6,680	10,700	12,800	12,300	505
RUSSIA	1	189	169	226	197	28
JAPAN	6	3,680	5,070	7,800	7,290	515
SOUTH AFRICA	2	24	27	30	29	0
INDIA	6	5,540	13,900	20,600	18,900	1,670
BRAZIL	10	555	864	940	926	14
MEXICO	0	0	0	0	0	0
CANADA	2	308	489	614	599	15
AUSTRALIA	5	99	175	196	190	6
INDONESIA	4	602	1,530	2,680	2,520	156
REP. OF KOREA	3	294	303	377	343	34
UK	2	414	569	716	665	51
FRANCE	1	13	18	23	20	2
ITALY	1	2	4	6	6	0
GERMANY	1	261	280	309	295	15
SAUDI ARABIA	1	15	29	38	35	3

***Table 16**. Exposed port city population (1,000s) in present (current), and in the 2070s in the absence of climate change (no climate change), with unmitigated climate change (A1B un-mitigated), and mitigated climate change (mitigated 2016-5-L), under the rapid urbanisation and FAC water level scenarios. The final column shows the potential avoided exposure, as a result of mitigation. Data is from Hanson et al. (2010) and has been rounded down to three significant figures.*

To further quantify the impact of SLR and some of the inherent uncertainties, the DIVA model was used to calculate the number of people flooded per year for global mean sea level increases (Brown et al., 2011). The DIVA model (DINAS-COAST, 2006) is an integrated model of coastal systems that combines scenarios of water level changes with socio-economic information, such as increases in population. The study uses two climate scenarios; 1) the SRES A1B scenario and 2) a mitigation scenario, RCP2.6. In both cases an SRES A1B population scenario was used. The results are shown in Table 17.

	A1B		RCP	
	Low	**High**	**Low**	**High**
Additional people flooded (1000s)	44.58	277.17	34.07	215.33
Loss of wetlands area (% of country's total wetland)	28.76%	38.42%	26.92%	32.94%

Table 17. *Number of additional people flooded (1000s), and percentage of total wetlands lost by the 2080s under the high and low SRES A1B and mitigation (RCP 2.6) scenarios (Brown et al., 2011).*

National-scale or sub-national scale assessments

Mexico's fourth national communication to the United Nations Framework on Climate Change (2009) has incorporated national-scale and sub-national scale studies published in the Spanish literature including institutional reports. In the English summary (main report not yet available in English) the Mexican government reports that studies on climate change impacts, vulnerability and adaptation have highlighted three main areas of concern: the lack of water in some states, the increase in distribution areas and number of dengue cases, as well as the gradual reduction of biodiversity in large areas of central and northern Mexico.

Friedman (2009 ed.) reports on wetland management pilot studies conducted at eight sites in Mexico. The English Executive Summary shows that the book (in Spanish) describes stresses on wetlands including land use and climate change. It concludes that the Gulf of Mexico is a priority for adaptation measures because of its vulnerability to climate change and provision of important economic and ecological services.

References

AINSWORTH, E. A. & MCGRATH, J. M. 2010. Direct Effects of Rising Atmospheric Carbon Dioxide and Ozone on Crop Yields. *In:* LOBELL, D. & BURKE, M. (eds.) *Climate Change and Food Security.* Springer Netherlands.

ALLISON, E. H., PERRY, A. L., BADJECK, M.-C., NEIL ADGER, W., BROWN, K., CONWAY, D., HALLS, A. S., PILLING, G. M., REYNOLDS, J. D., ANDREW, N. L. & DULVY, N. K. 2009. Vulnerability of national economies to the impacts of climate change on fisheries. *Fish and Fisheries,* 10**,** 173-196.

ARNELL, N., OSBORNE, T., HOOKER, J., DAWSON, T., PERRYMAN, A. & WHEELER, T. 2010a. Simulation of AVOIDed impacts on crop productivity and food security. *Work stream 2, Report 17 of the AVOID programme (AV/WS2/D1/R17).*

ARNELL, N., WHEELER, T., OSBORNE, T., ROSE, G., GOSLING, S., DAWSON, T., PENN, A. & PERRYMAN, A. 2010b. The implications of climate policy for avoided impacts on water and food security. *Work stream 2, Report 6 of the AVOID programme (AV/WS2/D1/R06).* London: Department for Energy and Climate Change (DECC).

ARNELL, N. W. 2004. Climate change and global water resources: SRES emissions and socio-economic scenarios. *Global Environmental Change,* 14**,** 31-52.

ARRIAGA-RAMIREZ, S. & CAVAZOS, T. 2010. Regional trends of daily precipitation indices in northwest Mexico and southwest United States. *Journal of Geophysical Research-Atmospheres,* 115.

AVNERY, S., MAUZERALL, D. L., LIU, J. F. & HOROWITZ, L. W. 2011. Global crop yield reductions due to surface ozone exposure: 2. Year 2030 potential crop production losses and economic damage under two scenarios of O_3 pollution. *Atmospheric Environment,* 45**,** 2297-2309.

BENDER, M. A., KNUTSON, T. R., TULEYA, R. E., SIRUTIS, J. J., VECCHI, G. A., GARNER, S. T. & HELD, I. M. 2010. Modeled impact of anthropogenic warming on the frequency of intense Atlantic hurricanes. *Science,* 327**,** 454-8.

BENGTSSON, L., HODGES, K. I., ESCH, M., KEENLYSIDE, N., KORNBLUEH, L., LUO, J.-J. & YAMAGATA, T. 2007. How may tropical cyclones change in a warmer climate? *Tellus A,* 59**,** 539-561.

BROWN, S., NICHOLLS, R., LOWE, J.A. and PARDAENS, A. (2011), Sea level rise impacts in 24 countries. Faculty of Engineering and the Environment and Tyndall Centre for Climate Change Research, University of Southampton.

CASTILLO-ALVAREZ, M., NIKOLSKII-GAVRILOV, I., ORTIZ-SOLORIO, C. A., VAQUERA-HUERTA, H., CRUZ-BELLO, G., MEJIA-SAENZ, E. & GONZALEZ-HERNANDEZ, A. 2007. Soil fertility alteration due to the climate change and its effect on agricultural crop productivity. *Interciencia,* 32**,** 368-375.

CAVAZOS, T. & RIVAS, D. 2004. Variability of extreme precipitation events in Tijuana, Mexico. *Climate Research,* 25**,** 229-242.

CHAKRABORTY, S. & NEWTON, A. C. 2011. Climate change, plant diseases and food security: an overview. *Plant Pathology,* 60**,** 2-14.

CHAUVIN, F., ROYER, J.-F. & DÉQUÉ, M. 2006. Response of hurricane-type vortices to global warming as simulated by ARPEGE-Climat at high resolution. *Climate Dynamics,* 27**,** 377-399.

CHEUNG, W. W. L., LAM, V. W. Y., SARMIENTO, J. L., KEARNEY, K., WATSON, R. E. G., ZELLER, D. & PAULY, D. 2010. Large-scale redistribution of maximum fisheries catch potential in the global ocean under climate change. *Global Change Biology,* 16**,** 24-35.

DASGUPTA, S., LAPLANTE, B., MEISNER, C., WHEELER, D. & YAN, J. 2009a. The impact of sea level rise on developing countries: a comparative analysis. *Climatic Change,* 93**,** 379-388.

DASGUPTA, S., LAPLANTE, B., MURRAY, S. & WHEELER, D. 2009b. Sea-level rise and storm surges: a comparative analysis of impacts in developing countries. Washington DC, USA: World Bank.

DASGUPTA, S., LAPLANTE, B., MURRAY, S. & WHEELER, D. 2010. Exposure of developing countries to sea-level rise and storm surges. *Climatic Change***,** 1-13.

DINAS-COAST Consortium. 2006 DIVA 1.5.5. Potsdam, Germany: Potsdam Institute for Climate Impact Research (on CD-ROM).

DOLL, P. 2009. Vulnerability to the impact of climate change on renewable groundwater resources: a global-scale assessment. *Environmental Research Letters,* 4.

DOLL, P. & SIEBERT, S. 2002. Global modeling of irrigation water requirements. *Water Resources Research*. Vol: 38 Issue: 4. Doi: 10.1029/2001WR000355

EMANUEL, K., SUNDARARAJAN, R. & WILLIAMS, J. 2008. Hurricanes and Global Warming: Results from Downscaling IPCC AR4 Simulations. *Bulletin of the American Meteorological Society,* 89**,** 347-367.

FALKENMARK, M., ROCKSTRÖM, J. & KARLBERG, L. 2009. Present and future water requirements for feeding humanity. *Food Security,* 1**,** 59-69.

FAO. 2008. *Food and Agricultural commodities production* [Online]. Available: http://faostat.fao.org/site/339/default.aspx [Accessed 1 June 2011].

FAO. 2010. Food Security county profiles [Online]. Available: http://www.fao.org/economic/ess/ess-fs/ess-fs-country/en/ [Accessed 1 Sept 2011].

FISCHER, G. 2009. World Food and Agriculture to 2030/50: How do climate change and bioenergy alter the long-term outlook for food, agriculture and resource availability? *Expert Meeting on How to Feed the World in 2050.* Food and Agriculture Organization of the United Nations, Economic and Social Development Department.

FISCHER, G., VELTHUIZEN, H. V., HIZSNYIK, E. & WIBERG, D. 2009. Potentially obtainable yields in the semi-arid tropics. *Global Theme on Agroecosystems Report.* Patancheru: International Crops Research Institute for the Semi-Arid Tropics (ICRISAT).

FRIEDMAN, , J . 2009 (Editor) English Executive Summary in Volume I of " Adaptación a los impactos del cambio climático en los humedales costeros del Golfo de México " ISBN 978-968-817-928-4

GARNER, S. T., HELD, I. M., KNUTSON, T. & SIRUTIS, J. 2009. The Roles of Wind Shear and Thermal Stratification in Past and Projected Changes of Atlantic Tropical Cyclone Activity. *Journal of Climate,* 22**,** 4723-4734.

GERTEN D., SCHAPHOFF S., HABERLANDT U., LUCHT W., SITCH S. 2004 . Terrestrial vegetation and water balance: hydrological evaluation of a dynamic global vegetation model International Journal Water Resource Development 286:249–270.

GORNALL, J., BETTS, R., BURKE, E., CLARK, R., CAMP, J., WILLETT, K., WILTSHIRE, A. 2010. Implications of climate change for agricultural productivity in the early twenty-first century. *Phil. Trans. R. Soc. B*, DOI: 10.1098/rstb.2010.0158

GOSLING, S., TAYLOR, R., ARNELL, N. & TODD, M. 2011. A comparative analysis of projected impacts of climate change on river runoff from global and catchment-scale hydrological models. *Hydrology and Earth System Sciences,* 15**,** 279–294.

GOSLING, S. N. & ARNELL, N. W. 2011. Simulating current global river runoff with a global hydrological model: model revisions, validation, and sensitivity analysis. *Hydrological Processes,* 25**,** 1129-1145.

GOSLING, S. N., BRETHERTON, D., HAINES, K. & ARNELL, N. W. 2010. Global hydrology modelling and uncertainty: running multiple ensembles with a campus grid. *Philosophical Transactions of the Royal Society A: Mathematical, Physical and Engineering Sciences,* 368**,** 4005-4021.

GRATIOT, N., DUVERT, C., COLLET, L., VINSON, D., NEMERY, J. & SÁENZ-ROMERO, C. 2010. Increase in surface runoff in the central mountains of Mexico: lessons from the past and predictive scenario for the next century. *Hydrology and Earth System Sciences,* 14**,** 291-300.

GROISMAN, P. Y., KNIGHT, R. W., EASTERLING, D. R., KARL, T. R., HEGERL, G. C. & RAZUVAEV, V. A. N. 2005. Trends in intense precipitation in the climate record. *Journal of Climate,* 18**,** 1326-1350.

GUALDI, S., SCOCCIMARRO, E. & NAVARRA, A. 2008. Changes in Tropical Cyclone Activity due to Global Warming: Results from a High-Resolution Coupled General Circulation Model. *Journal of Climate,* 21**,** 5204-5228.

HANSON, S., NICHOLLS, R., RANGER, N., HALLEGATTE, S., CORFEE-MORLOT, J., HERWEIJER, C. & CHATEAU, J. 2011. A global ranking of port cities with high exposure to climate extremes. *Climatic Change,* 104**,** 89-111.

HANSON, S., NICHOLLS, R., S, H. & CORFEE-MORLOT, J. 2010. The effects of climate mitigation on the exposure of worlds large port cities to extreme coastal water levels. London, UK.

HARDING, R., BEST, M., BLYTH, E., HAGEMANN, D., KABAT, P., TALLAKSEN, L.M., WARNAARS, T., WIBERG, D., WEEDON, G.P., van LANEN, H., LUDWIG, F., HADDELAND, I. 2011. Preface to the “Water and Global Change (WATCH)” special collection: Current knowledge of the terrestrial global water cycle. *Journal of Hydrometeorology*, DOI: 10.1175/JHM-D-11-024.1

HASEGAWA, A. & EMORI, S. 2005. Tropical Cyclones and Associated Precipitation over the Western North Pacific : T106 Atmospheric GCM Simulation for Present-day and Doubled CO 2 Climates. *Simulation,* 1**,** 148-151.

HIRABAYASHI, Y., KANAE, S., EMORI, S., OKI, T. & KIMOTO, M. 2008. Global projections of changing risks of floods and droughts in a changing climate. *Hydrological Sciences Journal-Journal Des Sciences Hydrologiques,* 53**,** 754-772.

IFPRI. 2010. *International Food Policy Research Institute (IFPRI) Food Security CASE maps. Generated by IFPRI in collaboration with StatPlanet.* [Online]. Available: www.ifpri.org/climatechange/casemaps.html [Accessed 21 June 2010].

IGLESIAS, A., GARROTE, L., QUIROGA, S. & MONEO, M. 2009. Impacts of climate change in agriculture in Europe. PESETA-Agriculture study. *JRC Scientific and Technical Reports.*

IGLESIAS, A. & ROSENZWEIG, C. 2009. Effects of Climate Change on Global Food Production under Special Report on Emissions Scenarios (SRES) Emissions and Socioeconomic Scenarios: Data from a Crop Modeling Study. Palisades, NY: Socioeconomic Data and Applications Center (SEDAC), Columbia University.

IPCC 2007a. Climate Change 2007: Impacts, Adaptation and Vulnerability. Contribution of Working Group II to the Fourth Assessment Report of the Intergovernmental Panel on Climate Change. *In:* PARRY, M. L., CANZIANI, O. F., PALUTIKOF, J. P., VAN DER LINDEN, P. J. & HANSON, C. E. (eds.). Cambridge, UK.

IPCC 2007b. Climate Change 2007: The Physical Science Basis. Contribution of Working Group I to the Fourth Assessment Report of the Intergovernmental Panel on Climate Change *In:* SOLOMON, S., QIN, D., MANNING, M., CHEN, Z., MARQUIS, M., AVERYT, K. B., TIGNOR, M. & MILLER, H. L. (eds.). Cambridge, United Kingdom and New York, NY, USA.

KITOH, A., OSE, T., KURIHARA, K., KUSUNOKI, S., SUGI, M. & GROUP, K. T.-M. 2009. Projection of changes in future weather extremes using super-high-resolution global and regional atmospheric models in the KAKUSHIN Program : Results of preliminary experiments Abstract :. *Group,* 53**,** 49-53.

KNUTSON, T. R., SIRUTIS, J. J., GARNER, S. T., VECCHI, G. A. & HELD, I. M. 2008. Simulated reduction in Atlantic hurricane frequency under twenty-first-century warming conditions. *Nature Geosci,* 1**,** 359-364.

KNUTSON, T. R. & TULEYA, R. E. 2004. Impact of CO_2-Induced Warming on Simulated Hurricane Intensity and Precipitation : Sensitivity to the Choice of Climate Model and Convective Parameterization. *Journal of Climate***,** 3477-3495.

LATIF, M. & KEENLYSIDE, N. S. 2009. El Niño/Southern Oscillation response to global warming. *Proceedings of the National Academy of Sciences of the United States of America,* 106**,** 20578-20583.

LOBELL, D. B., BURKE, M. B., TEBALDI, C., MASTRANDREA, M. D., FALCON, W. P. & NAYLOR, R. L. 2008. Prioritizing climate change adaptation needs for food security in 2030. *Science,* 319**,** 607-610.

LOBELL, D., SCHLENKER, W. and COSTA-ROBERTS, J. (2011) Climate Trends and Global Crop Production Since 1980. *Science,* 333, 616-620 [DOI:10.1126/science.1204531]

LUCK, J., SPACKMAN, M., FREEMAN, A., TRE¸BICKI, P., GRIFFITHS, W., FINLAY, K. & CHAKRABORTY, S. 2011. Climate change and diseases of food crops. *Plant Pathology,* 60**,** 113-121.

MCDONALD, R. E., BLEAKEN, D. G., CRESSWELL, D. R., POPE, V. D. & SENIOR, C. A. 2005. Tropical storms: representation and diagnosis in climate models and the impacts of climate change. *Climate Dynamics,* 25**,** 19-36.

MENDELSOHN, R., EMANUEL, K. & CHONABAYASHI, S. 2011. The Impact of Climate Change on Global Tropical Cyclone Damages.

Mexico's Third National Communication to the United Nations Framework Convention on Climate Change (2007)

Mexico's Fourth National Communication to the United Nations Framework Convention on Climate Change (2009) English Executive Summary

MONTERROSO RIVAS, A. I., CONDE ÁLVAREZ, C. & ROSALES DORANTES, G. 2011. Assessing current and potential rainfed maize suitability under climate change scenarios in México. *Atmósfera,* 24**,** 53-67.

MURAKAMI, H. & WANG, B. 2010. Future Change of North Atlantic Tropical Cyclone Tracks: Projection by a 20-km-Mesh Global Atmospheric Model*. *Journal of Climate,* 23**,** 2699-2721.

NELSON, G. C., ROSEGRANT, M. W., KOO, J., ROBERTSON, R., SULSER, T., ZHU, T., RINGLER, C., MSANGI, S., PALAZZO, A., BATKA, M., MAGALHAES, M., VALMONTE-SANTOS, R., EWING, M. & LEE, D. 2009. Climate change. Impact on Agriculture and Costs of Adaptation. Washington, D.C.: International Food Policy Research Institute.

NELSON, G. C., ROSEGRANT, M. W., PALAZZO, A., GRAY, I., INGERSOLL, C., ROBERTSON, R., TOKGOZ, S., ZHU, T., SULSER, T. & RINGLER, C. 2010. Food Security, Farming and Climate Change to 2050. *Research Monograph, International Food Policy Research Institute.* Washington, DC.

NICHOLLS, R. J. and LOWE, J. A. (2004). "Benefits of mitigation of climate change for coastal areas." *Global Environmental Change* **14**(3): 229-244.

NICHOLLS, R. J., MARINOVA, N., LOWE, J. A., BROWN, S., VELLINGA, P., DE GUSMÃO, G., HINKEL, J. and TOL, R. S. J. (2011). "Sea-level rise and its possible impacts given a 'beyond 4◦C world' in the twenty-first century." *Philosophical Transactions of the Royal Society A* **369**: 1-21.

NOHARA, D., KITOH, A., HOSAKA, M. & OKI, T. 2006. Impact of climate change on river discharge projected by multimodel ensemble. *Journal of Hydrometeorology,* 7**,** 1076-1089.

OOUCHI, K., YOSHIMURA, J., YOSHIMURA, H., MIZUTA, R., KUSUNOKI, S. & NODA, A. 2006. Tropical Cyclone Climatology in a Global-Warming Climate as Simulated in a 20 km-Mesh Global Atmospheric Model: Frequency and Wind Intensity Analyses. *Journal of the Meteorological Society of Japan,* 84**,** 259-276.

PARDAENS, A. K., LOWE, J., S, B., NICHOLLS, R. & DE GUSMÃO, D. 2011. Sea-level rise and impacts projections under a future scenario with large greenhouse gas emission reductions. *Geophysical Research Letters,* 38**,** L12604.

PARRY, M. L., ROSENZWEIG, C., IGLESIAS, A., LIVERMORE, M. & FISCHER, G. 2004. Effects of climate change on global food production under SRES emissions and socio-

economic scenarios. *Global Environmental Change-Human and Policy Dimensions,* 14**,** 53-67.

PERALTA-HERNANDEZ, A. R., BARBA-MARTINEZ, L. R., MAGANA-RUEDA, V. O., MATTHIAS, A. D. & LUNA-RUIZ, J. J. 2008. Temporal and spatial behavior of temperature and precipitation during the canicula (midsummer drought) under El Niño conditions in central Mexico. *Atmosfera,* 21**,** 265-280.

PETERSON, T. C., ZHANG, X. B., BRUNET-INDIA, M. & VAZQUEZ-AGUIRRE, J. L. 2008. Changes in North American extremes derived from daily weather data. *Journal of Geophysical Research-Atmospheres,* 113.

RAMANKUTTY, N., EVAN, A. T., MONFREDA, C. & FOLEY, J. A. 2008. Farming the planet: 1. Geographic distribution of global agricultural lands in the year 2000. *Global Biogeochemical Cycles,* 22**,** GB1003.

RAMANKUTTY, N., FOLEY, J. A., NORMAN, J. & MCSWEENEY, K. 2002. The global distribution of cultivable lands: current patterns and sensitivity to possible climate change. *Global Ecology and Biogeography,* 11**,** 377-392.

REICHLER, T. & KIM, J. 2008. How well do coupled models simulate today's climate? *Bulletin of the American Meteorological Society,* 89**,** 303-+.

ROCKSTROM, J., FALKENMARK, M., KARLBERG, L., HOFF, H., ROST, S. & GERTEN, D. 2009. Future water availability for global food production: The potential of green water for increasing resilience to global change. *Water Resources Research,* 45.

SAENZ-ROMERO, C., REHFELDT, G. E., CROOKSTON, N. L., DUVAL, P., ST-AMANT, R., BEAULIEU, J. & RICHARDSON, B. A. 2010. Spline models of contemporary, 2030, 2060 and 2090 climates for Mexico and their use in understanding climate-change impacts on the vegetation. *Climatic Change,* 102**,** 595-623.

SMAKHTIN, V., REVENGA, C. & DOLL, P. 2004. A pilot global assessment of environmental water requirements and scarcity. *Water International,* 29**,** 307-317.

SUGI, M., MURAKAMI, H. & YOSHIMURA, J. 2009. A reduction in global tropical cyclone frequency due to global warming. *SOLA,* 5**,** 164-167.

TATSUMI, K., YAMASHIKI, Y., VALMIR DA SILVA, R., TAKARA, K., MATSUOKA, Y., TAKAHASHI, K., MARUYAMA, K. & KAWAHARA, N. 2011. Estimation of potential changes

in cereals production under climate change scenarios. *Hydrological Processes,* Special Issue: Japan Society of Hydrology and water resources, 25 (17), 2715-2725.

VAN VUUREN, D., DEN ELZEN, M., LUCAS, P., EICKHOUT, B., STRENGERS, B., VAN RUIJVEN, B., WONINK, S. & VAN HOUDT, R. 2007. Stabilizing greenhouse gas concentrations at low levels: an assessment of reduction strategies and costs. *Climatic Change,* 81**,** 119-159.

VAN VUUREN, D. P., ISAAC, M., KUNDZEWICZ, Z. W., ARNELL, N., BARKER, T., CRIQUI, P., BERKHOUT, F., HILDERINK, H., HINKEL, J., HOF, A., KITOUS, A., KRAM, T., MECHLER, R. & SCRIECIU, S. 2011. The use of scenarios as the basis for combined assessment of climate change mitigation and adaptation. *Global Environmental Change,* 21**,** 575-591.

VECCHI, G. A. & SODEN, B. J. 2007. Effect of remote sea surface temperature change on tropical cyclone potential intensity. *Nature,* 450**,** 1066-70.

VOROSMARTY, C. J., MCINTYRE, P. B., GESSNER, M. O., DUDGEON, D., PRUSEVICH, A., GREEN, P., GLIDDEN, S., BUNN, S. E., SULLIVAN, C. A., LIERMANN, C. R. & DAVIES, P. M. 2010. Global threats to human water security and river biodiversity. *Nature,* 467**,** 555-561.

WARREN, R., ARNELL, N., BERRY, P., BROWN, S., DICKS, L., GOSLING, S., HANKIN, R., HOPE, C., LOWE, J., MATSUMOTO, K., MASUI, T., NICHOLLS, R., O'HANLEY, J., OSBORN, T., SCRIECRU, S. (2010) The Economics and Climate Change Impacts of Various Greenhouse Gas Emissions Pathways: A comparison between baseline and policy emissions scenarios, *AVOID Report*, AV/WS1/D3/R01. http://www.metoffice.gov.uk/avoid/files/resources-researchers/AVOID_ WS1_D3_01_20100122.pdf

WEHNER, M., EASTERLING, D. R., LAWRIMORE, J. H., HEIM, R. R., VOSE, R. S. & SANTER, B. D. 2011. Projections of Future Drought in the Continental United States and Mexico. *Journal of Hydrometeorology*.

WOOD, E.F., ROUNDY, J.K., TROY, T.J., van BEEK, L.P.H., BIERKENS, M.F.P., BLYTH, E., de ROO, A., DOLL, P., EK, M., FAMIGLIETTI, J., GOCHIS, D., van de GIESEN, N., HOUSER, P., JAFFE, P.R., KOLLET, S., LEHNER, B., LETTENMAIER, D.P., PETERS-LIDARD, C., SIVAPALAN, M., SHEFFIELD, J., WADE, A. & WHITEHEAD, P. 2011.

Hyperresolution global land surface modelling: Meeting a grand challenge for monitoring Earth's terrestrial water. *Water Resources Research,* 47, W05301.

WOS. 2011. *Web of Science* [Online]. Available: http://thomsonreuters.com/products_services/science/science_products/a-z/web_of_science [Accessed August 2011].

WU, W., TANG, H., YANG, P., YOU, L., ZHOU, Q., CHEN, Z. & SHIBASAKI, R. 2011. Scenario-based assessment of future food security. *Journal of Geographical Sciences,* 21**,** 3-17.

YOSHIMURA, J., SUGI, M. & NODA, A. 2006. Influence of Greenhouse Warming on Tropical Cyclone Frequency. *Journal of the Meteorological Society of Japan,* 84**,** 405-428.

ZHAO, M. & HELD, I. M. 2010. An Analysis of the Effect of Global Warming on the Intensity of Atlantic Hurricanes Using a GCM with Statistical Refinement. *Journal of Climate,* 23**,** 6382-6393.

ZHAO, M., HELD, I. M., LIN, S.-J. & VECCHI, G. A. 2009. Simulations of Global Hurricane Climatology, Interannual Variability, and Response to Global Warming Using a 50-km Resolution GCM. *Journal of Climate,* 22**,** 6653.

Acknowledgements

Funding for this work was provided by the UK Government Department of Energy and Climate Change, along with information on the policy relevance of the results.

The research was led by the UK Met Office in collaboration with experts from the University of Nottingham, Walker Institute at the University of Reading, Centre for Ecology and Hydrology, University of Leeds, Tyndall Centre — University of East Anglia, and Tyndall Centre — University of Southampton.

Some of the results described in this report are from work done in the AVOID programme by the UK Met Office, Walker Institute at the University of Reading, Tyndall Centre — University of East Anglia, and Tyndall Centre — University of Southampton.

The AVOID results are built on a wider body of research conducted by experts in climate and impact models at these institutions, and in supporting techniques such as statistical downscaling and pattern scaling.

The help provided by experts in each country is gratefully acknowledged — for the climate information they suggested and the reviews they provided, which enhanced the content and scientific integrity of the reports.

The work of the independent expert reviewers at the Centre for Ecology and Hydrology, University of Oxford, and Fiona's Red Kite Climate Consultancy is gratefully acknowledged.

Finally, thanks go to the designers, copy editors and project managers who worked on the reports.

Met Office
FitzRoy Road, Exeter
Devon, EX1 3PB
United Kingdom

Tel: 0870 900 0100
Fax: 0870 900 5050
enquiries@metoffice.gov.uk
www.metoffice.gov.uk

Produced by the Met Office.